Molecular Genetics of Leber Congenital Amaurosis (LCA) in Indian Patients

Thesis submitted for the degree of

DOCTOR OF PHILOSOPHY

By

Rachna Shukla

Kallam Anji Reddy Molecular Genetics Laboratory
L. V. Prasad Eye Institute
Hyderabad – 500 034

December 2014

Enrolment No: 09LBPH19

To

THE DEPARTMENT OF BIOCHEMISTRY
SCHOOL OF LIFE SCIENCES
UNIVERSITY OF HYDERABAD
HYDERABAD-500 046
INDIA

Dedicated
to
My Parents

UNIVERSITY OF HYDERABAD
SCHOOL OF LIFE SCIENCES
DEPARTMENT OF BIOCHEMISTRY
HYDERABAD-500 046
INDIA

DECLARATION

The research work embodied in this thesis entitled, **"Molecular genetics of Leber Congenital Amaurosis (LCA) in Indian patients"**, has been carried out by me at the L.V. Prasad Eye Institute, Hyderabad, under the guidance of Dr. Chitra Kannabiran. I hereby declare that this work is original and has not been submitted in part or full for any other degree or diploma of any other university.

Rachna Shukla

Dr. Chitra Kannabiran
Supervisor
Kallam Anji Reddy Molecular Genetics Laboratory
L. V. Prasad Eye Institute
Hyderabad – 500 034

UNIVERSITY OF HYDERABAD
SCHOOL OF LIFE SCIENCES
DEPARTMENT OF BIOCHEMISTRY
HYDERABAD-500 046
INDIA

CERTIFICATE

This is to certify that this thesis entitled, **"Molecular genetics of Leber Congenital Amaurosis (LCA) in Indian patients"**, submitted by Rachna Shukla, ID No. 09LBPH19, for the award of Doctor of Philosophy degree to the University of Hyderabad is based on the work carried out by her at the L.V. Prasad Eye Institute, Hyderabad, under the my supervision. This work has not been submitted for any diploma or degree of any other university or Institution.

Dr. Chitra Kannabiran
Supervisor
Kallam Anji Reddy Molecular Genetics Laboratory
L. V. Prasad Eye Institute
Hyderabad – 500 034

Acknowledgements

I would like to thank my mentor Dr. Chitra Kannabiran for her valuable guidance during the course of my work. Her intense devotion to science has left a lasting impression on me. This has inspired me all along and will also prove as a valuable asset for the rest of my career. I would not have imagined of a better adviser and mentor for my PhD, and without her knowledge, perseverance, vision and inspiration I would never have finished.

I wish to express my sincere and deep gratitude to Prof. D. Balasubramanian, Director of Research, L V Prasad Eye Institute for his unconditional support. Without which, it was impossible for me to pursue PhD. Personally I always looked upon him as a great scholar and researcher. I always enjoyed his simple explanations of complex scientific problems during our research presentations. His accounts about the days of yore, always kept me spell-bound.

I would like to thank Dr. G.N. Rao for making an outstanding research institute like L V Prasad. His vision to bring clinicians and researchers together to reduce the gap between bench and bed, lead to this outstanding place called LVPEI. The motto of LVPEI, vision for all and the philanthropy left an indelible impression.

I am profoundly grateful to Dr. Subhadra Jalali for helping me in sample collection and clinical data analysis. Her untiring endeavor to learn more about her patients through research left a lasting impression on me.

I would also like to thank Dr. Shubo and Dr. Inderjeet for their timely help to arrange and furnish reagents that bailed me out in many situations. Dr. Geetha was an ever enthusiastic scientist. My

interactions with her always filled me with hope and energy. I admire Dr. Indumati, for her exemplary nature and her aptitude for science. Dr. Vivek and Dr. Sanhita were the soothsayers who believed I will be done someday. The discussions with Dr. Srikant and Dr. Charanya have boosted my understanding of various nuances of science and life, which I will always cherish.

The 5th floor research labs were the best place as it was populated with guys like Sarita, Shubha and Maithali who constitute the advisory board, who bailed me out of tough situations with their timely counsel. Purushtottam, Sagar and Surya, the triad formed the Bermuda triangle of 5th floor; where all miseries disappeared with their humor.

Almas, Sushma and Santvana were wonderful lab-mates and took my side in sickness and health. The present floor-mates including Ganesh, Pulla Rao, Meha, Hameed, Shiva, Pravin and Pravin always have been good company.

Past members such as Hardeep and Neeraja were wonderful friends. I would like to thank Vidya and Gayatri for helping me in sample collection when needed. I fondly remember Subhash and Nageshwar.

I would like to thank Savitri in dispelling my anxiety during the last legs of my PhD.

Mr. Jagdish has been the unsung hero; all I could conclude is that he never says " NO". He has the infallible ability to procure reagents, when our stock was running short.

Dr. Chandak at CCMB and Dr. V.K. Namdev were my pervious mentors; and I learnt time and life-management from them.

I would like to thank Arvind and Joseph at biochemistry lab, Kishore Ji at MRD, Banu ji and Sudhakar in library, Karthik and Kishor at

communication, Shweta and Uma (optometrist), Jai Ganesh, Moinuddin and Ilens at administration, Aparijita at stores for their help and cooperation extended to me.

I sincerely thank LVPEI and CSIR for the fellowship.

Finally, I would like to thank my family for always supporting me. My mother was a source constant of inspiration. My family stood as a rock through thick and thin. My special thanks to Nishant and my mother-in-law took care of responsibilities at home, so that I can pursue my doctoral degree. Last but not the least; for my kids Ishita and Sejal, for providing chronic happiness in my life.

ABSTRACT

Leber congenital amaurosis (LCA) is a severe form of retinal dystrophy that is congenital in onset, clinically and genetically heterogeneous and leads to severe visual impairment or blindness at birth. LCA is mostly inherited as an autosomal recessive disorder with mutations in at least 21 genes reported so far.

LCA is largely untreatable. However, recent advances in specific gene replacement therapies have opened up the possibility of using this approach for various genetic forms of LCA. This requires knowledge of the mutation spectrum of different genes in LCA patients so that appropriate gene-specific therapies can be designed to treat this condition.

The present study was undertaken to identify pathogenic mutations in various genes in LCA patients of Indian origin. The aims of this study were to characterize the molecular genetic basis of LCA in Indian patients by screening 100 unrelated probands for pathogenic changes in: 1) LCA-associated genes known in literature and 2) novel genes that are putative candidates for LCA based on their roles in retinal physiology/pathology.

The study protocol was approved by the Institutional Review Board and adhered to the guidelines of the Declaration of Helsinki. Patients diagnosed with LCA, seen at the outpatient clinic of the retina service of LVPEI were recruited for the study. A total of 100 LCA probands and their family members were recruited for the study with informed consent. Pathogenicity of any sequence variations found was tested by screening for the presence of the relevant alteration in 150 normal unrelated controls and by co-segregation analyses in family members of the probands.

The known LCA genes taken for screening were guanylate cyclase 2D (*GUCY2D),* retinal degeneration 3 (*RD3)* and crumbs homologue 1 (*CRB1*). The novel genes were nicotinamide nucleotide adenylyltransferase 1 (*NMNAT1)* and the membrane protein palmitoylated 5 (*MPP5/PALS1*).

A total of 7 novel and 7 reported variations were identified in the *GUCY2D* gene. Of the 7 novel variations, four were found to be pathogenic including 2 homozygous missense variations and 2 homozygous nonsense variations (Ala353Val, Trp640Arg, Gln791X and Gln939X) observed in 1 proband each out of 100 probands tested.

In the *RD3* gene, 4 non-synonymous sequence changes were observed; all were detected in heterozygous probands. Among these, 3 were reported and one was novel (Arg47His/c.140G>A).

Screening of the *CRB1* gene revealed 7 novel variations including 4 exonic and 3 intronic changes. Two homozygous exonic variations (Gln1124X and Tyr1269X) were found to be pathogenic and confirmed by co-segregation analysis in available family members and absence in 150 normal control individuals. 7 SNPs were also observed.

In the *NMNAT1* gene, 5 sequence changes were found in 4 probands- 3 probands were homozygous for the novel missense changes - Val9Met, Asp33Gly, Leu72His, one in each proband. One proband was compound heterozygous for two variants Ala189Leufs*25 and Arg237Cys. One proband carrying a change of Val178Met was heterozygous for the same.

Screening of the *PALS1* led to the identification of 8 SNPs. No disease-associated changes were detected in 100 probands screened.

In conclusion this study revealed that mutations in the 4 genes tested together occur in 10 % of LCA cases of Indian origin. Other genes need to be explored for determining the genetic basis of LCA in the majority of patients.

LIST OF ABBREVIATIONS

AD	Autosomal Dominant
AR	Autosomal Recessive
bp	Base Pair
^{0}C	Degree Centigrade
cDNA	complementary DNA
DNA	Deoxyribonucleic Acid
dNTP	Deoxynucleotide triphosphate
D	Diopters
EDTA	Ethylenediaminetetraacetic acid
ERG	Electroretinogram
kDa	Kilodaltons
KO	Knockout
mg	Milligram
ml	Millilitre
mm	Millimetre
NGS	Next Generation Sequencing
nm	Nanometer
ng	Nanogram
ONL	Outer Nuclear Layer
OS	Outer Segment
IS	Inner Segment
OD	Right Eye
OS	Left Eye
OU	Both Eyes
PCR	Polymerase Chain Reaction
PPRPE	Preserved Para-Arteriolar RPE
RBC	Red blood cell
RFLP	Restriction Fragment Length Polymorphism
RP	Retinitis Pigmentosa
RPE	Retinal Pigment Epithelium
RPM	Revolutions Per Minute
OCT	Optical Coherence Tomography
SDS	Sodium Dodecyl Sulphate
SNP	Single Nucleotide Polymorphism
µl	Microlitre
VA	Visual Acuity
UV	Ultraviolet
X	Termination Codon

TABLE OF CONTENTS

LIST OF TABLES

Appendix tables

LIST OF FIGURES **Page Number**

1.1 Retina

The human eye is a nearly spherical structure with an antero-posterior diameter of about 25 mm in adults. The eyeball consists of an outer shell made up of three layers-sclera, choroid and retina.

Retina is the innermost layer, lining the posterior two-thirds of the interior of the eye, and consisting of multiple types of photosensitive neurons. The retina extends from the optic disc to the ora serrata. The oras serrata are at the junction of the retina and ciliary body. The retina is firmly attached only at the margins of optic disc posteriorly and at the ora serrata anteriorly. The retina is 0.1 mm thick at the ora serrata and 0.23 mm thick at the posterior pole. The retina has dual blood supply, the inner two-thirds of the retina is covered by central retinal vessels whereas the outer one-third is nourished by the choriodal circulation or the choriocapillaris. These two circulations do not overlap and form the blood retinal barrier (Bron ,Tripathi *et al.*, 1997).

Near the centre of retina, a highly pigmented yellow spot called macula is present. The yellow colour is due to the presence of carotenoid pigments-xeaxanthin and lutein in the axons. The macula is 5.5 mm in diameter. The centre of the macula is called fovea (1.5 mm in diameter). Within fovea, foveola or foveal pit (0.35 mm in diameter) is present, which has the largest density of cone cells. Towards the peripheral retina, the density of rods increases and number of cones and thus visual acuity decreases. The optic disc which appears as a pale pink/whitish area is present 3 mm medial to the central of the macula. All the axons of retinal ganglion cells form optic nerve, which exits from the eye through the optic disc. Optic nerve fibers are not myelinated in the intraocular portion. This area from where optic nerve exits lacks photoreceptors and hence is known as the blind spot (Bron ,Tripathi *et al.*, 1997; Anathony J. Bron *et al.*1997). Detailed descriptions of different parts of eye are shown in Figure 1.1.

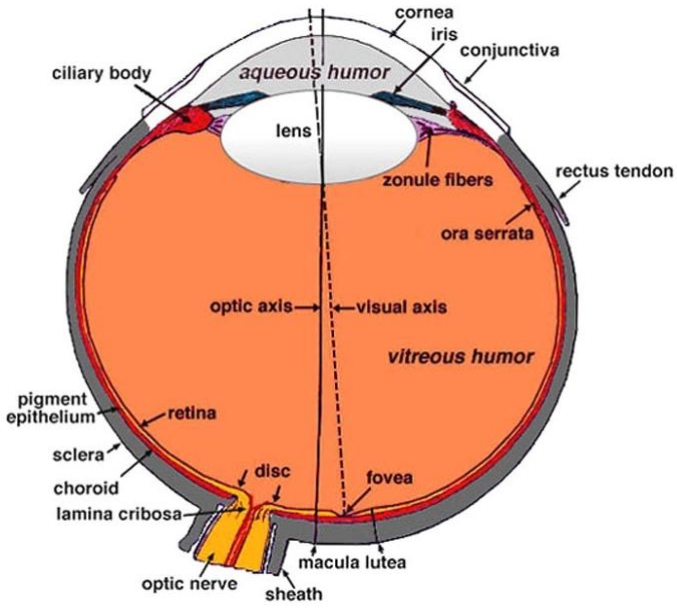

Figure- 1.1: Anatomy of the eye.

[Source -http://www.ncbi.nlm.nih.gov/books/NBK11534/figure/A11]

1.2 Development of the retina

The development of the retina is a complex and orderly designed process**.** Prenatal development of the eye can be divided into 3 major periods-embryogenesis, organogenesis and retinal differentiation (retinogenesis).

1.2.1 Embryogenesis

Development of the embryo involves mitotic subdivisions and formation of two groups of cells- the peripheral outer cell mass (trophoblast) and the inner cell mass (embryoblast). The trophoblast forms the placenta, whereas the embryoblast divides and forms the epiblast and hypoblast. At the beginning of 3rd week, cells of epiblast in the medial region of the embryonic disc form the primitive streak. Proliferation and migration of these cells results in the formation of three primary germinal layers- the ectoderm, mesoderm and endoderm. The anterior end of the primitive streak forms the notochord and induces the overlying ectoderm to differentiate as neuroectoderm. These cells proliferate and thicken to form a curved ridge called neural plate. During

cleavage stage, a subset of pluripotent embryonic cells become competent precursors to form retina. A specific set of cells of this lineage becomes retinal stem cell (RSCs) and form the eye field at the anterior end of the neural plate (Zaghloul, Yan *et al*. 2005).

1.2.2 Organogenesis

Formation of the primitive eye begins in the 4^{th} week. Initially the eye appears as a single field which is located in the center of the anterior neural plate. During neural plate maturation, the RSCs separate into right and left optic primordial. During neural tube morphogenesis, each optic primordium gives rise to an optic vesicle. Folding of the optic vesicles result in the formation of optic cup and stalk. By the end of the embryonic period (8^{th} week), the retina is differentiated into presumptive neural retina (PNR) and retinal pigment epithelium (RPE). The space between the two layers of the optic cup is called the subretinal space. The proximal region gives rise to presumptive ventral optic stalk (POS). Neural retina contains retinal progenitor cells (RPCs) which give rise to differentiated cell types of retina (Figure 1.2) (Duke-Elder 1963; Anathony J. Bron 1997; Zaghloul, Yan *et al*. 2005).

1.2.3 Retinogenesis

The formation of different retinal cell layers is called retinogenesis. All retinal cells are derived from a common population of multipotent retinal progenitor cells (RPCs) located in the inner neuroepithelium of the optic cup. RPCs form several different specialised cells: photoreceptors (rods and cones), horizontal, bipolar, amacrine, muller and ganglion cells. Cell differentiation starts in a wave-like manner and is initiated in the inner layer of the central optic cup and progresses concentrically towards the peripheral edges of the retina.

The most characteristic feature of retinogenesis is a relatively fixed chronological sequence. The various types of retinal cells are not produced at a time, by the progenitor cells. One type of cells induces the progenitor cells to make next cell type. Retinal ganglion cells are generated first, followed in overlapping phases by horizontal cells, cone photoreceptor, amacrine, rod photoreceptor, bipolar cells and

finally muller glial cells (Heavner, Pevny, 2012) (Figure 1.3). Thus the process of photoreceptor development can be divided into five major steps which are: 1) proliferation of multipotent RPCs, 2) restriction of the competence of RPCs, 3) cell fate specification and commitment to a neural cell precursors, 4) expression of cell specific genes, 5) axonal growth and synapse formation. Retinogenesis is controlled by both intrinsic as well as extrinsic factors (Duke-Elder 1963; Anathony J. Bron 1997; Chow and Lang 2001).

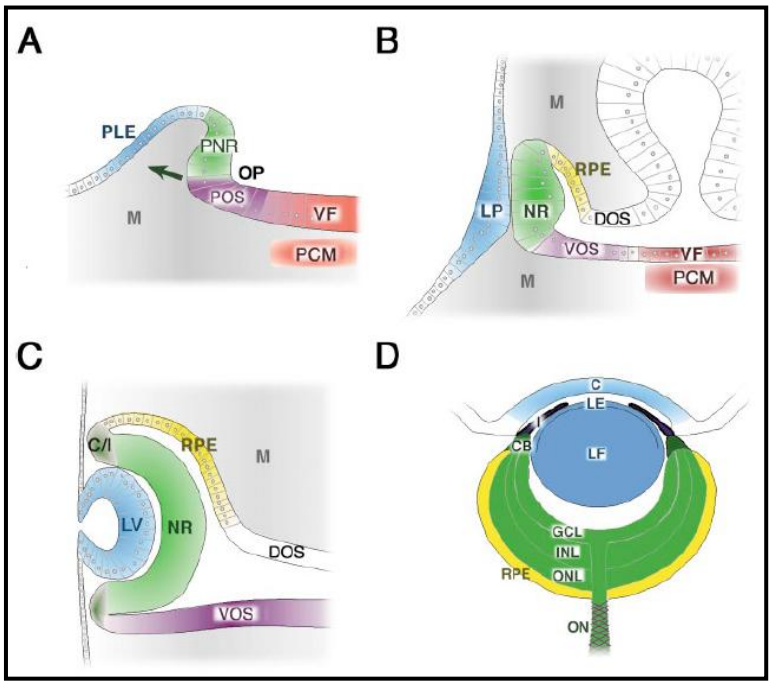

Figure 1.2: Different stages of eye development humans.

[Figure is inserted with permission from (Chow and Lang 2001)].

A) Formation of optic vesicles, B) Formation of lens placode, C) Formation of lens vesicle and optic cup, D) Establishment of the overall structure of the eye.

CB-ciliary body, C/I-ciliary body and iris, C-cornea, DOS-dorsal optic stalk, GCL-ganglion cell layer, INL- inner nuclear layer, LE-lens epithelium, LF- lens fiber cells, LP- lens placode, LV- lens vesicle, M- mesenchyme, NR-neural retina, ONL- outer nuclear layer, ON-optic nerve, PCM- prechordal mesoderm, PLE- presumptive lens ectoderm, PNR-presumptive neural retina, POS- presumptive ventral optic stalk, RPE-retinal pigmented epithelium, VF-ventral forebrain, VOS-ventral optic stalk.

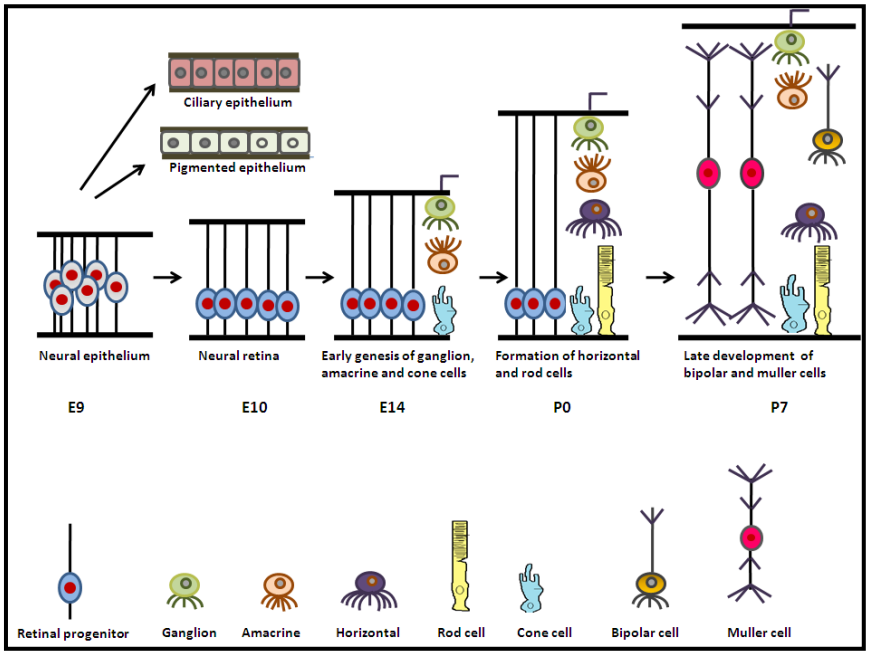

Figure 1.3: Different stages of retinogenesis.

[Figure is adapted from (Heavner and Pevny 2012)].

1.3 Histology of retina

The neural retina consists of several cell types including six major types of neural cells -photoreceptors, bipolar cells, horizontal cells, amacrine cells, ganglion cells and the muller glial cells. The retina is organized into a 10- layered structure (Figure-1.4). From the outer retina to inner, these layers are present in the following order:

1) Retinal pigment epithelium (RPE)

2) Layer of rods and cones: consists of photoreceptor cells.

3) Outer limiting membrane: formed by continuous band of junctional complexes between muller cells as well as between muller cells and photoreceptor cells.

4) Outer nuclear layer (ONL): containing the nuclei of the photoreceptor cells.

5) Outer plexiform layer (OPL): made up of the synapses of photoreceptors with bipolar, amacrine and horizontal cells.

6) Inner nuclear layer (INL): containing the nuclei of muller glial cells, bipolar cells, amacrine and horizontal cells.

7) Inner plexiform layer (IPL): formed by synapses between bipolar, horizontal and amacrine cells with retinal ganglion cells.

8) Ganglion cell layer: consisting of nuclei of the retinal ganglion cells (RGCs).

9) Nerve fiber layer: made up of axons of the retinal ganglion cells leading to the optic nerve.

10) Internal limiting membrane: formed by the enlarged and flattened innermost processes of muller cells.

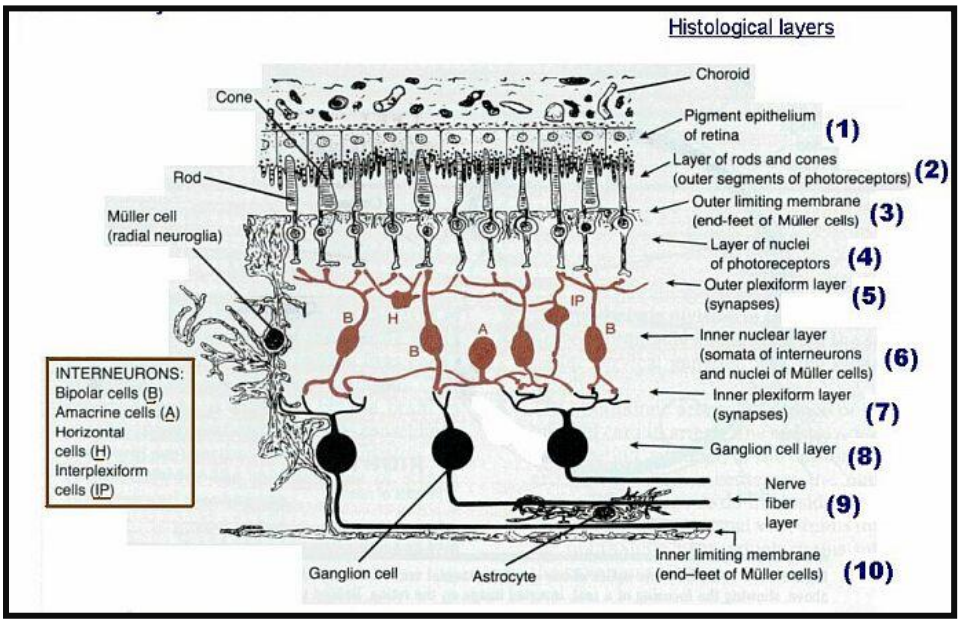

Figure-1.4: Diagrammatic representation of the organisation of the retina showing the different retinal layers.

[Source- http://instruct.uwo.ca/anatomy/530/retina.jpg].

1.4 Cellular organization of retina

The major cellular components of retina are the retinal pigmented epithelial cells, photoreceptors, horizontal cells, bipolar cells, amacrine cells and ganglion cells.

1.4.1 Retinal pigment epithelium (RPE)

The RPE is the outermost layer of the retina. It consists of a monolayer of hexagonal pigmented cells. There are ~3.5 million RPE cells in the human retina. RPE cells have highest cell density in the central retina (fovea-5000 cells/mm^2) and their number reduces towards periphery (2000 cells/mm^2). The RPE performs diverse functions: (a) absorption of light and protection against photo-oxidative damage with the help of melanin, (b) regeneration of all-*cis*-retinal, (c) phagocytosis of shedded photoreceptor outer segments, (d) uptake, processing, storage and release of vitamin A, (e) transport of nutrients, ions, and water, (f) secretion of various essential growth factors (PEDF, VEGF, FGF-1, FGF-2, and FGF-5, IGF-I, TGF-β) for maintaining the structural integrity of the retina (Gabriele Thumann 1998; Simo, Villarroel *et al*. 2010).

1.4.2 Photoreceptors

Photoreceptor cells are of two types-cones and rods. Cones are very densely packed in the fovea, but their density drops rapidly towards the periphery of retina. Rods are absent in the fovea, but their density is maximum towards the periphery of retina. Each photoreceptor consists of an outer segment, inner segment, a cell body and the synaptic terminal. Outer segment of photoreceptor have membranous discs which contain photopigments and other phototransduction proteins. The inner segment contains the protein synthesis (endoplasmic reticulum, golgi body) and metabolic machinery (mitochondria, nucleus). The cilium connects the inner segment to the outer segment and is involved in transport of proteins from inner segment to outer

segment (Figure-1.5). Rods and cones differ from each other in their shape, type of photopigment, retinal distribution and pattern of synaptic connections.

1.4.2.1 Rod cells: Rods are responsible for scotopic (dim light or night) vision. The number of rods is approximately 77–107 million. Rods are extremely sensitive to light but have low spatial resolution. The longer outer segment (OS) of rods is composed of individual discs. The number of discs varies from 600-1000 per rod (Bron AJ 1997). Disc membranes form by evagination of the plasma membrane. Old discs are continually shedded from the ends and are replaced by new discs at the base of the outer segments. These discs contain 90% of the visual pigment (rhodopsin) in rod while the remaining visual pigment is scattered on the surface of plasma membrane. Rhodopsin is composed of a chromophore (11-*cis*-retinal) and a protein moiety (rhodopsin). Many rods form synaptic connections with a single rod bipolar cell. Further many rod bipolar cells contact a single amacrine cell. Thus the degree of convergence is high. Rods can detect a single photon but have slow response to dim light and saturate quickly. These characteristics make rods suitable for scotopic vision.

1.4.2.2 Cone cells: Cones are responsible for fine details and colour vision. The number of cones is ~4 to 5 million (Bron AJ 1997). Cones show very fast response in dim light and do not saturate even in high light intensity. These properties make cones suitable for photopic vision. The outer segment of cones consists of series of discs, which are attached to each other as well as to the surface of plasma membrane. Humans have three types of cones with varying sensitivity towards light spectrum - long wavelength cones (L or red; peak sensitivity at 564 nm), medium wavelength cones (M or green; peak sensitivity at 533 nm), and short wavelength cones (S or blue; peak sensitivity at 437 nm). The S cone population is much smaller than those of the L and M cones (only 5-10 % of the total cone population). The L and M type cone cells are randomly intermixed with ~2 times more L cones than M cones. S cones are totally absent in the foveal area but concentration of M and L cones is high in this region (Mustafi, Engel *et al*. 2009).

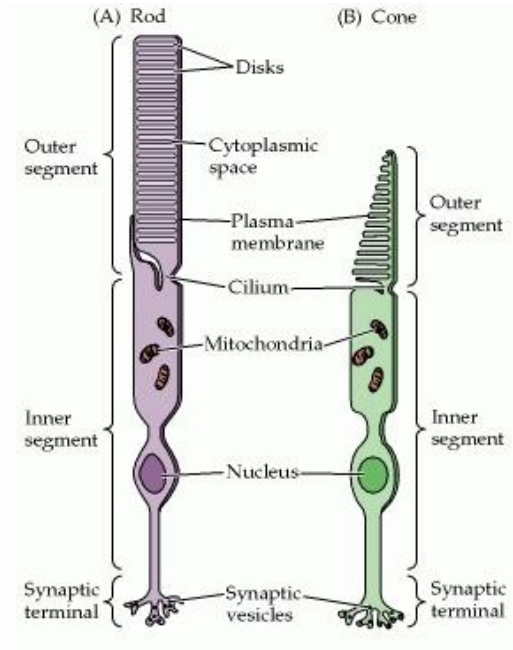

Figure-1.5: Structure of rod and cone photoreceptor

[Source-http://www.ncbi.nlm.nih.gov/books/NBK10850/bin/ch11f8.gif]

1.4.3 Muller cells

These are the principal glial cells of the retina. These cells extend from the outer limiting membrane to the inner limiting membrane. Retinal neurons are nourished by these cells. Muller cells control the homeostasis by mediating the intracellular transport of ions, water and bicarbonates. They are also protects the neurons by taking up excess neurotransmitters and clearing waste products like carbon dioxide and ammonia (Bringmann, Pannicke *et al*. 2006).

1.4.4 Bipolar Cells

Bipolar cells (BCs) receive direct input from the photoreceptors and indirect input from the horizontal cells and pass it on to the ganglion cells directly or indirectly (via amacrine cells). Cones send signals through two parallel pathways, ON and OFF pathways. The ON bipolar cells become depolarized due to decrease in glutamate release during light phase. This results in increased neurotransmitter release by bipolar cells. The reverse is true for OFF bipolar cells. All rod bipolar cells are ON bipolar cells. Bipolar cells are classified according to their anatomic features (Diffuse, Midget & S-cone bipolar cells) and whether they contact rods or cones. Bipolar cells

branch at different levels in inner plexiform layer. The ON bipolar cells have axon terminals in the inner half of the IPL (ON sub lamina) whereas the axons of OFF bipolar cells terminate in the outer half of IPL (OFF sublamina) (Masland 2001).

1.4.5 Amacrine cells

Amacrine cells are interneurons that are present in the inner nuclear layer of the vertebrate retina. Amacrine cells make synapses with bipolar cells, ganglion cells and other amacrine cells. Almost 40 different amacrine cells are known which are classified based on 1) width of the receptive field, 2) location in stratum in IPL, 3) type of neurotransmitter (GABA, glycine or both). These cells are involved in the processing of retinal images, specifically adjustment of image brightness and detecting motion. (Lagnado 1998).

1.4.6 Horizontal cells

Horizontal cells (HC) are lateral inter neurons in the outer retina. There are three different types of horizontal cells in the human retina -HI, HII & HIII. These cells form synapses with all three types of cones. Horizontal cells are not colour selective, but they are differentiated based on the relative inputs they receive from three cone classes.

Dendritic processes of horizontal cells are interconnected with the axon terminals of the one or more photoreceptors to receive inputs. On the other side they contact with bipolar cells that are innervated directly. These cells provide a negative feed-back signal to photoreceptors. In darkness, horizontal cells are depolarized by the release of glutamate from photoreceptors and releases of the inhibitory neurotransmitter GABA (γ-arninobutyric acid). GABA in turn hyperpolarizes the center photoreceptors. Hyperpolarization of the photoreceptors prevents the release of glutamate and thus forming negative feedback. The combined signal from the photoreceptors and the horizontal cells is sent to the bipolar cells (Wu 1992; Kamermans and Spekreijse 1999).

1.4.7 Ganglion cells

Ganglion cells receive visual inputs from the photoreceptors via the bipolar, amacrine and horizontal cells. The receptive field of ganglion cells is organized as concentric circles. In the human retina two main type of ganglion cells are present-ON center and OFF center. ON-center ganglion cells are activated when a spot of light falls in the center of their receptive field and are inactivated when light falls on the field's periphery. OFF-center ganglion cells react in the opposite way. Ganglion cells can also be broadly divided into three major categories -Midget, Parasol and Bistratified ganglion cells based on their axon projection and function (Lee, Martin *et al*. 2010).

1.5 The mechanism of visual perception in retina

Vision perception by human eye starts with the conversion of light into electrical signals, processing by the retinal cells and transfer of this information to the brain. This process consists of phototransduction, visual cycle and synaptic transmission and information processing.

1.5.1. Phototransduction

Vision is brought about by the retina through the actions of photoreceptors which convert light energy into neuronal impulses through phototransduction. This process takes place in the outer segments of rods and cones. Phototransduction can be divided into three phases- light phase (A-C; Figure 1.6), cGMP restoration or restoration of dark phase (D; Figure 1.6) and deactivation of photo-transduction cascade (E; Figure 1.6). Visual pigments are regenerated by visual cycle (F-H; Figure 1.6).

1.5.1.1 Light phase

Photoreceptors contain rhodopsin (rods) or other opsins (cones) which are photon capturing molecules. In its inactive ground state, the opsin apoprotein is covalently attached to a light-sensitive chromophore (11-*cis*-retinal). Upon absorbing a photon, rhodopsin is activated to meta-rhodopsin II or R* with the photochemical isomerization of 11-*cis*-retinal to all-*trans*-retinal which dissociates from metarhodopsin.

Activated rhodopsin (R*) activates the G protein transducin (T) by catalyzing GDP/GTP exchange. Transducin is a G protein consisting of -α, β and γ subunits. At this stage the signal is amplified as a single rhodopsin molecule can activate >800 transducin molecules per second (Leskov, Klenchin *et al*. 2000). The activated transducin in turn activates cGMP-phosphodiesterase (PDE). PDE consists of two catalytic subunits (α and β) and two inhibitory subunits (γ). One molecule of activated transducin activates only one molecule of PDE by binding to inhibitory γ subunits and releasing the catalytic subunits. This leads to the hydrolysis of cyclic guanosine monophosphate (cGMP) to 5'GMP. One activated PDE can convert approximately 6 cGMP molecules to GMP (Leskov, Klenchin *et al*. 2000).

Outer segment contains cGMP-gated ion channels and Na^+-K^+ pump and inner segment contains $Na^+/Ca^{2+}K^+$ exchanger channels. In the dark state cGMP-gated ion channels actively transport cations (Na^+ and Ca^{2+}) into the outer segment from extracellular space. $Na^+/Ca^{2+}K^+$ exchanger channels are responsible for continuous influx of Na^+ and efflux of Ca^{2+} and K^+ from the inner segment. This process establishes an inward current (the "dark" current of -40mV) that depolarizes the membrane and results in continuous release of the neurotransmitter glutamate. During the light phase, hydrolysis of cGMP results in reduction in cGMP levels leading to the closure of cGMP-gated cation channels (CNCG). This causes reduction in Na^+ and Ca^{2+} levels in outer segment, hyperpolarization of the cell plasma membrane and reduced neurotransmitter secretion (Pugh and Lamb 1993; Jindrova 1998).

1.5.1.2 cGMP re-synthesis

Light-induced reduction of intracellular calcium levels activates guanylate cyclase-activating proteins (GCAPs). These Ca^{2+}-binding proteins rapidly stimulate guanylate cyclase (ret GC1) enzyme to catalyze cGMP synthesis**.** Restoration of cGMP levels leads to the reopening of the cGMP-gated channels and influx of calcium that leads to restoration of the dark state (Miller, Picones *et al*. 1994; Burns and Arshavsky 2005; Lamb and Pugh 2006).

1.5.1.3 Deactivation of photo-transduction cascade

All the activated intermediates (R*, Gα–GTP or G* and PDE*) have to be deactivated to restore their native states. Decline in Ca^{2+} concentration helps in the photoreceptor regeneration. Deactivation of activated rhodopsin (R*) starts with its phosphorylation by rhodopsin kinase (RK). During the light phase, recoverin (Rec; a C^{a2+}-binding protein) binds with rhodopsin kinase and inhibits its activity. In the dark, when intracellular calcium level goes down, recoverin is released from rhodopsin kinase which in turn deactivates the R*. Inactivation of R* is completed by the binding of arrestin (Arr) to the phosphorylated rhodopsin. This prevents the further activation of transducin. Arrestin also promotes the separation of all-*trans*-retinal from opsin. All-*trans*-retinal diffuses into the cytosol of the photoreceptor outer segment. The inactivation of active transducin (Gα–GTP) is achieved by the hydrolysis of bound GTP to GDP by GTPase-activating-protein (GAP) complex. This complex consists of Regulator of G-protein signalling 9 (RGS9), RGS9-anchoring protein (R9AP), an orphan $_{G\beta}$ subunit ($_{G\beta5}$) and PDE. Transducin Gα–GDP then re-associates with the βγ subunits to form native transducin. Dissociation of Gα–GDP from PDE leads to the binding of inhibitory γ subunits of PDE with the catalytic αβ subunits to keep it in an inactive state (Jindrova 1998; Burns and Arshavsky 2005).

1.5.2. Retinoid or Visual cycle

To regenerate rhodopsin, all-*trans*-retinal must be converted back to 11-*cis*-retinal and reattached to opsin. The regeneration of 11-*cis*-retinal can occur either by all-*trans*-retinol present in the choroidal circulation or by regeneration of 11-*cis*- retinal by the visual cycle in the RPE. During visual cycle, all-*trans*-retinal is released from rhodopsin in the rod outer segments. All-trans-retinal is highly reactive and short lived in photoreceptors. It is transported with the help of membrane lipid phosphatidylethanolamine (PE) to the cytoplasm of photoreceptors by ATP binding cassette transporter gene (*ABCA4*) where it is converted into all-*trans*-retinol by retinol dehydrogenase 12 (RDH12). Interphotoreceptor retinoid-binding proteins (IRBPs) help in the transportation of all-*trans*-retinol from the interphotoreceptor matrix into RPE cells.

Inside the RPE, all-*trans* retinol is recognized by cellular retinoid binding proteins (CRBP), which are highly specific for binding to all-*trans*-retinol in comparison to other isomers such as 11-*cis*-retinol. Lecithin retinol acyltransferase (LRAT) catalyzes *trans*-esterification of all-*trans*-retinol and forms all-*trans*-retinyl esters which are further isomerised and hydrolyzed to 11-*cis*-retinol by the isomerohydrolase activity of RPE65(Moiseyev, Chen *et al*. 2005). Cellular retinaldehyde-binding protein (CRalBP) binds to 11-*cis*-retinol (Rando 2001; Lamb and Pugh 2004). In its bound state, retinol dehydrogenase 5 (RDH5) converts 11-*cis*-retinol to 11-*cis*-retinal which is transported back to the photoreceptor outer segment by IRBP. In the rod outer segment, 11-*cis* retinal binds to opsin apoprotein and regenerates rhodopsin (Carlson and Bok 1992; Simon, Romert *et al*. 1999).

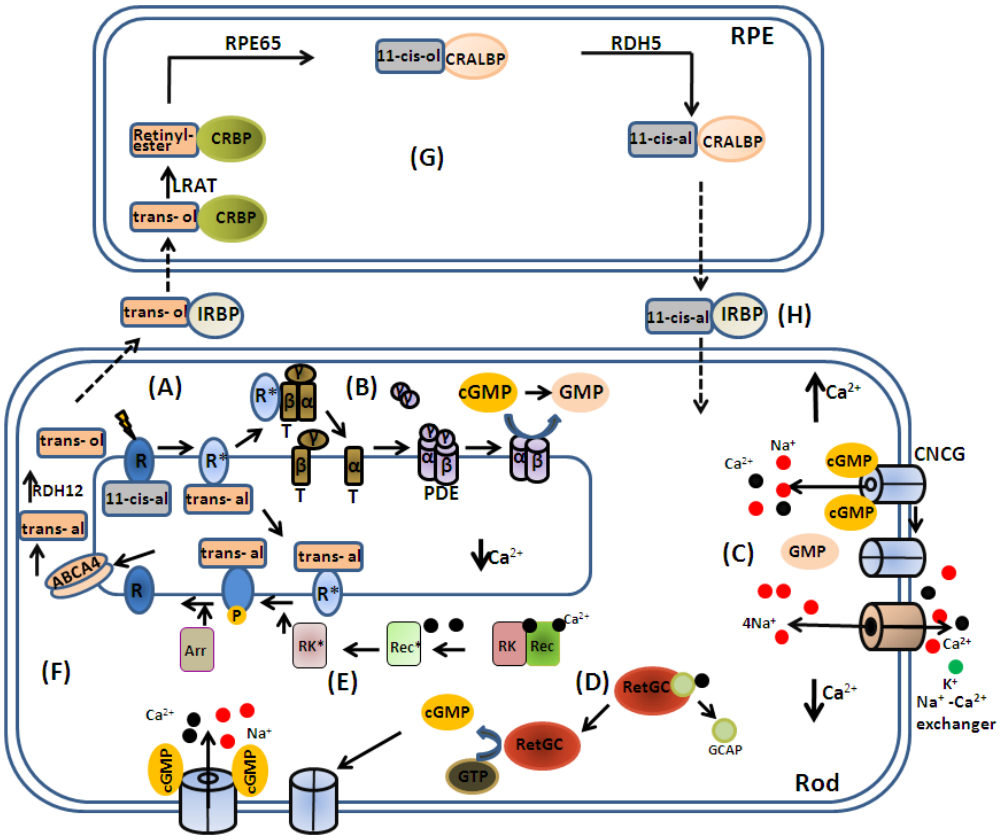

Figure-1.6: Schematic diagram of the different stages of phototransduction cascade and visual cycle in vertebrate photoreceptors

[Figure is adapted from (Smith, Bainbridge *et al*. 2009)]

11-*cis*-retinal (11-*cis*-al), 11-*trans*-retinol (11-*trans*-ol), arrestin (Arr), CRBP - cellular retinoid-binding protein, CRALBP – cellular retinaldehyde-binding protein, guanylyl cyclase activating protein (GCAP), guanylyl cyclase (GC), interphotoreceptor retinoid-binding proteins (IRBP), PDE- phosphodiesterase, R-rhodopsin, R*-activated rhodopsin, recoverin (Rec), rhodopsin kinase (RK), retinal pigment epithelium (RPE), T-transducin.

1.5.2.1 Difference between retinoid cycle in rods and cones of vertebrate retina

Despite having similar phototransduction and visual cycle components, rods and cones have different pigment regeneration pathways. In cones this regeneration involves the muller cells instead of RPE cells as in the case of rods (Mata, Radu *et al*. 2002). In cone cells, the released all-*trans*-retinol is absorbed by Muller cells and converted to 11-*cis*-retinol by all-*trans*-retinol isomerase enzyme. A novel cone-specific 11-*cis* retinyl ester (11*c*RE) synthase catalyzes the esterification of 11-*cis* retinol to 11-cis-retinyl ester. (Mata, Radu *et al*. 2002). Retinyl ester hydrolase (REH) converts 11-cis-retinyl ester into 11-*cis*-retinol which is which is released by the Müller cell and with the help of IRBP enters in the cones. 11-*cis*-retinol is converted to 11-*cis* retinal by a cone specific 11-*cis*-retinol dehydrogenase (11*c*RDH). 11-*cis* retinal combines with apo-opsin to regenerate cone opsin pigment (Rando 2001; Arshavsky 2002; Mata, Radu *et al*. 2002). The different retinoid cycles of rods and cones are presented in Figure 1.7.

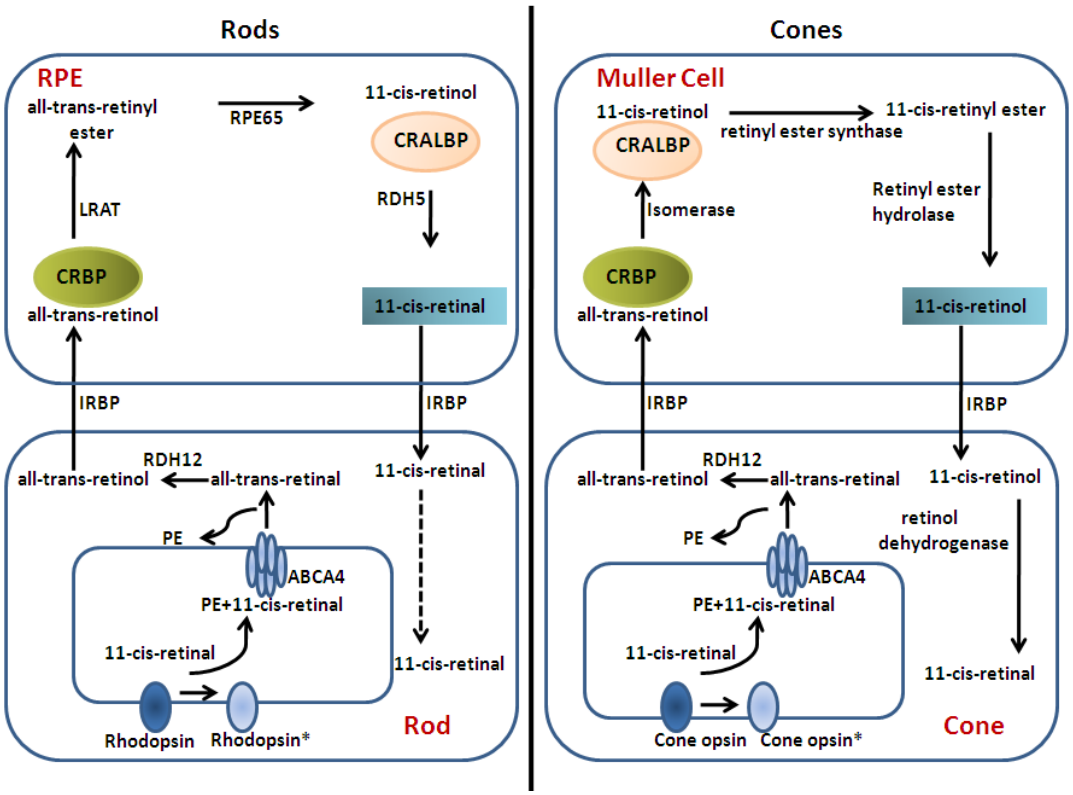

Figure-1.7: Retinoid cycle in rod and cones.

[Figure is adapted from Arshavsky (2002)].

1.5.3 Information processing in the retina

Visual signals received by the retina are transmitted as neuronal impulses from photoreceptors to higher order retinal neurons and finally to the brain through a complex network of synapses. Rods and cones form pre-synaptic connections with different second order retinal neurons-horizontal cells, amacrine cells and bipolar cells and finally transmit these signals to ganglion cells. These cells transmit the signal to the brain either via a direct pathway or a lateral pathway (Masland 2001).

Photoreceptors form complex multiple interconnected circuits. At the foveal region a one-to-one vertical pathway is present where one photoreceptor makes synaptic contact with a bipolar cell which in turn passes this signal to a ganglion cell. In the area surrounding the fovea, divergent wiring occurs where a single cone is divided into many signals and conveyed to contacts with many bipolar cells, which in turn make contact with ganglion cells. Thus many ganglion cells get information

originating from a single cone. Towards the peripheral area, convergent wiring is present, where each ganglion cell collects signals originating from many photoreceptors. Lateral interactions mediated by horizontal and amacrine cells, help to integrate information from different parts of retina. Lateral pathways modify and control the signal that passes through the direct pathway

1.6 Retinal dystrophies

Retinal dystrophies are a group of hereditary disorders characterized by degeneration of the RPE and/or photoreceptor cells. They are genetically and clinically heterogeneous disorders. Till date, 261 retinal disease loci/genes have been identified (http://www.sph.uth.tmc.edu/RetNet/).

Retinal dystrophies can be classified on the basis of the primary site of retinal dysfunction (rods, cones, RPE or whether the central retina or peripheral retina is affected), the age of onset, rate of progression, syndromic or non-syndromic and the mode of inheritance (Figure 1.8).

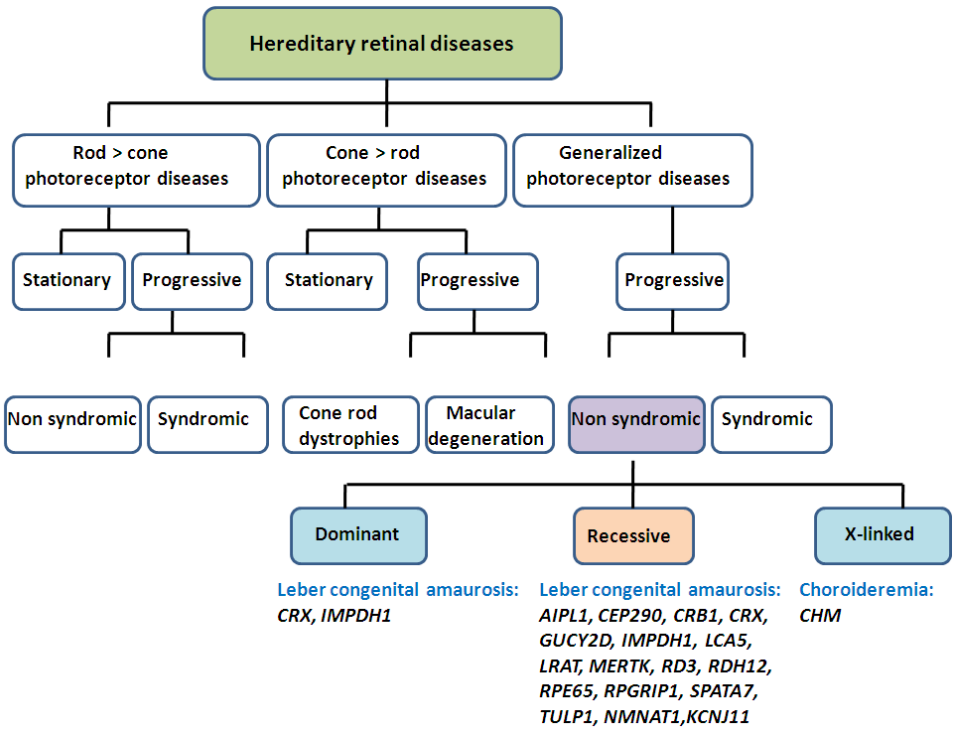

Figure 1.8: Classification of monogenic hereditary retinal diseases

The classification is based on photoreceptor cell type or structures affected by the disease and on the basis of other characteristics such as stationary versus progressive nature, syndromic vs non-syndromic. [Figure is Adapted from (Berger, Kloeckener-Gruissem *et al*. 2010)]

1.6.1 Leber Congenital Amaurosis

Leber congenital amaurosis (LCA) is most severe form of retinal dystrophy. It was first described in 1869 by the German ophthalmologist Theodor Leber as *tapetoretinale Degeneration mit Amblyopie* which belonged to retinitis pigmentosa (RP) group.Severe vision loss at or near birth, amaurotic pupils, wandering nystagmus and a pigmentary retinopathy were the most characteristic clinical features documented. Franceschetti and Dieterle in 1954, reported the presence of severely reduced or non-detectable ERG early in the disease (Franceschetti and Dieterle 1954). LCA is mostly autosomal recessive in inheritance as first observed by Alstom and Olson in 1957 (Alstrom CH 1957). However, autosomal dominant (AD) LCA has also been reported though it appears to be rare (Sohocki, Sullivan *et al*. 1998).

LCA accounts for ≥5% of all inherited retinopathies with the disease prevalence of 1/30,000 - 1/81,000 as reported in mainly in Western populations (Stone 2007; Kaplan 2008). Currently used diagnostic criteria for LCA was proposed by De Laey in 1991 which is as follows-

1. Onset of blindness or poor vision (appearing early in the first year of life, before 6 months of age.
2. Sluggish pupillary reaction.
3. Roving eye movements/nystagmus.
4. Oculo-digital signs (eye-poking and eye rubbing).
5. Extinguished or severely reduced electroretinogram **(**ERGs).
6. Absent or abnormal visually evoked potential (VEPs).
7. Variable fundus appearance (normal, marbled fundus, bone spicule pigmentation, salt and pepper and macular coloboma etc).

Apart from these ocular symptoms, other associated ocular signs include: cataract, keratoconus and more frequently, enophthalmos. Mostly LCA patients are hyperopic but myopic cases are also known. Oculodigital signs (eye poking, rubbing) are often characteristic of LCA and may lead to keratoconous, infection and enophthalmos. These patients also experience photophobia and difficulty in focusing. Other clinical findings such as neuro-developmental delay, hearing impairment, mental retardation and associated systemic anomalies may also be present (Janaky, Deak *et al*. 1994).

Visual acuity ranges from light perception (LP) to a visual acuity of 20/400 in LCA patients. Longitudinal studies on the pattern of visual acuity changes indicated that visual acuity deteriorates only in 15% patients where as in 75% of cases it remains stable (Walia, Fishman, *et al*.2010). The fundus may appear normal or show abnormalities such as attenuation of retinal vessels, atrophy of RPE, salt and pepper pigmentation, preserved para-arteriolar RPE (PPRPE), Coat's reaction, keratoconous, white retinal spots, maculopathy and bone spicule pigmentation (Chung and Traboulsi 2009).

Many patients with non-syndromic and syndromic ocular diseases may present with ''LCA-like ocular phenotypes" which can overlap with LCA. Non-syndromic LCA can be distinguished from other retinal degeneration disorders through detailed evaluation combined with (mostly) an autosomal recessive (AR) inheritance pattern. Syndromic disorders associated with LCA can be diagnosed on the basis of associated systemic defects (Koenekoop, Lopez, *et al*. 2007).

1.6.1.1 Genetics of LCA

Advances in the molecular genetics of LCA have progressed rapidly since the mapping and identification of the first locus (LCA1) in the year 1995 (Camuzat, Dollfus *et al*. 1995). In a span of one and a half decades, 21 genes known to be associated with LCA were identified using various approaches like classical linkage mapping or identity-by-descent (IBD) mapping. Few genes were discovered using candidate genes approach on the basis of their preferential expression in the retina or associated retinal function or their involvement in retinal degeneration in animal

models. Recently novel LCA genes have been added to this list using SNP microarrays and exome sequencing approaches as mentioned in Table 1.1.

Frequencies of mutations in LCA genes range from rare causes of disease like *RD3*, *LRAT* and *MERTK* to very high frequency of mutations for *NMNAT1*, *GUCY2D* and *CRB1* as given in Table 1 (Appendix).

The most frequently mutated gene known till date is *CEP290* with a mutation frequency in some Caucasian populations of ~20-30% of cases (Coppieters, Casteels *et al.* 2010; Perrault, Delphin *et al.* 2007).

The *KCNJ13*, *MYO7A*, *CNGA3*, and *ALMS1* genes are reported till date in one study each (Sergouniotis, Davidson *et al.* 2011; Wang, Wang *et al.* 2011) and hence their mutation frequencies as shown, may not be reliable.

There are variations in the overall frequency of mutations between different studies as shown in Figure 1.9. Screening in a Saudi Arabian patient population revealed about 24% of cases to have mutations when 13 of the LCA genes were tested (Li, Wang *et al*. 2009). In a study in Chinese patients with LCA, 50% of patients had mutations when 15 genes were tested, but the percentage of patients with at least 2 mutant alleles was less than 50%. In Chinese patients, *GUCY2D* (16.1%) was the major cause of LCA cases followed by *CRB1* (11.5%) (Li, Xiao *et al*. 2011). A smaller study in Korean patients covering 9 genes found mutations in 3/20 cases (15%) (Seong, Kim *et al*. 2008). A survey of most common 784 variations present in 15 genes responsible for LCA using LCA chip, showed mutations in 11 /30 (36%) cases of Indian origin, where *RPE65* (16.6) and *GUCY2D*(10%) accounted for majority of cases(Verma, Perumalsamy *et al*. 2013). Similarly screening of Belgium patients with using LCA chip for 8 genes revealed mutations in 69% patients, with highest frequency of *CEP290* gene (30%) (Coppieters, Casteels *et al*. 2010). Screening of 8 most common disease causing LCA genes using Microarray chip identified mutations in 28% (27/95) and 30% (13/42) of Italian and Spanish patients respectively. *CRB1* (23%) accounted for the majority of cases in Spanish cohort where as the mutation frequency of *RPE65* (8.4%) was highest followed by *CRB1* (7.4%) in the Italian cohort. (Simonelli, Ziviello *et al*. 2007; Vallespin, Cantalapiedra *et al*. 2007). Mutations were

reported in 61% (14/23) families of Pakistani origin using microarray and direct sequencing (McKibbin, Ali *et al*. 2010).

Thus frequencies of mutations in specific genes can be a useful guide to prioritize efforts at developing therapies that can target larger numbers of patients in a particular population.

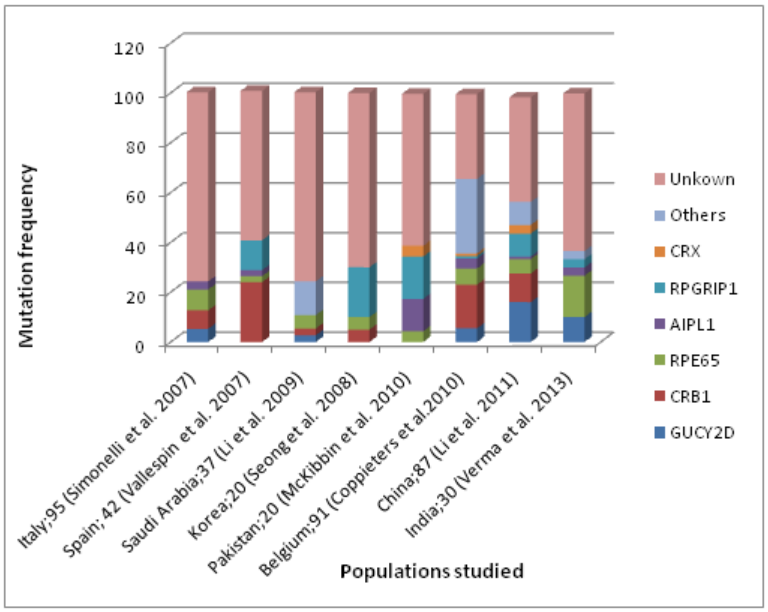

Figure 1.9: Relative mutation frequencies of LCA associated genes found in different ethnic groups

The frequency of mutations (%) in LCA associated genes in different populations; the number of probands and reference (in bracket) are shown.

1.6.1.2 Genotype-phenotype correlations

LCA patients show considerable heterogeneity in phenotypes. Variable features that are exhibited by LCA patients include eye poking behaviour, cataract, keratoconus, hyperopia and myopia. Hearing impairment and possible developmental delay have also been reported. Clinical heterogeneity can be seen in fundus appearance, sensitivity towards light and refractive error. Some patients have normal fundus appearance, but others exhibits abnormalities in the form of attenuation of retinal vessels, atrophy of RPE, salt and pepper pigmentation, preserved para-arteriolar RPE

(PPRPE), Coat's reaction, white retinal spots, macular coloboma and bone spicule pigmentation. Visual acuity in LCA patients can range from 20/200 to only light perception (Kaplan, 2008; Hanein, Perrault, *et al.* 2004; Dharmaraj, Silva, *et al.* 2000).

Evaluation of patients having LCA associated with mutations in different genes has suggested gene-specific patterns in phenotypes although there is considerable degree of variation between individuals and overlaps between different genes (Dharmaraj, Silva *et al*. 2000; Hanein, Perrault *et al*. 2004; Kaplan 2008).

Presence of measurable visual acuity and nyctalopia is associated with *RPE65* gene mutation while poor vision, lack of nyctalopia and normal appearing fundus are associated with mutations in *GUCY2D*. (Dharmaraj, Silva *et al*. 2000; Galvin, Fishman *et al*. 2005). Visual acuities (VA) of patients with *RPE65* mutations may vary from mild, moderate or severe loss of VA in the first 3 decades, with worsening after the 3rd decade (Walia, Fishman *et al*.2010). The retinas of *GUCY2D*-LCA patients show preservation of retinal layers and organization comparable with normal individuals as showed by macular imaging with spectral domain optical coherence tomography (SD-OCT) (Pasadhika, Fishman *et al*. 2010). Pigmentary retinopathy of varying degrees and progressive decline in visual acuities with increasing age is a feature of *RDH12* mutations, although patients are found to have useful levels of visual acuity during childhood (Schuster, Janecke *et al*. 2007). Maculopathy is found to be a predominant feature of *AIPL1*-LCA. *RPGRIP1* patients have severe loss of vision from early infancy (Dharmaraj, Leroy *et al.* 2004; McKibbin, Ali *et al.* 2010).

The presence of preserved para-arteriolar retinal pigment epithelium (PPRPE), Coat's like exudative vasculopathy and thick retina with abnormal lamination pattern are usually associated with *CRB1* gene mutations apart from nummular pigmentation especially in later ages, macular atrophy and hyperopia (Jacobson, Cideciyan *et al.* 2003; McKay, Clarke *et al.* 2005; Henderson, Mackay *et al.* 2011).

In case of *CEP290*, patients have severe but stable vision loss (Galvin, Fishman *et al.* 2005; Chung and Traboulsi 2009). VA of counting fingers or less was found in *CEP290* cases with an early decline of vision (Perrault, Delphin *et al.* 2007; Walia,

Fishman *et al*. 2010). Patients with *CEP290* mutations are found to have sparing of the macular area on gross retinal examination, with marbleized fundus in the first decade and retinal atrophy in later stages (Coppieters, Casteels *et al.* 2010). Preservation of photoreceptors in the foveal and macular regions has also been detected on OCT in these patients (Pasadhika, Fishman *et al*.2010).

1.6.1.3 Molecular diagnosis of LCA

Molecular diagnosis involves determining the underlying disease-associated gene mutations that can aid in counselling and recruitment of cases for prospective therapies. Though no therapeutic options are available for LCA except for gene replacement therapy for the *RPE65* gene, which is in process of phase III clinical trials (Bainbridge, Smith *et al.* 2008; Hauswirth, Aleman *et al.* 2008; Maguire, Simonelli, *et al.* 2008). In this scenario categorising patients on the basis of gene mutations could help in planning appropriate therapeutic interventions.

Recent advances have greatly decreased the cost, time and effectiveness of mutation detection. Microarray-based mutation detection is available for many retinal degenerative disorders including LCA (Yzer, Leroy *et al.* 2006; Henderson, Waseem *et al.* 2007; Coppieters, Casteels *et al.* 2010; Pomares, Riera *et al.* 2010). The screening by disease chip is rapid, reliable and affordable. The LCA microarray chip version -9.0 developed by Asper Ophthalmics, Estonia (http://www.asperbio.com) contains 784 known disease-associated mutations in 15 LCA genes (*GUCY2D*, *CRX*, *RPE65*, *CRB1*, *RPGRIP1*, *AIPL1*, *LRAT MERTK*, *TULP1*, *LCA5*, *RDH12*, *CEP290*, *SPATA*, *IQCB* and *RD3*) and is being updated as information on new genes and mutations becomes available.

Direct sequencing of LCA-associated genes or novel candidate genes is a widely used technique for finding mutations in patients. This approach is time-consuming due to the high degree of genetic heterogeneity as seen in LCA and related retinal diseases.

Next generation sequencing (NGS) is a newer technique in which sequencing of the whole exome from clonally amplified or single DNA molecules is performed by repeated cycles of polymerase-mediated nucleotide extensions or by iterative cycles

of oligonucleotide ligation. Depending on the platform used, NGS can generate hundreds of megabases to gigabases of nucleotide sequence output in a single instrument run. Recently, whole exome sequencing is being increasingly applied to identify novel genes in genetic disorders including LCA (Sergouniotis, Davidson *et al.* 2011; Wang, Wang *et al.* 2011; Falk, Zhang *et al.* 2012)

1.6.1.4 Functions of genes associated with LCA

Most of the genes associated with LCA are expressed exclusively or predominantly in the eye and are involved in a variety of retinal functions such as phototransduction pathway, vitamin A cycle, nucleotide biosynthesis, phagocytosis as well as genes encoding structural proteins, cilia/centrosomal proteins and transcription factors. Table 1.1 summarizes the data for all LCA known genes, their functions, expression pattern, major phenotypes associated with a gene mutation, method of gene identification and range of mutation frequencies as reported in literature.

Table 1.1: LCA associated genes and their functions.

S.N.	Gene Symbol/ Associated diseases	Gene name/Chromosomal location	Function	Expression	Phenotype associated with the gene	Mutation frequency (LCA)	Discovered/ References
1	*GUCY2D/ RETGC1* [*CORD 6*]	Guanylate cyclase 2D (17p13.1)	Photo-transduction (cGMP synthesis)	Photoreceptors	Poor vision, normal fundus appearance, photophobia, early macular & peripheral degeneration	2.7-21%	Linkage mapping (Perrault, Rozet *et al.* 1996)
2	*RPE65* [*RP20*]	Retinal pigment epithelium specific protein, 65- kD (1p31)	Visual cycle	RPE	Relatively good vision in early life & later deterioration, diffuse retinal degeneration with fundus depigmentation especially in the posterior pole	1.7-9%	Candidate gene method (Marlhens, Bareil *et al.* 1997)

3	*CRX* [CORD2]	Cone-rod homeobox (19q13.3)	Transcription factor	Photoreceptors, retinal inner nuclear layer, pineal gland	Severe vision loss, infantile nystagmus, AD inheritance pattern	0.6-3.4%	Candidate gene method (Freund, Wang *et al.* 1998)
4	*MERTK* [RP38]	Mer tyrosine kinase protooncogene (2q14.1)	OS phagocytosis	Macrophages, dendritic cells, RPE	Attenuated vessels, carpet-like retinal degeneration & no foveal reflex	0.9-2.3%	Candidate gene method (Gal, Li *et al.* 2000)
5	*AIPL1* [CORD 2, RP]	Aryl hydrocarbon-interacting receptor protein-like1 (17p13.1)	Maintenance of rod photoreceptor, chaperone, farnesylation	Early stages- Central & peripheral retina Adults- only in rods & pineal gland	Poor vision, progressive retinal changes, pigmentary changes & maculopathy in the form of a bull's eye lesion or atrophic lesion, keratoconus or cataracts	1.1-7.8%	Linkage mapping (Sohocki, Bowne *et al.* 2000)
6	*CRB1* [PPCRA, RP 12]	CRUMBS, Drosophila, Homolog of, 1 (1q31-q32.1)	Cell-cell interaction	Photoreceptor, retinal inner nuclear layer, iris, brain	PPRPE, Coats-like response, thickened & disorganized retina on OCT	2.7-16.7%	Candidate gene method (Lotery, Jacobson *et al.* 2001)

7	*LRAT* [RP]	Lecithin retinol acyltransferase (4q31)	Visual cycle	RPE	Clinically like juvenile retinitis pigmentosa	0.5-1.1%	Candidate gene method (Thompson, Li *et al.* 2001)
8	*RPGRIP1* [CORD 13]	Retinitis pigmentosa GTPase regulator-interacting protein 1 (14q11)	Protein transport	OS of rod photoreceptor, kidney, brain, heart, liver, spleen	Initially normal retinal appearance, progress to pigmentary retinopathy & progressively vision loss	4.5-29%	Candidate gene method (Dryja, Adams *et al.* 2001)
9	*RDH12*	Retinol dehydrogenase 12 (14q23.3)	Visual cycle	RPE, IS of photoreceptors	RPE atrophy, pronounced attenuation of retinal arterioles & intra-retinal bone spicule pigmentation, maculopathy, good visual function in early life followed by a progressive decline	1.1-7.2%	Linkage mapping (Janecke, Thompson *et al.* 2004)

10	*TULP1*, [RP14]	Tubby-like protein 1 (6p21.3)	Protein transport	IS of photoreceptors	Pigmentary retinopathy, able to read in early stages	0.4-13%	Candidate gene method (Hanein, Perrault *et al.* 2004)
11	*CEP290*/ NPHP6 [BBS 14, JBTS 5, MKS 4, SLSN 6]	Centrosomal Protein, 290-kD (12q21.3)	Protein transport	Ubiquitous	Extremely poor vision, cataracts & keratoconus, well-preserved macular area	1.4-30%	IBD mapping (den Hollander, Koenekoop *et al.* 2006)
12	*RD3*	Retinal degeneration 3 (1q32.3)	GUCY2D transport	Retina, photoreceptors	Poor vision & atrophic macular lesion	1.0%	Candidate gene method (Friedman, Chang *et al.* 2006)

13	*IMPDH1* [RP10]	Inosine-5prime-monophosphate dehydrogenase Type 1 (7q31.3-q32)	Involved in the *de novo* synthesis of guanine nucleotide	Ubiquitous	Rare, diffuse RPE mottling, no pigmentary deposits	8.3%	Candidate gene method (Bowne, Sullivan *et al.* 2006)
14	*LCA 5*/ Lebercilin	Lebercilin (6q14.1)	Protein transport	Ubiquitous expression in early embryonic stages, connecting cilium, centriole & microtubules in adults	Macular colobomas in older patients, ciliary defect	1.7-21%	IBD mapping (den Hollander, Koenekoop *et al.* 2007)
15	*SPATA7* [RP]	Spermatogenesis -associated protein (14q24)	-	Retina, testis & brain	Poor vision, retinal atrophy, attenuated vessels	1.7-2.9%	Homozygosity mapping & SNP array (Wang, den Hollander *et al.* 2009)
16	*KCNJ13* [SVD]	Potassium channels, Inwardly rectifying, subfamily J, member 13	Regulation of K^+ transport	Epithelial cells of kidney, lung, testis, small intestine & CNS	Pigmentary retinopathy, macular atrophy, cataract, nummular pigmented lesions, myopia	0.9%	Homozygosity mapping & exome sequencing (Sergouniotis, Davidson *et al.* 2011)

17	*IQCB1*/ NPHP5 [SLSN5, NPHP1]	Iq motif-containing protein B1 (3q21.1)	Protein transport	Connecting cilia of photoreceptors & primary cilia of RPE	Lobular pattern of hypo & hyper-pigmentation around the vascular arcades	2-2.6%	Homozygosity mapping & exome sequencing (Stone, Cideciyan *et al.* 2011)
18	*ALMS1* [ALMS, SLSN 5]	ALMS1 (2p13.1)	Probably intracellular trafficking	Ubiquitous	Nystagmus, anterior & posterior spoke-like cataracts, vascular attenuation, pigmentary maculopathy & coarse granular diffuse RPE peripheral atrophy	5.1%	Exome sequencing (Wang, Wang *et al.* 2011)
19	*CNGA3* [ACHM 2]	Cyclic nucleotide-gated channel, alpha-3 (2q11.2)	Phototransduction	Cones	Nystagmus, very sluggish pupils & nonrecordable ERG	0.8%	Exome sequencing (Wang, Wang *et al.* 2011)
20	*MYO7A* [USH,	Myosin 7A (11q13.5)	Translocation of RPE melanosomes, removal of	Kidney, liver & retina	Poor vision since birth, nystagmus, neuroepithelial atrophy	3.4%	Exome sequencing (Wang, Wang *et al.* 2011)

	DFN]		phagosomes				
21	*NMNAT1*	Nicotinamide nucleotide adenylyl-transferase 1 (1p36.22)	NAD biosynthesis	Nucleus	Macular atrophy, pigmentary clumping, attenuated retinal blood vessels & optic disc pallor	4.5-22%	Exome sequencing (Falk, Zhang *et al.* 2012)

LCA associated genes, characteristic clinical features and various other diseases associated with LCA genes (given in bracket) are mentioned.

ACHM-Achromatopsia, ALMS-Alstrom syndrome, BBS-Bardet-biedl syndrome, CORD-cone-rod dystrophy, CNS-central nervous system, DFN-deafness, ERG-electroretinography, JBTS- Joubert syndrome, LCA-Leber congenital amaurosis, MKS-Meckel syndrome, NPHP-Nephronophthisis, OCT-optical coherence tomography, OS-outer segment of photoreceptors, PPCRA- pigmented paravenous chorioretinal atrophy, PPRPE- preserved para-arteriolar retinal pigment epithelium, RP- Retinitis pigmentosa, SLSN-Senior-loken syndrome, SVD-Vitreoretinal degeneration, snowflake type, USH-Usher syndrome.

1.6.1.5 Therapeutic approaches in LCA

Research in this area has focused mainly on three approaches gene therapy, stem cell-based therapy and neuro-prosthetic devices.

1.6.1.5.1 Gene Therapy

The first gene therapy for LCA in a large mammal (Briard dog) with the replacement of the *RPE65* gene resulted in vision improvement. Sub-retinal injection of recombinant adeno-associated virus serotype 2 (AAV2/2) carrying a chicken h-actin-promoter/CMV enhancer-driven canine *RPE65* cDNA led to a restoration of rod and cone photoreceptor functions, which was observed to be stable even after 3 years (Acland, Aguirre *et al.* 2001; Acland, Aguirre *et al.* 2005).

Successful gene replacements have also been done for 6 LCA subtypes in knockout models of LCA (*GUCY2D, AIPL1*, *RPGRIP1*, *LRAT*, *MERTK* and *CEP290*) (Boye, Boye *et al.* 2010; Smith, Schlichtenbrede *et al.* 2003; Batten, Imanishi *et al.* 2005; Pawlyk, Bulgakov *et al.* 2010; Sun, Pawlyk *et al.* 2010; Baye, Patrinostro *et al.* 2011).

The mouse model of GC1 deficiency (GC1KO) exhibits loss of cone function whereas rod ERG amplitude are partially preserved. Subretinal delivery of GC1 using viral vector restored cone mediated visual functions (Boye, Boye *et al.* 2010).

Efficacy of gene therapy for *AIPL1* gene was assessed using adenovirus AAV8-RK-*hAIPL1* vector in both null (*Aipl1*$^{-/-}$) and hypomorphic (*Aipl1*$^{h/h}$) mice. RK (rhodopsin kinase) promoter is specific to both rods and cones. Gene transfer using this promoter resulted in increased *Aipl1* expression followed by PDE synthesis in both rod and cone photoreceptors in both models which was evident by the improved ERG. Improved photoreceptor cell survival, stabilization of retinal functions, preservation of outer segment morphology was also observed. AAV5 mediated gene delivery was reported to be stable after ~ 2 years of injection (Sun, Pawlyk *et al.* 2010).

In *RPGRIP*$^{-/-}$ mice, photoreceptor degeneration starts at around postnatal day 15 and by the 3 months of age, most of the cells degenerate. Subretinal delivery of AAV- *RPGRIP*

in *RPGRIP*$^{-/-}$ mutant mice using murine opsin promoter fragment (mOps) was able to restore retinal functions. Restored localization of RPGR to connecting cilia, thicker photoreceptor nuclear layer, well organized outer segments and higher ERG amplitude as compared to controls were significant features of this study (Pawlyk, Smith *et al.* 2005). Human gene and human RK promoter was also used to prove the efficacy of gene therapy for *RPGRIP1*. Improved retinal function was observed at the 5th month as measured by ERG amplitude. Introduced human *RPGRIP1* localized correctly in mouse retina and was able to anchor *RPGR*. Incomplete rescue of wild type phenotype in treated mice could be due to the low expression level of transgenic human RPGRIP1 compared to endogenous RPGRIP1. Despite this fact, this model set the background for human trial (Pawlyk, Bulgakov *et al.* 2010).

Adenoviral mediated delivery of *Mertk* using either CMV (cytomegalo virus) or RPE65 promoter *(*AAV-CMV-*Mertk* or AAV-RPE-*Mertk*) in RPE of RCS rat restored the phagocytotic function of RPE cells. Prolonged survival of photoreceptor cells, upto 9 weeks after treatment, was observed in treated eye. The number of photoreceptors were also ~2.5 times higher than in control eye after 9 months (Smith, Schlichtenbrede *et al.* 2003).

Similarly, rAAV mediated gene transfer in *Lrat*$^{-/-}$ mice restored visual functions by increasing visual pigment levels. Increased pupillary light responses (PLRs) indicated the restoration of retinal signaling to the brain. ~ 50% increase in ERG amplitude was recorded in treated mice as compared to wild type. Similar results were observed through oral administration of retinoids in *Lrat*$^{-/-}$ mice (Batten, Imanishi *et al.* 2005).

CEP290, another suitable candidate gene for gene therapy is the most frequently mutated gene. Patients with *CEP290* gene mutations showed preservation of ONL at the fovea and decreased thickening (Cideciyan, Aleman *et al.* 2007; Pasadhika, Fishman *et al.* 2010). The huge size of this gene (54exons; 290 kD) makes it difficult to pack into adeno virus for delivery. CEP290 protein was divided into two part -N terminal region (first 1059 amino acids containing c.2991 + 1655A > G region) and C terminal (1765–2479 amino acids). cep290 knockdown zebra fish embryos (mimicking hypomorphic c.2991 + 1655A

> G mutation in human) who received N-terminal CEP290 construct, had normal retinal structure yet reduced visual acuity (Baye, Patrinostro *et al.* 2011).

A. Human gene therapy clinical trials for *RPE65* gene

The success of the canine model of R*PE65* gene therapy set the background for human clinical trials. Three human gene therapy clinical trials for *RPE65* gene replacement were started simultaneously in University College and Moorefield's Eye Hospital and Institute of Ophthalmology, University college London; Schie Eye Hospital, Department of Ophthalmology University of Pennsylvania, Philadelphia, USA and the Department of Ophthalmology, University of Florida, USA. Adeno-associated virus (AAV) was chosen because of its ability to efficiently transduce both rod and cone photoreceptors and the RPE (AAV2/4), non-toxic nature, non-immunogenicity and long-lasting effect (Weber, Rabinowitz *et al.* 2003). The summary of all these trials is given in Table 1.5, which shows the number of patients included in each trial and trial ID, their ages and type of *RPE65* gene mutations, promoter used for each gene therapy, follow-up period and the clinical outcome.

Table 1.5: Summary of outcome measures of human clinical trials of the *RPE65* gene therapy

Clinical trial ID	No. of patients / type of mutation	Promoter	Age of patients	Follow up	Results	Reference
NCT006543747	3 /missense	Human RPE65	17–23 years	4 months to 1 year	No adverse effects, no retinal damage, significant improvement in retinal sensitivity & mobility (1/3), no significant changes in VA, peripheral visual fields & ERG.	(Bainbridge, Smith *et al.* 2008)
NCT00516477	12 / missense & nonsense	CBA	8–44 years	4 months to 2 years	No adverse effects, significant improvements in nystagmus & visual fields (12/12), retinal sensitivity (11/11), VA (7/12), mobility (3/12), development of electrical responses from the macula & visual cortex activation (2/2), no significant changes in ERG (12/12).	(Maguire, Simonelli *et al.* 2008)
NCT00481546	15/ missense, splice site, deletion, nonsense	CBA	11–30 years	1 month to 3 years	No serious adverse events, improvement in retinal function in treated eyes (14/15), retinal sensitivity (13/15), VA (2/3), mobility (3/6).	(Hauswirth, Aleman *et al.* 2008)

NCT01208389	3 (27–46 years)	CBA		6 months (2nd eye); 3–4 years (1st eye)	No serious adverse events; improvement of retinal function in the second treated eye (2/3), retina sensitivity (3/3), improved VA (1/3), improved mobility (2/3), significant visual cortex activation (3/3).	(Bennett, Ashtari *et al*. 2012)

CBA-chicken β actin promoter, fMRI- functional magnetic resonance imaging, FST- Full-field sensitivity testing, mfERG- multifocal Electroretinography, PLR- Pupillary light reflex, VA-visual acuity

1.6.1.5.2 Stem cell Therapy

Despite undergoing III phase clinical trials for *RPE65* gene replacement therapy (Cideciyan 2010), this approach has some limitations. It can be used only in patients with mutations in a given gene. Hence, one cannot target majority of patients with LCA since the frequency of mutations in a particular gene such as *RPE65* is small. For the success of this approach, early intervention is needed when the photoreceptor layer is still intact. For these reasons, stem cell therapy may present an alternative approach that can potentially be used in all LCA patients.

Studies of photoreceptor transplantation using committed progenitor or precursor cells as donor have shown the integration capabilities in the adult or degenerating retina. These transplanted cells were also able to differentiate into rod photoreceptors, form synaptic connections resulting in improved visual functions (MacLaren, Pearson *et al.* 2006). Similarly successful transplantation of cone photoreceptors has been done using Crx positive mouse donor cells in two genetic models of Leber congenital amaurosis, the *Crb1*$^{rd8/rd8}$ and *Gucy2e*$^{2/2}$ (Lakowski, Baron *et al.* 2010). Feasibility of precursor of rod photoreceptor transplantation in severe retinal degeneration models (*Prph2*$^{+/\Delta 307}$, *Crb1*$^{rd8/rd8}$,*Gnat1*$^{-/-}$, *Rho*$^{-/-}$, *PDE6β*$^{rd1/rd1}$, *Prph2*$^{rd2/rd2}$) was also studied. Data suggested that repair of degenerating retina is possible even in late-stage but recipient environment plays a significant role in the successes of transplantation. Disease models where outer limiting membrane was disrupted (*Crb1*$^{rd8/rd8}$) showed higher Integration efficiency (Barber, Hippert *et al.* 2013; Singh, Charbel Issa *et al.* 2013). This suggested the possibility of combining the correction of genetic defect with photoreceptor transplantation for better results.

1.6.1.5.3 Retinal prosthesis

Retinal prostheses are electronic devices that convert light into electrical signals that stimulate neurons. These prosthetic devices are of two types-non-retinal (cortical, optic nerve and epiretinal prostheses) and retinal. Various studies and clinical trials for these devices (Optobionics, ARGUS II, Epi-ret3 and Bionic eye) are underway (Zrenner, Bartz-Schmidt *et al.* 2011; Humayun, Dorn *et al.* 2012)

1.7 Overview of genes screened in this study

1.7.1 Guanylate cyclase 2D (*GUCY2D*)

Guanylate cyclase 2D (*GUCY2D*) was the first LCA gene to be identified in 1995 in a consanguineous North African family by homozygosity mapping (Camuzat, Dollfus *et al.* 1995; Perrault, Rozet *et al.* 1996). This gene is located on chromosome 17p13.1 and consists of 19 exons. *GUCY2D* belongs to membrane- bound guanylate cyclases (GCs) family and encodes retinal guanylate cyclase (RetGC-1) enzyme. In humans, Guanylate cyclase has two isoforms, retGC1 and retGC2 (encoded by *GUCY2D* and *GUCY2F*). The mouse homologues of these genes are referred as GC-E and GC-F respectively. retGC1 and retGC2, both are responsible for resynthesis of cGMP in photoreceptors for the recovery of dark state. RetGC1 is also involved in the transport of transmembrane and peripheral membrane proteins from endoplasmic reticulum to outer segment (Karan, Frederick *et al.* 2010). The retGC1 expression has been reported in the retina, pineal gland, and olfactory bulb, cochlear nerve and the organ of corti whereas the retGC2 expression is restricted to retina (Seebacher, Beitz *et al.* 1999).

retGC1 consists of an extracellular domain, a trans membrane domain, an intracellular protein kinase-like homology domain (KHD), a dimerization (hinge) domain (DD) and a C-terminal catalytic domain (CAT). At high intracellular Ca^{2+} concentration (500nM) GC-1 exists in a monomer form with basal level of GC activity. Guanylate cyclase-activating proteins (GCAP1, GCAP2 or GCAP3), the Ca^{2}+ binding proteins modulate retGCs function. GCAP1 and GCAP2 are expressed in rod and cone photoreceptors, whereas GCAP3 is expressed only in cones. GCAPs bind to GCs and stimulate synthesis of cGMP in a feedback manner (Figure 1.10). At low Ca^{2+} concentration (300nM), GCAPs are converted from their Ca^{2+} bound (inhibitor) state to the Mg^{2+} bound (activator) state. This causes formation of retGC1 homodimer and increase in catalytic activity of retGC1 (Dizhoor, Olshevskaya, *et al.* 2010; Yu, Olshevskaya, *et al.* 1999).

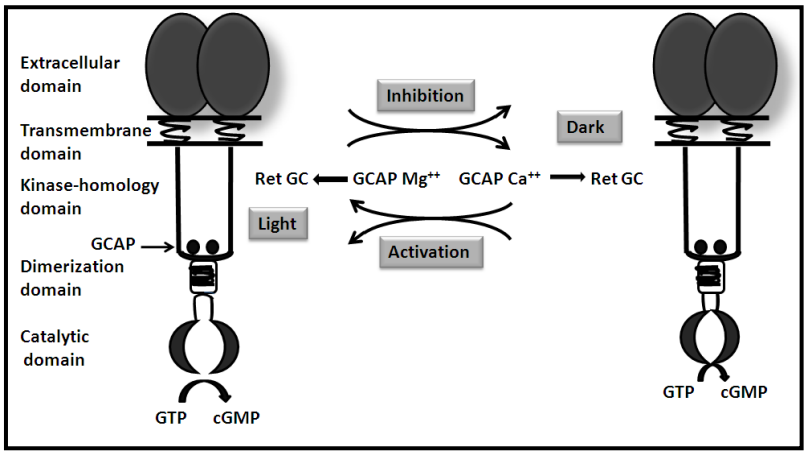

Figure 1.10: Schematic model of the regulation of retGC1 by GCAP1 under light and dark conditions

Knockout mice studies suggested that GC2 can compensate for the absence of GC1 in rods to a certain extent, therefore mutations in *GUCY2F* gene mainly affects cones. However double knockout mice (GC1/GC2 double knock-out or GCdko) showed degenerated outer segments and extinguished ERG, similar to human LCA1 patients (Baehr, Karan *et al.* 2007).

In humans, dominant mutations affect mainly cones and causes cone–rod dystrophy (CORD). Cone–rod dystrophy is characterized by early degeneration of cones followed by rod cells degeneration in later stages. It results in an early decrease in visual acuity and colour vision. Recessive mutations in *GUCY2D* gene are known to cause Leber congenital amaurosis. However, recently *GUCY2D* gene mutations have been identified in a CORD family with autosomal recessive inheritance using whole genome linkage analysis (Ugur Iseri, Durlu *et al.* 2010).

Mutations in the *GUCY2F* gene have not been reported. Mutations reported in *GUCY2D* can be grouped in two type 1) loss of function mutations result in decreased RetGC1 enzyme activity leading to LCA (Tucker, Ramamurthy, *et al.* 2004). Gain of function mutations can cause later onset but less severe cone–rod dystrophy (CORD) due to decrease in the Ca^{2+} sensitivity of the GCAP-RetGC1 complex. This leads to an abnormal increase in the cGMP levels in photoreceptors in the dark (Tucker, Woodcock, *et al.* 1999). The percentage of patients with mutation in this gene which are reported in major studies are reviewed in the Table 1(Appendix).

Animal models help to study the gene function. The rd chicken is a naturally occurring blind mutant for *GUCY2D*, discovered in a Rhode Island Red flock. It exhibits retinal degeneration, due to a 22-kb deletion in the *GUCY2D* orthologue, *GUCY1B*. Deletion in this gene leads to decreased cGMP in rods and cones leading to reduced phototransduction and finally photoreceptors degeneration (Semple-Rowland, Lee *et al.* 1998). In rd chicken, degenerative changes first appear in the outer segments of the rod and cone photoreceptor cells, 7-10 days after the birds hatch in the central retina and proceeds progressively towards the periphery and is complete by 6-8 months (Ulshafer, Allen *et al.* 1984). Gene therapy using this model showed restoration of vision using lentiviral-mediated transfer of GC1 in Prehatch embryo (Williams, Coleman *et al.* 2006).

The homozygous *Gucy2e* knockout mouse (GC1KO), was created by replacing a portion of exon 5, which codes for the transmembrane region, with a neomycin-resistance gene cassette. These null mice had overall normal retinal structure. Drastic reduction in number of cones was observed initially but then number remain stable by 5 weeks of age (Yang, Robinson *et al.* 1999). The residual rod activity was due to the presence of *gucy2f* gene which can compensate the loss due to *Gucy2e* gene (Baehr, Karan *et al.* 2007). GC1KO resembles with the human LCA1 where cone starts degenerating followed by loss of cone function. But rods cells remain unaffected. Stable restoration of visual functions was observed in this model using adenoviral assisted subretinal gene transfer (Boye, Boye *et al.* 2010; Mihelec, Pearson *et al.* 2011). Maintenance of retinal structure in LCA1 patients makes *GUCY2D* suitable for the successful gene therapy candidate in humans.

1.7.2 Retinal degeneration 3 (*RD3*)

Rd3 mice (RBF/DnJ mice strain) were first identified in Switzerland in 1969 (Chang, Heckenlively *et al.* 1993). The *rd-3* gene, responsible for the retinal degeneration phenotypes was mapped on to chromosome 1 (Chang, Heckenlively *et al.* 1993). These mice carried a homozygous mutation (R107X) in exon 3 of *rd3* gene leading to a truncated protein (Friedman, Chang *et al.* 2006).

The homologous human *RD3* gene was identified on 1q32.3 and designated as c1orf36. It consists of 3 exons. Initial screening of this gene in retinal degeneration probands did not identify any mutations (Lavorgna, Lestingi *et al.* 2003). *RD3* gene screening in a large

cohort of 881 probands from North America, India and Europe with various retinal degeneration phenotypes (cone dystrophy, LCA, AD RP and AR RP) was done. A splice mutation was identified in a single LCA proband of Indian origin, recruited at LVPEI (Friedman, Chang *et al.* 2006).

RD3 co-localizes with photoreceptor guanylate cyclases (GC1 and GC2) in the photoreceptor outer segments (Azadi, Molday *et al.* 2010). GC1 and GC2 expression was undetectable in the retinas of rd3 mice due to RD3 deficiency. A short segment of C terminus region of GC is required for the binding with RD3. RD3 is involved in the vesicle trafficking of GCs from inner to outer segments and also acts as a high-affinity allosteric inhibitor of GC (Azadi, Molday *et al.* 2010). *In vitro* studies showed the restoration of GCs expression and trafficking through viral vector mediated delivery of *Rd3* gene in rd3 mice model. This resulted in improved visual and photoreceptor survival (Molday, Djajadi *et al.* 2013). RD3 also act as an inhibitor for basal retGC1 catalytic activity. GCs activity is controlled by a feed-back mechanism where GCAP switch from a Ca^{2+}-bound (inhibitor) state to Mg^{2+}-bound (GC activator) state. It also acts as a negative modulator of the RetGC by preventing it's the activation by GCAPs (Peshenko, Olshevskaya *et al.* 2011).

Mutations in *RD3* gene cause LCA12 and early onset severe retinal dystrophy (EOSRD) (Friedman, Chang *et al.* 2006; Preising, Hausotter-Will *et al.* 2012). *RD3* forms the rarest form of LCA with only 3 reports have been published so far. Mutation spectrum of this gene is given in Table 1(Appendix).

1.7.3 Crumbs, Drosophila, Homolog of, 1 (*CRB1*)

CRB1 gene is located on chromosome position 1q31.3. CRB1 is a homologous to the crumbs (CRB) protein of the *Drosophila melanogaster* with 35% sequence homology. It was identified by a suppression subtractive hybridization (SSH) method using cDNA library of human retina and RPE (den Hollander, ten Brink *et al.* 1999). It consists of 12 exons and alternative splicing results in two isoforms, an extracellular protein (1376 amino acid), or a transmembrane protein (1406 amino acid). Crumbs protein consists of 19 EGF- like domains, three laminin AG-like domains, a transmembrane domain and a cytoplasmic domain consisting of FERM protein domain and PDZ binding domain. In

humans, two other homologues to *CRB1* gene (*CRB2* and *CRB3)* are present. *CRB1* gene is expressed in the retina and brain (den Hollander, ten Brink *et al.* 1999). *CRB2* expression has been observed mainly in retina, kidney, heart and lung (van den Hurk, Rashbass *et al.* 2005) and *CRB3* has wider expression in various tissues including retina (Makarova, Roh *et al.* 2003).

The exact role of *CRB1* in humans is still not clear. In *Drosophila* Crb forms Crumbs complex with Stardust (Sdt), protein associated with tight junctions or Pals1-associated tight junction protein (PATJ) and Lin-7. This complex is located in the subapical region of epithelial cells and the stalk in photoreceptor cells (PRCs) of *Drosophila*. Crumbs complex acts as molecular scaffold and controls the apical-basal polarity of embryonic epithelial cells and is required for photoreceptor cell morphogenesis in *Drosophila* (Pellikka, Tanentzapf *et al.* 2002)

Mammalian Crumbs complex consists of CRB1-3, MUPP1 (multiple PDZ domain protein), PATJ (PALS1-associated tight junction protein) and PALS1/MPP5 (protein associated with Lin seven1) (Lemmers, Medina *et al.* 2002; van de Pavert, Kantardzhieva *et al.* 2004; Kantardzhieva, Gosens *et al.* 2005; van Rossum, Aartsen *et al.* 2006). In CRUMBs complex PALS1 acts as linker by binding with both CRB1 and PATJ (Roh, Makarova *et al.* 2002). Crumbs complex is localized in the subapical region (SAR) adjacent to adherens junctions at the outer limiting membrane in retina (van de Pavert, Kantardzhieva *et al.* 2004; van Rossum, Aartsen *et al.* 2006). Crumbs complex is required for muller glia-photoreceptor cell interaction. It plays a key role in establishing the polarity of retina by maintaining the integrity of adherens junctions at the outer limiting membrane (van de Pavert, Kantardzhieva *et al.* 2004).

Lack of Crb results in light-induced retinal degeneration as shown in *Drosophila* (Johnson, Grawe *et al.* 2002). Similar results were observed in *Crb1*$^{-/-}$ knockout mice. These mice showed disruption of adherens junctions between muller and photoreceptor cells followed by neuronal cell death in the inner and outer nuclear layers of the *Crb1*$^{-/-}$ retina during light exposure (van de Pavert, Kantardzhieva *et al.* 2004).

In vivo studies in *Drosophila* had shown that Crb regulates the epithelial cell polarity and integrity by inhibiting phosphoinositides 3-kinase (PI3K) - Rac1 pathway. Balance

between Crb and the Rac1–PI3K module is required to maintain apico-basolateral polarity in epithelial cells (Chartier, Hardy, *et al.* 2011). Rac1 is also involved in the production of superoxide and other reactive oxygen species (ROS) through NADPH oxidase and Crb is a negative regulator for the ROS production. Increased ROS levels as compared to wild type, has been observed in crb mutant retinas. Inhibition of Rac1 or NADPH oxidase in *Drosophila* with *crb* mutations showed increased survival of photoreceptors against ROS related retinal degeneration (Chartier, Hardy, *et al.* 2012).

Mutations in *CRB1* are reported to be associated with LCA as well as with other retinal dystrophies including retinitis pigmentosa (RP) with or without preserved paraarteriolar retinal pigment epithelium (PPRPE) (den Hollander, ten Brink *et al.* 1999), retinitis pigmentosa with Coats-like exudative vasculopathy (den Hollander, Heckenlively *et al.* 2001; den Hollander, Davis *et al.* 2004) and pigmented paravenous chorioretinal atrophy (McKay, Clarke *et al.* 2005).

LCA patients with *CRB1* gene mutations exhibit a range of overlapping clinical features including PPRPE, Coats-like exudative vasculopathy & keratoconous. Keratoconous may be due to *CRB1* mutations leading to corneal shape abnormality. Apart from these features hyperopia, retinal thickening with delaminated retina, nummular pigment clumps, macular coloboma and white spots on fundus are other features often reported to be associated with *CRB1* mutations (Lotery, Jacobson *et al.* 2001; Jacobson, Cideciyan *et al.* 2003; Yzer, Leroy *et al.* 2006; Henderson, Mackay *et al.* 2011).

Photoreceptor degeneration leads to a thin retina as reported in LCA patients with mutations in either *RPE65* or *GUCY2D* genes (Pasadhika, Fishman *et al.* 2010). Contrary to this, patients with *CRB1* gene mutations have been reported with thicker, disorganization retina without distinct layering (Aleman, Cideciyan *et al.* 2011).

1.7.4 Nicotinamide mononucleotide adenylyltransferase 1 (*NMNAT1*)

The *NMNAT1* gene was mapped to chromosome 1p36.22 and consists of 4 exons. This gene is located in the previously identified LCA 9 locus (Koenekoop, Wang *et al.* 2012). *NMNAT1* gene encodes nicotinamide mononucleotide adenylyltransferase enzyme. NMNAT1 forms a barrel shaped hexamer and a nuclear localization signal (NLS)

sequences is located at the surface of the barrel (Werner, Ziegler, *et al.* 2002; Zhou, Kurnasov, *et al.* 2002). It shows dual specificity for both NMN and NaMN and is involved in the biosynthesis of nicotinamide adenine dinucleotide (NAD) and nicotinic acid adenine dinucleotide (NAAD) as shown is Figure 1.11.

NMNAT1 is a member of the nucleotidyltransferase α/β phosphodiesterases superfamily. NMNAT has 3 isoforms in humans-NMNAT1, NMNAT2 and NMNAT3. NMNAT1 localizes to the nucleus (Raffaelli, Sorci *et al.* 2002; Berger, Lau *et al.* 2005). The other 2 isoforms *NMNAT2* and *NMNAT3* are encoded by 2 different genes and the proteins are localized in the Golgi complex and mitochondria respectively (Berger, Lau *et al.* 2005).

NMNAT1 participates both in *de novo* as well as in salvage pathways of NAD biosynthesis (Sauve 2008). In the *de novo* pathway, tryptophan is converted into nicotinic acid mononucleotide (NaMN) and then to nicotinic acid adenine dinucleotide (NaAD) by the NMNAT enzyme. NaAD is finally converted into NAD with the help of NAD synthetase. In salvage pathway four different precursors - nicotinic acid or vitamin B3 (NA), nicotinamide (NAM), nicotinamide riboside(NR) and nicotinic acid riboside (NAR) can be converted into NAD+, as shown in figure 1.11 (Nikiforov, Dolle, *et al.* 2011; Zhou, Kurnasov, *et al.* 2002).

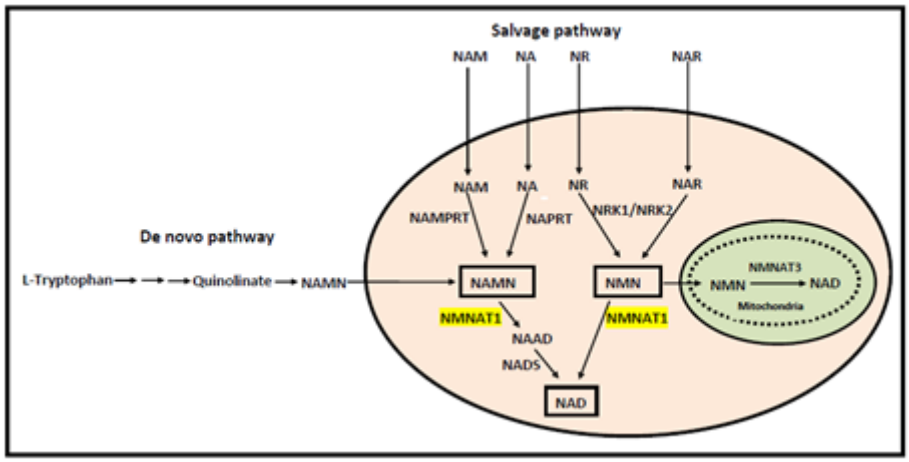

Figure 1.11: A schematic representation of *de novo* and salvage pathways of NAD^+ biosynthesis in human cells.

The *de novo* pathway starts with tryptophan. In the salvage pathway, nicotinamide (NAM), niacin or nicotinic acid (NA), nicotinic acid riboside (NAR) and nicotinamide riboside (NR) are recycled to synthesize NAD.

NMNAT1 is a stress response protein and plays a protective role during axonal degeneration in various neurodegenerative conditions such as neonatal hypoxic-ischemic (H-I) injury (Press and Milbrandt 2008; Verghese, Sasaki *et al.* 2011). Overexpression of *nmnat* in *Drosophila* provides neuronal protection by preventing unfolding and promoting refolding of proteins. (Zhai, Zhang *et al.* 2008). *In vivo* studies in *Drosophila* showed the up-regulation of nmnat during various stress conditions like heat shock, oxidative stress or hypoxia (Ali, McCormack, *et al.* 2011). Similarly *Nmnat1* overexpression in mice prevents axonal degeneration due to injury (Wallerian degeneration) or stress (Araki, Sasaki *et al.* 2004; Press and Milbrandt 2008)

Nmnat1 is a part of Wallerian fusion protein (Wld^S), found in the slow Wallerian degeneration mouse (C57BL/Wld) as a result of a spontaneous mutation. This translocation mutation results in a fusion protein consisting of the N-terminal 70 amino acids of the ubiquitin fusion degradation protein 2a (Ufd2a), a linker region of 18 amino acids, and the full length Nmnatl protein (Mack, Reiner *et al.* 2001). In Wallerian degeneration, following an injury to a nerve such as cut or crush, the peripheral nerve axons, distal to its site of injury undergoes degeneration. *Nmnat1* overexpression in mice provides protection against axonal degeneration after injury (Araki, Sasaki *et al.* 2004; Sasaki, Vohra *et al.* 2009a).

Some reports suggest that there is a requirement of the N-terminal end of fusion protein consisting of Ufd2a together with Nmnat1 enzyme activity that is required for protection against degeneration (Conforti, Fang *et al.* 2007; Conforti, Wilbrey *et al.* 2009). Many studies have been published till now to understand the exact mechanism of protection conferred by Nmnat1. These studies suggest that Nmnat1 enzymatic activity is required but NAD^+ levels do not appear to have a role in protection against neurodegeneration (Sasaki, Vohra *et al.* 2009b). *In vitro* studies using mouse neurons also suggested that it also has a role in neuronal morphogenesis (Zhao, Zhang *et al.* 2011).

NMNAT1 regulates the functions of many NAD+ dependent enzymes such as-SIRT1 (Sirtuin 1) and PARP-1(poly (ADP-ribose) polymerase 1). SIRT1 is a NAD^+-dependent histone deacetylase involved in chromatin remodelling. NMNAT1 regulates SIRT1 dependent transcription of many genes like *TGFβ, ATXN10, SOCS2* (Zhang, Berrocal *et al.* 2009). SIRT1 recruits NMNAT1 at target gene promoters which in turn regulates gene expression (Zhang, Berrocal *et al.* 2009). NMNAT1 also regulates PARP-1, another chromatin and transcription modulating enzyme. PARP-1 is activated by cellular stress like DNA damage and stimulates poly-(ADP-ribosyl)ation of target proteins. NMNAT-1 binds to PARP-1 and regulates this NAD+ consuming process (Berger, Lau *et al.* 2007a). Thus the neuroprotective role of NMNAT1 is attributed to its chaperone activity and its interaction with DNA repair proteins such as PARP-1 and SIRT1. Its chaperone function is independent of its enzyme activity (Araki, Sasaki *et al.* 2004; Berger, Lau *et al.* 2007; Zhai, Zhang *et al.* 2008; Zhang, Berrocal *et al.* 2009).

1.7.5 Membrane protein palmitoylated 5 (*MPP5/PALS1*)

PALS1 gene located on chromosome 14q23.3 and consists of 13 exons. PALS1 belongs to the MAGUK (membrane-associated guanylate kinase) family of proteins, which are scaffold proteins. PALS1 contains one PDZ, one SH3 and two L27 domains. *In- vitro* studies suggested that the PDZ domain of Pals1 links it to Crb, whereas the N-terminal L27 domain links it to Pals1-associated tight junction (Patj) protein (Roh, Makarova *et al.* 2002).

Pals1 is involved in the organization of intracellular Pals1-Crb-Patj protein scaffolds which localize in the mammalian epithelial cells. This complex plays a role in determining cell polarity (Roh, Makarova *et al.* 2002; Makarova, Roh *et al.* 2003). Another macromolecular complex Par3-Par6-aPKC, located in the tight junction of mammalian epithelial cells is involved in epithelial cell polarity. Pals1 links these two complexes by binding to Par6 (Hurd, Gao *et al.* 2003). Thus loss of PALS1 function affects the PATJ levels and delay in tight junction formation as shown in MDCKII cells (Madin-Darby canine kidney) (Straight, Shin *et al.* 2004).

Crb/Pals1/Patj protein complex is also located in the region (SAR) of outer limiting membrane (OLM) of photoreceptors and muller glial cells and is involved in maintenance

of cell adhesions between photoreceptors and muller glial cells (van Rossum, Aartsen *et al.* 2006). Similarly, Stardust (*Sdt*), the *PALS1* orthologue in *Drosophila* also shown play an important role in retinal development (Bulgakova, Kempkens *et al.* 2008). Mutations in *Sdt* gene results in light-induced retinal degeneration (Berger, Bulgakova *et al.* 2007b).

Since Pals1 is required for polarity and cell adhesion in neural retina, conditional knock-out of *Pals1* causes the retinal neuronal death, defects in retinal lamination, pseudorosette formation, adhesion defects, disrupted apical structure and photoreceptor degeneration. The *Pals1* knockout mice exhibited disorganized lamination and apical junctions and retinal degeneration leading to early visual impairment as assessed by electroretinogram (Cho, Kim *et al.* 2012).

Mutations in the *CRB1* gene have been reported in patients with Leber congenital amaurosis (LCA), retinitis pigmentosa (RP) with preservation of para-arteriolar retinal pigment epithelium (PPRPE), early-onset RP without PPRPE and RP with Coats-like exudative vasculopathy (den Hollander, Davis *et al.* 2004; Ehrenberg, Pierce *et al.* 2013). Existing literature suggests that the genetic background of patients influence the phenotype and severity of disease as different mutations in *CRB1* gene results in different retinal disease phenotypes (den Hollander, Davis *et al.* 2004; Ehrenberg, Pierce *et al.* 2013).The various phenotypes caused by mutations in *CRB1* gene could be due to the involvement of other components of Crumbs complex like *PALS1*. Mutations in *PALS1* gene have not been reported in humans. However in a conditional knock-out of *Pals1* in mice with premature protein termination at amino acid 122, resulted in photoreceptor degeneration leading to early visual impairment (Cho, Kim *et al.* 2012).

2.1 Enrolment of study participants

The study was approved by the Institutional Review Board of L.V. Prasad Eye Institute and the protocol was in accordance with the Tenets of Declaration of Helsinki. The study participants were enrolled at L.V. Prasad Eye Institute with prior written informed consent. Patients (n = 100) who reported at the retina outpatient clinic were enrolled after confirmed diagnosis of LCA and documentation of clinical features, by a retina specialist. In addition, available family members of the probands were also included for collection of samples and clinical examination, if required. Pedigrees were recorded based on information provided by the parents/guardians of the proband.

Clinical evaluation involved a comprehensive and detailed eye examination including measurement of best corrected visual acuity and fundus examination by indirect ophthalmoscopy. Fundus photographs were taken. Electroretinography (ERG) and optical coherence tomography (OCT) were performed wherever possible. Full-field electroretinograms were recorded using Metrovision ERG system monitor (Perenchies, France) for both scotopic and photopic responses. OCT scans were performed on Optovue (RTVue; Optovue, Inc., Fremont, CA). Available family members also underwent a comprehensive eye examination.

2.2.1 Diagnostic criteria for LCA patients

Inclusion criteria of patients recruited in this study were-

a. Visual loss since birth as noted within 6 months of birth.

b. A normal fundus or variable fundus appearance including white retinal spots, salt and pepper pigmentation, bone spicule pigmentation, marbleized retinal changes or nummular pigmentation, preserved para-arteriolar RPE (PPRPE) and macular coloboma.

c. Nystagmus since birth/ infancy

In addition to the above mentioned essential clinical features, additional features were also considered for the inclusion of subjects, as listed below:

d. Eye poking
e. Arterial narrowing
f. Disc pallor
g. AR inheritance
h. Extinguished ERG
i. VA < 20/200 in better eye
j. Hyperopia> 4D sph
k. Keratoconus and astigmatism
l. Coats'- like retinal exudation

Exclusion criteria included absence of nystagmus, patchy retinal involvement, no loss of vision at birth, presence of trauma, inflammation or any other systemic conditions, and patients or in case of minors, family members not willing to participate in the study.

2.2.2 Enrolment criteria for normal subjects

Normal subjects (n=150) without any signs of retinal disease were included as controls. Blood samples from control individuals were collected after obtaining informed written consent.

2.3 Sample collection from study participants

Subjects who met the inclusion criteria were asked to participate in the study with prior written informed consent. 3-4 ml of venous blood was collected from patients and available family members in sodium EDTA vacuetainers (BD Biosciences, USA) by venipuncture. Blood samples were stored at -20 ^{o}C until further processing. A total of 100 probands and 150 unrelated healthy controls were included in this study.

2.4 Isolation of genomic DNA from blood samples

Genomic DNA isolation was performed according to standard protocols (Sambrook *et al*., 1989) with some modifications**.** Frozen blood samples were thawed at room temperature under a laminar flow hood and transferred to 50 ml polypropylene centrifuge tubes [Tarsons, Kolkata, India]. Four volumes of reagent A (made up of- 320 mM Sucrose, 5 mM $MgCl_2$, 1% Triton-X 100 and 10 mM Tris-HCl (pH-8.0) was added to one volume of blood (about 3-4 ml) and mixed well by vortexing. The tubes

were then centrifuged at 3000 rpm for 8-10 minutes to obtain a pellet, free of RBCs. The resulting supernatant with lysed and RBCs was discarded carefully either with a Pasteur pipette or by decanting. This step was repeated 2-3 times until a clear pellet was obtained. The pellet was resuspended in half the volume (as that of blood sample) of reagent B (400 mM Tris-HCl (pH-8.0), 60 mM Na-EDTA, 150 mM NaCl, and 1% SDS). The contents in the tube were mixed thoroughly by inverting the tube for about 2-3 minutes until a viscous solution was obtained. After a homogenous solution was obtained, 5-20 µl of Proteinase K (25 mg/ml stock solution; at 5 µl/ml of blood) was added and the tubes were incubated at 37^{o}C for 30 minutes. Reagent C (5 mM sodium perchlorate) was then added at one-fourth the volume of the blood taken for extraction and the solution was thoroughly mixed. Subsequently equal volumes (as that of reagent B and C) of chloroform (Qualigens, Mumbai, India) and Tris-equilibrated phenol (Sigma-Aldrich, St Louis, USA) were added, mixed well by inverting the tubes several times gently until an emulsion was formed. The tube was then centrifuged at 3000 rpm for 10 minutes resulting in separation of the solution in to three layers – a clear aqueous phase, a turbid protein phase and the bottom most organic solvent phase comprising phenol-chloroform. The aqueous layer was transferred to a 15 ml centrifuge tube using a broad mouth tip without disturbing the protein phase. The aqueous phase was re-extracted with an equal volume of chloroform, and centrifuged for 5 minutes at 2500 rpm. It was then was transferred to a fresh centrifuge tube, 2 volumes of chilled absolute ethanol [Qualigens, Mumbai, India] were added and gently swirled to precipitate out the DNA, which was transferred with a broad mouth tip into a 1.5 ml microfuge tube and the DNA pellet was washed two times with 500 µl of 70% ethanol. The tube was air-dried to obtain an ethanol-free DNA pellet. The DNA pellet was then dissolved in autoclaved de-ionized water and incubated at 37°C overnight. The DNA was quantitated by measuring its absorbance on a UV spectrophotometer (UV-1601, Shimadzu, Japan). 5 µl of genomic DNA was diluted with autoclaved de-ionized water to a final volume of 1ml in 1.5 ml microfuge tube and transferred to a quartz cuvette. The absorbance was measured at 260 nm and 280 nm. The readings at 260 nm and 280 nm were used to calculate the absorbance ratios A260/A280, which were used to assess the purity of DNA. The concentration of DNA in the samples was calculated by taking the absorbance of 1mg/ml of double-stranded DNA as equal to 20 OD units.

2.5 Screening of candidate genes

The present study was undertaken to identify pathogenic mutations in five genes in Indian LCA patients. Genes taken for screening were either known to be associated with LCA or other retinal dystrophies, or were candidates for LCA based on retinal function and expression. These included guanylate cyclase 2D (*GUCY2D),* retinal degeneration 3 (*RD3),* crumbs homologue 1 (*CRB1*) and membrane protein palmitoylated 5 (*MPP5/PALS1*). Nicotinamide nucleotide adenylyltransferase 1(*NMNAT1)* gene was identified by exome sequencing. Details of these genes are given in Table 2.1

Table 2.1: Details of genes selected for screening

Gene symbol	Gene name	Gene size (Kb)	No. of exons	Transcript ID	Protein ID
GUCY2D	Guanylate cyclase 2D	17.6	19	NM_000180.3	NP_000171.1
RD3	Retinal degeneration 3	16.3	3	NM_183059.2	NP_898882.1
CRB1	Crumbs homologue 1 (Drosophila)	276.9	12	NM_201253.2	NP_957705.1
PALS1/ MPP5	Membrane-associated palmitoylated protein 5	94.7	13	NM_022474.2	NP_071919.2
NMNAT1	Nicotinamide nucleotide adenylyltransferase 1	42.0	5	NM_022787.3	NP_073624.2

2.6 Amplification of target DNA by Polymerase chain reaction (PCR)

Primers for PCR-amplification of the genomic regions of interest were designed using either Primer 3 software, version 0.40 (http://frodo.wi.mit.edu/primer3) or Primer-Blast software (http://www.ncbi.nlm.nih.gov/tools/primerblast/).

PCR was carried out in a volume of 25 µl using 4-5 pmols of specific primers, 50 to 100 ng template DNA, 1.25-2.5 mM $MgCl_2$, 200 µM dNTPs, 1 unit of *Taq* DNA

polymerase (Bangalore Genei, Bangalore, India) and 1X reaction buffer (10 mM Tris (pH8.3), 50 mM KCl, 0.1% gelatin). Details of specific primers used for each of the genes screened in the study, are given in Appendix 1. The contents of the tube were thoroughly mixed by vortexing and centrifugation. The tubes were placed in the Veriti 96 well thermal cycler (Applied Biosystems, Foster City, USA) and set at required conditions (normal or touchdown PCR) for amplification of the specific products. The cycling parameters are given in Tables 2.2 and 2.3.

Table 2.2: Conditions for PCR

Step	**Process**	**Temperature**	**Time**
Step 1	Initial denaturation	95^0C	2 minutes
Step 2	Denaturation	95^0C	30 seconds
Step 3	Annealing	56-65^0C	30-45 seconds
Step 4	Elongation	72^0C	30 seconds
Step 5	Repeat steps 2-4 29 more times		
Step 6	Final elongation	72^0C	5 minutes
Step 7	Hold	4^0C	

Table 2.3: Conditions for touchdown PCR

Step	**Process**	**Temperature**	**Time**
Step 1	Initial denaturation	95^0C	2 minutes
Step 2	Denaturation 1	95^0C	30 seconds
Step 3	Annealing 1	62-55 ^{0}C (decrease 1^0C per cycle)	30 seconds
Step 4	Elongation 1	72^0C	30 seconds
Step 5	Repeat steps 2-4 7 times		
Step 7	Denaturation 2	95^0C	30 seconds
Step 8	Annealing 2	55-58^0C	30 seconds
Step 9	Elongation 2	72^0C	30 seconds
Step 10	Repeat steps 7-9 19 more times		
Step 11	Final elongation	72^0C	5 minutes
Step 12	Hold	4^0C	Forever

2.7 Visualization of PCR products by agarose gel electrophoresis

PCR products were visualized by agarose gel electrophoresis. The appropriate amount of agarose powder (1-2 g/100 ml volume to make 1-2% agarose gels) was taken in 1X TAE (Tris-acetate EDTA; 40 mM Tris, 20 mM acetic acid and 1 mM EDTA) buffer (pH 8.0). The agarose was melted by heating in a microwave oven. After cooling the gel to <65 ^{0}C, ethidium bromide (EtBr) was added from a 10mg/ml stock to make a final concentration of 0.25 µg/ml EtBr. The gel was cast in a tray and allowed to solidify at room temperature. After the gel solidified, the comb was removed and the gel was placed in a horizontal electrophoresis chamber, so as to submerge it in 1X TAE buffer. It was then loaded with 4-5 µl of the PCR products mixed with 6X loading dye (40% sucrose, 0.025% xylene cyanol and 0.025% bromophenol in deionised water). Sizes of DNA fragments were determined by comparison with 0.5-1.0 ug of DNA size standards (100 bp or 1000 bp DNA ladder, Fermentas, Hanover, MD) loaded on the same gel. The gel was electrophoresed at 80-100V for about 30 minutes until the bromophenol blue migrated to the end of the gel, and the DNA was visualized over a UV transilluminator (UVITec, Cambridge, UK).

2.8 PCR-RFLP

PCR-RFLP (polymerase chain reaction-restriction fragment length polymorphism) was used to test for the presence of specific sequence variations in normal control individuals, in those cases in which the sequence changes resulted in alteration (gain or loss) of a restriction enzyme site. Restriction enzyme sites in a given sequence were identified using the NEBcutter v 2.0 software (http://tools.neb.com/NEBcutter2/index.php). The relevant PCR products were subjected to digestion for durations ranging from 3 hour to overnight with 1.0 unit of specific restriction enzyme to a final volume of 10 ul using the recommended buffer. Digested PCR products were visualized upon polyacrylamide gel electrophoresis (PAGE) followed by EtBr staining. Depending on the expected sizes of digestion products, electrophoresis was carried out on 8-10% native polyacrylamide gels. The gels were stained by adding 10µl of EtBr (10mg/ml) for 15-20 minutes, washed in dH_2O and visualized on a UV transilluminator (UVITec, Cambridge, UK). The details of restriction enzymes used for RFLP in this study are given in Table 2.4.

Table 2.4: Details of restriction enzymes used for PCR-RFLP analyses of different genes

Gene/ Mutation	Enzyme	Restriction site	Tempe-rature	Size of uncut PCR product (bp)	Digested products (bp)	
					Normal	Mutant
GUCY2D (Ala353Val; Exon 4)	MaeII (gain of site)	A↓CGT	65^0C	468	468	101 & 367
GUCY2D (Trp640Arg; Exon 9)	BseN1 (loss of site)	ACTGGn↓n	65^0C	587	233 & 354	587
GUCY2D (Gln939X ; Exon 15)	BfaI (gain of site)	C↓TAG	37^0C	295	295	114 & 181
CRB1 (Gln1124X; Exon 9)	SapI (loss of site)	GCTCTTCn↓nnn	37^0C	558	84 & 474	558
NMNAT1 (Leu72His; Exon 3)	Nsp1 (gain of site)	RCATG↓Y	37^0C	512	512	250 & 262

2.9 Polyacrylamide gel electrophoresis (PAGE)

PAGE was performed in a vertical slab gel electrophoresis unit (Hoefer SE 600 Series, Amersham Biosciences, San Francisco, USA). The gel percentage was chosen based on the sizes of the PCR products to be displayed. Polyacrylamide gels of 8-10% were made in a total gel volume of 40 ml, with appropriate volumes of 30% acrylamide stock solution (29:1, acrylamide: bisacrylamide; Sigma-Aldrich, St Louis, USA), and 1X Tris- borate- EDTA (TBE) buffer,(0.09M Tris-borate, 0.002M EDTA; pH 8.3). Polymerization was initiated with 200 µl of 10 % Ammonium persulfate (APS; Sigma, St. Louis, USA) and 35 µl of TEMED (N,N,N',N'-tetramethylene diamine; USB, Cleveland, USA). The contents were mixed and poured in between glass plates (18 x16 cm) separated by 1.5 mm spacers. A 15 well comb was inserted for the formation of wells. After polymerization samples were loaded along with the 6X loading dye (0.25% bromophenol blue, 0.25% xylene cyanol, 40% w/v sucrose) and electrophoresis was done in an vertical electrophoresis unit (Hoefer SE 600 Series, Amersham Biosciences, San Francisco, USA) at a voltage of 80-100 V.

After electrophoresis, the gels were stained with EtBr (10mg/ml) by adding 8-10 µl of it in 1X TBE buffer. The DNA was visualized over a UV transilluminator (UVITec, Cambridge, UK).

2.10 Sequencing PCR

PCR products were sequenced using Big Dye version 3.1 cycle sequencing kit (Applied Biosystems Incorporated, Foster city, CA, USA). Sequencing PCR was set up in a reaction volume of 10 µl with 0.2 µl of Big Dye reaction mix consisting of DNA polymerase, dNTPs and ddNTPs tagged with specific fluorescent dyes, 5X sequencing buffer, 3 pmols of primer and 50-100 ng of amplified PCR product template. Sequencing was performed in a thermal cycler (VeritiTM, Applied Biosystems 9700, USA) with the conditions as mentioned in Table: 2.5

Table 2.5: Thermal cycler Conditions for sequencing PCR

Step	Process	Temperature	Time
Step 1	Initial Denaturation	96^0C	2 minutes
Step 2	Denaturation	96^0C	30 seconds
Step 3	Annealing	50^0C	6 seconds
Step 4	Extension	60^0C	4 minutes
Step 5	Repeat steps 2-4 29 more times		
Step 6	Hold	4^0C	

2.11 Precipitation of sequencing products

Precipitation of sequencing reaction products was performed in a 96 well plate. To the sequencing PCR product (10 µl), 1.0 µl of 0.125M EDTA was added and given a short spin at 1000 rpm. 1µl of 3M sodium acetate (pH 5.2) was added followed by 35 µl of 100% ethanol. The plate was sealed with a plastic flap, centrifuged at 1000 rpm for 10-15sec and incubated on ice for 20 minutes. The plates were centrifuged at 4000 rpm for 30 minutes at 4^0C. The plates were inverted to remove the supernatant completely. Pellets were then washed with 50µl of 70% ethanol followed by centrifugation for 20 minutes at 4000 rpm. Any residual ethanol was decanted as mentioned before. The wells in the plate were allowed to dry completely and the pellets were resuspended in 10 µl of 50% Hidi formamide (Applied Biosystems, Foster City, CA, USA). The samples were denatured at 95˚C for 5 minutes in a thermal cycler and snap chilled on ice.

2.12 Automated DNA sequencing and analysis

2.12.1 Protocol

Sequencing electrophoresis, data collection and analysis were performed on the ABI3130 XL according to the manufacturer's protocol. The plate containing the loaded samples was sealed with septa and placed on the automated DNA sequencer (3130XL Genetic Analyzer, Applied Biosystems Incorporated, Foster city, CA, USA). Details and order of samples loaded was entered into the sample file. The samples

were electrophoresed for the required time based on the size of the PCR product. The program was preset according to the product length. After the electrophoresis was completed electrophorograms were visualized using Chromas software (http://www.technelysium.com.au/chromas.html).

2.12.2 Data Interpretation

The sequences of patient and control DNA were compared with the reference gene sequences available in public databases -NCBI (http://www.ncbi.nlm.nih.gov/gene) and Ensembl (http://www.ensembl.org).

2.13 Prediction of pathogenicity

Variations were categorized as pathogenic or non-pathogenic based on the following criteria – a) absence of the variation in at least 150 unrelated normal control subjects; b) complete segregation of the variation in available family members of the proband. In addition, the potential effects of the sequence changes on the function of the gene were assessed as follows- 1) exonic changes that were predicted as missense substitutions, tools such as Polyphen and SIFT software were employed to interpret the impact of a sequence change on the protein; 2) intronic variants, especially those not involving canonical splice sites at the intron-exon junctions were analyzed by the splice prediction program Human Splicing Finder (http://www.umd.be/HSF) and ESE Finder (http://rulai.cshl.org/cgi-bin/tools/ESE/esefinder.cgi). If they were predicted to affect the protein/ mRNA by the above-mentioned methods in addition to absence in normal control populations and co-segregation with the disease, they were interpreted as pathogenic.

Bio-informatics tools used for prediction of putative effects of sequence changes:

1. Human splicing finder (http://www.umd.be/HSF)- It predicts the effect of mutation on the 5′ss, 3′ss splice sites , branch point and on the auxiliary *cis*-splicing sequences such as exonic splice enhancers (ESE) and exonic splicing silencers (ESS).

2. ESEfinder (http://rulai.cshl.org/cgi-bin/tools/ESE/esefinder.cgi)-It predicts the effect of exonic mutations on exonic splicing enhancer sequences (ESE).

To predict whether a particular amino acid change is likely to be pathogenic or not, two softwares were used-

3. SIFT (http://blocks.fhcrc.org/sift/SIFT.html)- Sorting intolerant from tolerant (SIFT) tool was used to predict the effect of sequence changes on the protein function. This software is based on homology search and the physical properties of the amino acids. This program predicts whether a variation will affect protein function by calculating a scaled probability for the substitution at that position. The probability score is derived from the observed frequencies of amino acids at that particular position in different species. A SIFT score of <0.05 for a substitution is interpreted as not tolerated (i.e., possibly pathogenic).

4. Polyphen (http://genetics.bwh.harvard.edu/pph2/)- Polyphen predicts possible impact of an amino acid substitution on the structure and function of a protein. It then estimates the probability of a missense substitution being damaging based on a combination of sequence-based homology and structure-based properties**.** A mutation is classified as "probably damaging" if its probabilistic score is above 0.85, and "possibly damaging" if the score is above 0.15. Remaining variations (<0.15) are categorized as benign.

Screening of LCA associated genes

Five genes (*GUCY2D, RD3, NMNAT1, CRB1* and *PALS1*) were screened in 100 unrelated probands with LCA and 150 normal controls in order to determine the role of these genes if any, in the pathogenesis of LCA in Indian patients. Out of 100 patients included in this study, 61 were male and 39 were female. About 75% of all probands included in this study were offspring of consanguineous marriages. The majority of patients were residents of Andhra Pradesh (n=74) whereas the remaining were from Maharashtra (n=10), Madhya Pradesh (n=8), West Bengal (n=4), Karnataka (n=3) and Bihar (n=1). Majority of the probands (n=65) did not have a family history (sporadic), where as 35 probands had at least one other affected family member.

3.1 Guanylate cyclase 2D (*GUCY2D*)

The *GUCY2D* gene consists of 19 exons and its open reading frame (ORF) starts in the second exon (Figure 3.1). Bi-directional sequencing of exons 2-19 of the *GUCY2D* gene in 100 probands showed 7 novel and 7 reported variations (Table 3.1).

Two probands LCA72 and LCA105 were homozygous for one of the following missense changes Ala353Val (c.1058C>T) and Trp640Arg (c.1918T>C) respectively (Figure 3.2; A and B). LCA5 and LCA15 harboured two nonsense changes one in each proband at positions Gln791X (c.2371C>T) and Gln939X (c.2815T>A) respectively (Figure 3.2; C and D). A synonymous variation His314His (c.942C>T) was present in 4 probands LCA27, LCA38, LCA57 and LCA64. All four probands were heterozygous for this variation. In addition, a silent change Pro753Pro (c.2259C>T) was detected in one proband, LCA23 who was heterozygous for the same. An intronic novel heterozygous variation c.721+37C>T was present in two probands.

Gln791X and Gln939X are expected to result in truncated proteins and thereby constitute functional null alleles. Ala353 and Trp640 are located in the highly conserved regions of GUCY2D protein (Figure: 3.3).

The potential effects of amino acid substitutions on protein function was assessed with different prediction tools (SIFT and Polyphen). Substitution Ala353Val gave a Polyphen score of 0.921 and a SIFT score of 0.15. Analysis of Trp640Arg yielded a Polyphen score of 0.985 and SIFT score of 0.36. SIFT scores for these two variations were beyond the conventional threshold, predicting these alterations to be tolerated but Polyphen scores predicted these amino acid substitutions to be probably damaging. Taken together, these predictions do not conclusively suggest a pathogenic role for these two substitutions.

The above-mentioned four variations (Ala353Val, Trp640Arg, Gln791X and Gln939X) were screened in family members of the respective probands for co-segregation with the disease (Figure 3.4).

Four members of the family of LCA72 (shown in Figure 3.4A) including the proband's mother, unaffected brother and two affected maternal uncles were screened for homozygous substitution of c.1058C>T (Ala353Val). Blood samples of the proband's father and two siblings (II-4, III-3, III-4) including one affected sibling, were not available for analysis. Both the maternal uncles (II-5, II-7) who were also diagnosed with LCA in our clinic, were homozygous for the same change, c.1058C>T. Mother and brother (II-3 and III-6) were heterozygous for this change (Figure 3.4A).

All members of the family of LCA105 including father, mother and one unaffected brother of the proband were screened for change c.1918T>C (Trp640Arg). All the three members were heterozygous for this change (Figure 3.4B)

Similarly co-segregation analysis for c.2371C>T (Gln791X) variation was carried out in family of LCA5 in father, mother and unaffected sibling (I-1, I-2, II-2) of the proband (Figure 3.4C). The blood sample of the affected sister could not be collected. Both the parents and unaffected sibling were heterozygous for c.2371C>T (Gln791X).

The mother of proband LCA15 was heterozygous for the c.2815A>T (Gln939X) (Figure 3.4D). Other family members could not be recruited.

These 4 sequence changes in the *GUCY2D* gene (c.1058C>T, c.1918T>C, c.2371C>T and c.2815A>T) were absent in a normal control population of 150 unrelated individuals by either PCR-RFLP or direct sequencing (as detailed in Chapter 2).

Absence of these variations in 150 unrelated normal controls and co-segregation in family members provided support for the idea that they are pathogenic.

An intronic change c.1956+21G>T; intron 9, was present in two homozygous probands (LCA27 and LCA74) and was absent in 150 normal controls. This variations was not reported in any database at the time of analysis. Bioinformatics analysis was employed to predict the consequence of this intronic change on splicing pattern using Human Splice Finder (http://www.umd.be/HSF) software. This analysis predicted the activation of a cryptic splice acceptor site with a consensus score of (78.38), which would be expected to lead to a premature termination. No difference in splicing pattern was observed between wild type and mutant clones using minigene construct (data not shown here). The frequency of this variation is 0.01 which indicate that it is a rare non-pathogenic variation.

This variation reported in the 1000 Genomes Database (rs139731548) with the frequency of 0.01. This indicates that it is a rare non-pathogenic variation.

Table 3.1: Variations observed in the *GUCY2D* gene.

S.N.	Exon/ Intron	cDNA change	Amino acid change	Novel/ Reported	No. of patients with variation	MAF*	Reference
1	Intron 2	c.721+37C>T	-	Novel	2 Heterozygous	-	
2	Exon 3	c.741C>T	His247His	rs3829789	4 Heterozygous	0.02 -0.24	1000 G, ESP
3	Exon 3	c.942C>T	His314His	Novel	4 Heterozygous	-	
4	Exon 4	c.1058C>T	Ala353Val	Novel	1 Homozygous	-	
5	Exon 9	c.1918T>C	Trp640Arg	Novel	1 Homozygous	-	
6	Intron 9	c.1956+21G>T	-	rs139731548	2 Homozygous	0.002-0.083	1000 G, ESP
7	Intron 9	c.1956+27C>T	-	rs368301973	23 Heterozygous	0.002	ESP,
8	Intron 10	c.2114+34G>A	-	rs112764660	1 Homozygous 2 Heterozygous	0.006	1000 G
9	Exon 11	c.2259C>T	Pro753Pro	Novel	1 Heterozygous	-	
10	Exon 12	c.2345C>T	Leu782His	rs8069344	1 Homozygous 6 Heterozygous	0.061-0.505	1000 G ESP, HapMap
11	Exon 12	c.2371C>T	Gln791X	Novel	1 Homozygous	-	
12	Intron 13	c.2576+37G>T	-	rs12103471	1 Homozygous 3 Heterozygous	0.030-0.361	1000 G, ESP
13	Exon 14	c.2577G>T	Pro859Pro	rs112372281	2 Homozygous 4 Heterozygous	0.005-0.026	1000 G, ESP
14	Exon 15	c.2815T>A	Gln939X	Novel	1 Homozygous	-	

*MAF- minor allele frequency. Source of allele frequencies- Ensembl genome browser (http://asia.ensembl.org) 1000G-1000 genomes browser (http://browser.1000genomes.org/), ESP-Exome Sequencing Project (http://evs.gs.washington.edu/EVS/) and HapMap -HapMap database (http://hapmap.ncbi.nlm.nih.gov/).

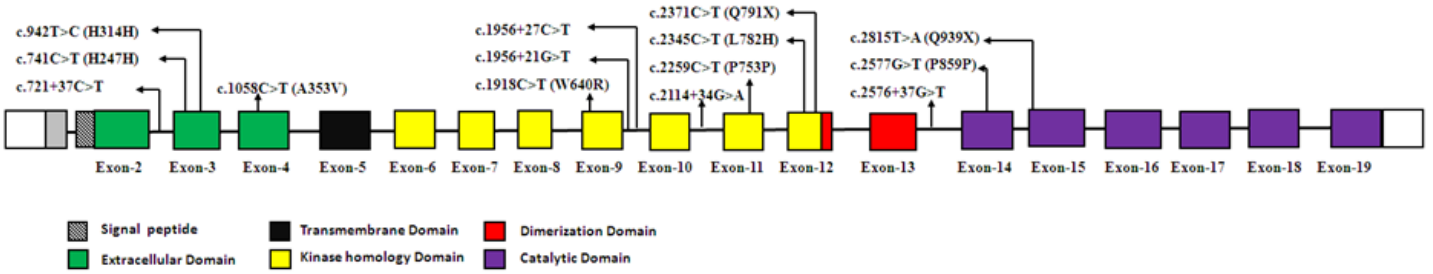

Figure 3.1: Schematic representation of the *GUCY2D* gene with all the variations identified in this study.

The filled boxes represent the coding region whereas the open boxes represent the untranslated regions of the gene. Protein motifs are shown by colored boxes. Grey shaded box is exon 1. Reference for domains: (Shyjan, de Sauvage et al. 1992).

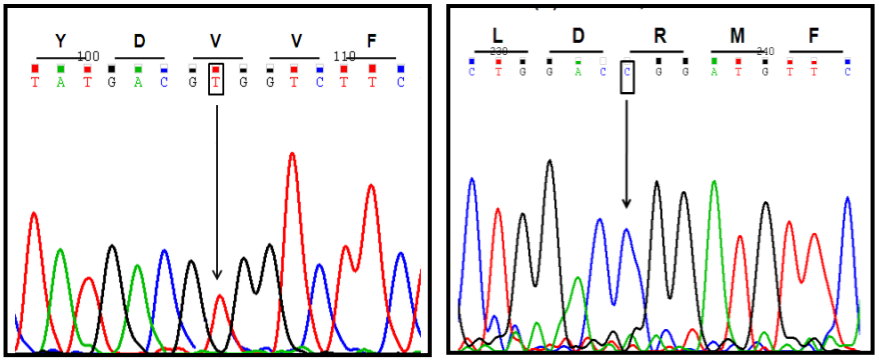

(A) LCA72 (c.1058C>T; Ala353Val) **(B) LCA105 (c.1918T>C; Trp640Arg)**

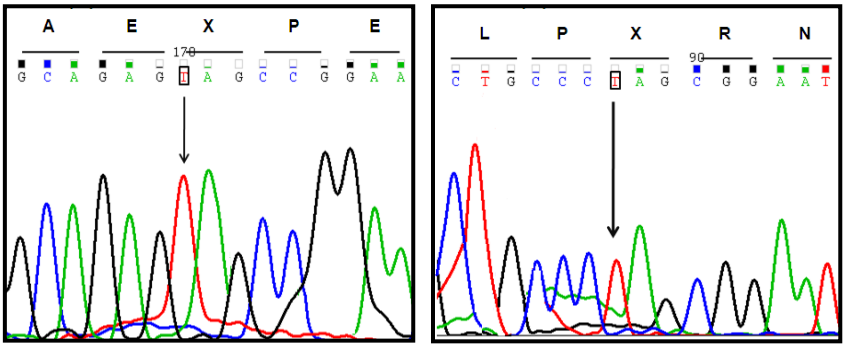

(C) LCA5 (c.2371 C>T; Gln791X) **(D) LCA15 (c.2815 A>T; Gln939X)**

Figure 3.2: Sequence electrophorograms showing pathogenic sequence changes (indicated by arrows) in the *GUCY2D* gene in LCA probands.

Codons are indicated by dashes above the sequence, with the corresponding amino acids.

	A353V	W640R
Homo sapiens|NP_000171.1	LQQVSPLFGTIYDAVFLLARGV	AQREIKLDWMFKSSLLLDLIK
Mus musculus|NP_001124165.1	PEQVSPLFGTIYDAVILLAHALN	QNENLRLDWTFKASLLLDLIR
Rattus norvegicus|XP_006229772.1	PEQVSPLFGTIYDAVILLAHALN	RNEDLRLDWTFKASLLLDLIR
Xenopus tropicalis|XP_002942678.2	PTEVSPLFATIYNSYLLGATAD	QNQDMKLDWMFKSSLLLDLIK
Pan troglodytes|XP_003315414.1	LQQVSPLFGTIYDAVFLLARGV	AQREIKLDWMFKSSLLLDLIK
Macaca mulatta|XP_001111670.1	LQQVSPLFGTIYDAVFLLVRGV	AQREIKLDWMFKSSLLLDLIK
Equus caballus|XP_005597817.1	LQQVSPLFGTIYDAVYLLAGGV	AQRDIKLDWMFKSSLLLDLIK
Canis lupusfamiliaris|NP_001003207.1	LQQVSPFFGTIYDAVLLLAGGV	AQRDIKLDWMFKSSLLLDLIK

Figure 3.3: Multiple sequence alignment of GUCY2D protein from different species. Two mutated residues, alanine at position 353 and tryptophan at 640, are boxed across different species.

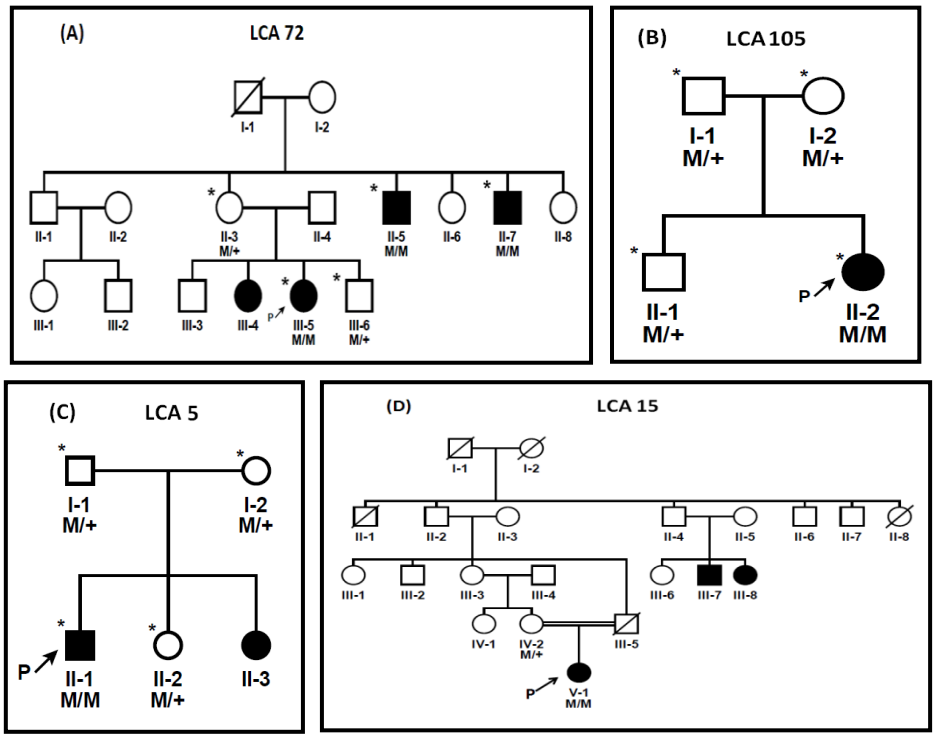

Figure 3.4: Pedigrees of LCA families with homozygous mutations in *GUCY2D*

Affected and unaffected members are represented by solid and open symbols respectively. Squares and circles represent males and females respectively. The proband is indicated by an arrow. Individuals that were tested are shown by asterisks '*'. M denotes the specific mutant and plus sign (+) denotes the wild type allele present in a family.

Clinical features of LCA probands with mutations in *GUCY2D*

Family LCA72 (Ala353Val): The proband was first seen in our clinic at the age of 6 years with complaints of vision loss. Her vision was counting fingers at 50 cm in both the eyes. She also had nystagmus, sluggishly reacting pupils, amblyopia and astigmatism. Fundus examination showed diffuse RPE degeneration and macular coloboma. Electroretinographic (ERG) responses were extinguished. Two maternal

uncles (II.5 and II.7 in Figure 3.4) who were also affected were homozygous for this mutation. Both of them had vision loss since birth, nystagmus and hyperopia. Patient II.7 also had keratoconous and eye poking behaviour.

Family LCA105 (Trp640Arg): The proband was diagnosed with LCA at the age of 3 months and had non-fixation of the eyes (nystagmus), eye poking and was hyperopic. Pupillary responses were relatively sluggish in both eyes and ERG responses were extinguished. On fundus examination, optic discs appeared to be within normal limits but arterial narrowing was present. RPE degeneration was diffuse and widespread in all over retina.

Family LCA5 (Gln791X): The proband presented at the retina clinic of our institution at the age of 3 months with a history of vision loss since birth. Examination showed optic disc pallor with macular and peripheral pigmentation and macular atrophy. Visual acuity was <20/200 in both the eyes. Additionally the proband had cataract in his left eye. Subsequently one of his younger sisters was also diagnosed with LCA. But molecular analysis could not be done due to unavailability of the blood sample.

Family LCA15 (Gln939X): This proband was diagnosed as having LCA at the age of 10 months. He had typical features of LCA such as vision loss since birth, eye poking, nystagmus, and hyperopia. Fundus evaluation showed RPE degeneration, pale optic disc and arterial narrowing. Additionally, this patient showed symptoms of mental retardation and developmental delay.

3.2 Retinal degeneration 3 (*RD3*)

The two coding exons (exons 2 and 3) of the *RD3* gene were screened. Figure 3.5 shows the gene structure with all the variations identified in this study. Four non-synonymous sequence changes were detected in 5 probands, all heterozygous (Table 3.2). These included one novel missense change, Arg47His (c.140G>A) in exon 2 of

the *RD3* gene in family LCA138. A second mutated allele could not be identified in this proband.

Other changes found in *RD3* include a heterozygous change c.191C>T (Ala64Val) in exon 2 found in proband LCA62. A SNP rs148242709, involving c.101C>T with amino acid change of Thr34Met was found in two probands, both heterozygous for the same. Another single nucleotide polymorphism, c.139C>T (Arg47Cys; rs34049451), was identified in only one proband, who was also heterozygous for this change.

Table 3.2: Variations observed in *RD3* gene

S.N.	Exon/Intron	cDNA Change	Amino acid Change	Novel/ Reported	No. of patients with variation	MAF*	Reference
1	Exon 2	c.101C>T	Thr34Met	rs148242709	2 Heterozygous	0.003-0.008	1000G,ESP
2	Exon 2	c.139C>T	Arg47Cys	rs34049451	1 Heterozygous	0.003-0.026	1000G,ESP
3	Exon 2	c.140G>A	Arg47His	Novel	1 Heterozygous	-	
4	Exon 2	c.191C>T	Ala64Val	COSM1172101[#]	1 Heterozygous	NA	COSMIC

Details of variations identified in *RD3* gene. *MAF- minor allele frequency, NA- not available. Source of allele frequencies- Ensembl genome browser (http://asia.ensembl.org), 1000G-1000 genomes browser (http://browser.1000genomes.org/), ESP-Exome Sequencing Project (http://evs.gs.washington.edu/EVS/), HapMap -HapMap database (http://hapmap.ncbi.nlm.nih.gov/) and .COSMIC-Catalogue of somatic mutations in cancer (http://cancer.sanger.ac.uk/cancergenome/projects/cosmic/).

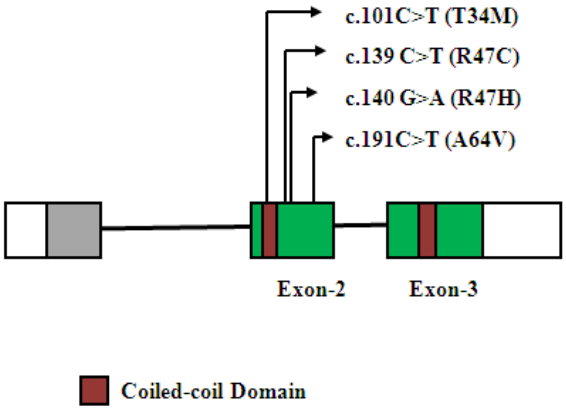

Figure 3.5: Schematic representation of the *RD3* gene showing the variations identified in this study.

The filled boxes represent the coding regions whereas the open boxes represent the untranslated region of the gene. Protein motifs are shown with colored boxes. Grey shaded box is exon 1. Reference for domains: (Friedman, Chang *et al.*2006).

3.3 Crumbs, Drosophila, Homolog of, 1 (*CRB1*)

Screening of 12 exons of *CRB1* gene revealed 7 novel variations, 4 of which were exonic and 3 were intronic variations. Figure 3.6 shows the graphic representation of *CRB1* gene and variations identified in this gene in our cohort. Details of these variations are given in Table 3.3

The exonic variations included two nonsense mutations -c.3579C>T (Gln1124X) and c.4016C>A (Tyr1269X). These mutations were found in 1 proband each, both of which were homozygous for the respective mutation. These 2 mutations co-segregated with the disease in family members who were tested (Figure-3.7). Both the parents and unaffected brother of LCA30 was screened for the c.3579C>T (Gln1124X) variation. All three family members were heterozygous for this change. In LCA40 family father and affected brother was analysed for c.4016C>A (Tyr1269X) variation. Mother's blood sample was not available for the analysis.

Father was found to be heterozygous and the affected brother was homozygous for the same variation (Tyr1269X).

Screening of 150 unrelated normal controls by PCR-RFLP / direct sequency revealed that these two variations were absent in controls.

Two patients (families LCA55 and LCA117) were heterozygous for either of two novel exonic variations Val243Glyfs*97 and S359A. The other mutant allele was not identified in both these cases. Three intronic variations (c.70+124insT, c.989-74C>T and c.989-72A>T) were also observed. Probands were heterozygous for these variations which were not reported previously. The details of 7 polymorphic changes, observed in our cohort in the *CRB1* gene are shown in Table 3.3

Table 3.3: Variations identified in the *CRB1* gene

S.N.	Exon/ Intron	cDNA Change	Amino acid Change	Novel/ Reported	No. of patients with variation	MAF	Reference
1	Intron 1	c.70+124insT	-	Novel	1 Heterozygous	-	
2	Intron 1	c.71-12A>T		rs12042179	27 Homozygous 19 Heterozygous	0.011-0.758	1000G,ESP
3	Exon 3	c.728delT	Val243Glyfs*97	Novel	1 Heterozygous	-	
4	Intron 3	c.849-62T>G	-	rs1572514	8 Heterozygous	0.006-0.721	1000G,HapMap
5	Intron 3	c.849-35T>C		rs1337167	1 Homozygous 5 Heterozygous	0.042-0.300	1000G,ESP, HapMap
6	Intron 4	c.988+35C>T	-	rs2275251	4 Homozygous 3 Heterozygous	0.009-0.180	1000G,ESP, HapMap
7	Intron 4	c.989-74C>T	-	Novel	2 Heterozygous	-	
8	Intron 4	c.989-72A>T	-	Novel	1 Heterozygous	-	
9	Intron 4	c.989-64T>C	-	rs148281370	1 Heterozygous	0.001-0.009	1000G
10	Intron 4	c.989-53T>G	-	rs2786098	1 Homozygous 19 Heterozygous	0.044-0.292	1000G, HapMap
11	Exon 5	c.1075T>G	Ser359Ala	Novel	1 Heterozygous	-	
12	Exon 6	c.1410A>G	Leu470Leu	rs3902057	2 Homozygous	0.001-0.314	1000G,ESP, HapMap
13	Exon 9	c.3579C>T	Gln1124X	Novel	1 Homozygous	-	
14	Exon 10	c.4016C>A	Tyr1269X	Novel	1 Homozygous	-	

Source of allele frequencies-Ensembl genome browser, 1000 genomes browser, ESP-Exome Sequencing Project and HapMap database.

*MAF- minor allele frequency, NA- not available

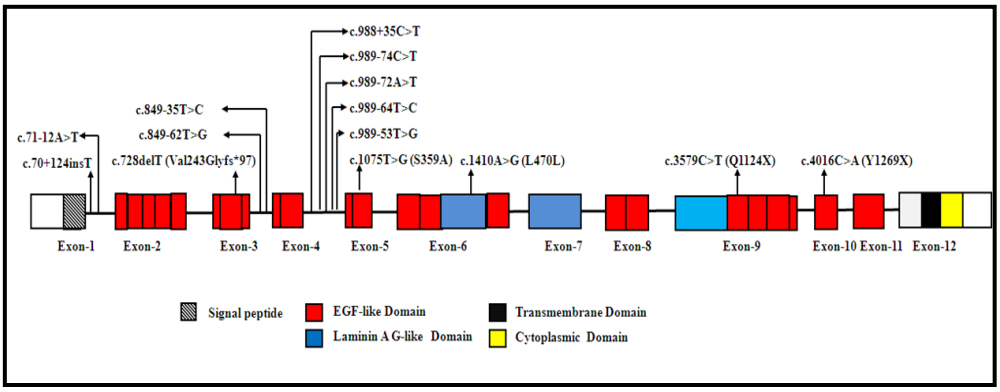

Figure 3.6: Schematic representation of the *CRB1* gene showing all the variations identified in this study.

The filled boxes represent the coding regions whereas the open boxes represent the untranslated region of the gene. Protein motifs are shown with colored boxes. References for the domains :(den Hollander, ten Brink et al. 1999).

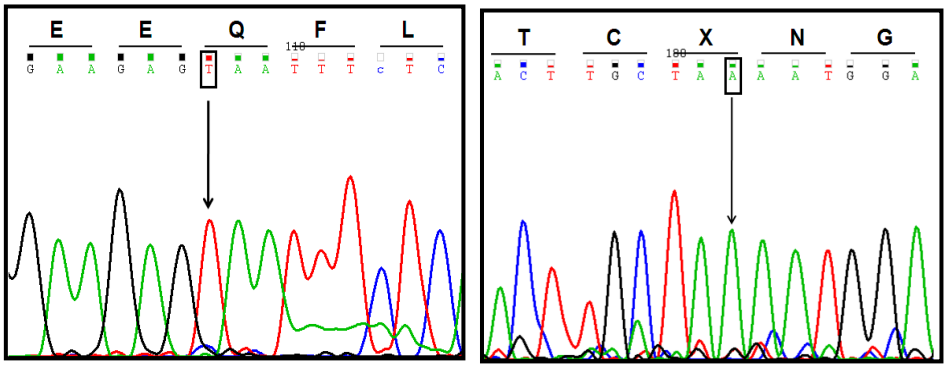

(A) LCA30 (c.3579C>T;Gln1124X) **(B) LCA40 (c.4016C>A;Tyr1269X)**

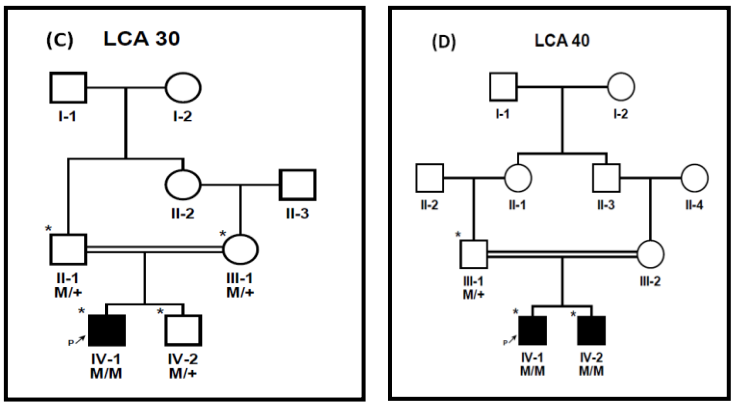

Figure 3.7: Sequence electrophorograms showing pathogenic sequence changes in *CRB1* gene in LCA families (A and B); Pedigrees of LCA families with homozygous pathogenic mutations in *CRB1* gene (C and D).

M denotes the specific mutant allele and plus sign (+) denotes the wild type allele present in that family.

Clinical features of patients with *CRB1* mutations

Family LCA30: The proband from family LCA30 having mutation Gln1124X presented to the clinic at the age of 6 years. He was born to unaffected consanguineously married parents and had an unaffected younger brother with myopic astigmatism and an otherwise normal eye examination. Genetic analysis of both the parents and the unaffected brother revealed that all of them were heterozygous for the Gln1124X gene mutation. The proband reportedly had visual loss and squint since birth with eye poking behaviour since childhood. He also had nystagmus wandering fixation with alternate esotropia and very sluggishly reacting pupils. Fundus evaluation showed diffuse RPE degeneration all over, arterial narrowing, disc pallor, partial macular atrophy with sclerosis of choriodal vessels, perivascular sparing of RPE degeneration especially in the periphery (Figure. 3.8. A and B). OCT showed an abnormal lamination pattern with increased foveal thickness of 276 µm (normal upto-190 µm). However imaging was difficult and imprecise due to poor vision and nystagmus (Figure.3.8.C)

Family LCA40: The 2nd proband (Family LCA40) with a mutation in *CRB1* had the Tyr1269X change and first presented to our clinic at the age of 10 years. The father and an affected brother were examined. The father was a heterozygous carrier whereas the brother was homozygous for the same mutation. Examination of proband revealed jerky nystagmus, ptosis of left upper eyelid, sluggishly reacting pupils, and a clear lens. Fundus evaluation showed diffuse RPE degeneration all over sparing the macular area; white spots and disc pallor (Figure 3.8.D).The affected brother had the same phenotype but no ptosis.

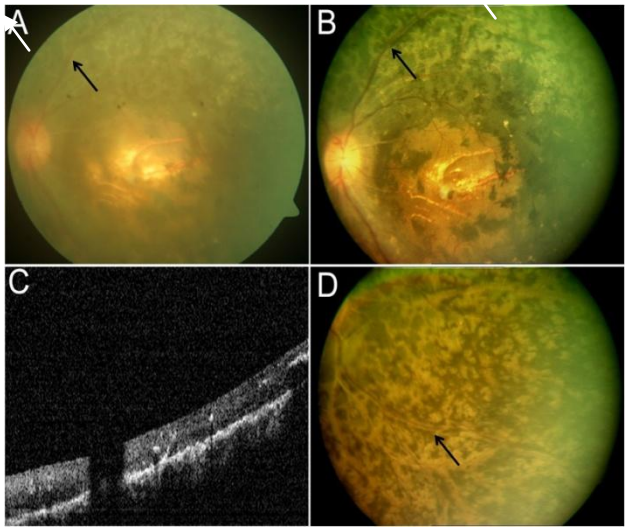

Figure 3.8: Fundus photographs of LCA30 (A and B) and LCA 40 (D), optical coherence tomography of patient 30 (C).

A- Patient at 12 years of age shows perivascular sparing of RPE degeneration especially in the periphery, arterial narrowing, disc pallor, partial macular atrophy with sclerosis of choriodal vessels. **B-** Fundus photograph of the same patient at the age of 22 years showing increased macular degeneration and pigmentation with persistence of the unusual perivascular sparing. Arrow indicates perivascular sparing. **C**- OCT image of proband from LCA30 showing delamination of the retina with increased retinal thickening and loss of foveal contour. **D-** Proband LCA40 (aged 10 yrs) shows perivascular sparing of RPE degeneration and white spots as indicated by arrow.

3.4. Membrane protein palmitoylated 5 (*MPP5/PALS1*)

The *PALS1* gene was selected in this study as a candidate gene for LCA because it is part of the Crumbs complex (van Rossum, Aartsen et al. 2006) and *Pals1* conditional knock-out mice exhibit features similar to human LCA phenotypes (Cho, Kim et al. 2012). No studies have reported mutations in the *PALS1* gene in LCA patients till date.

In the present study, the *PALS1* gene was screened in 100 LCA probands, to investigate its role if any, in the causation of human LCA.

A graphical representation of the *PALS1* gene with all the variations identified is given in Figure 3.9. Screening of coding regions of the *PALS1* gene revealed eight SNPs - rs140810601, rs7144928, rs12588292, rs12588355, rs5809338, rs1475128, rs1475129 and rs143175731 (Table 3.4).

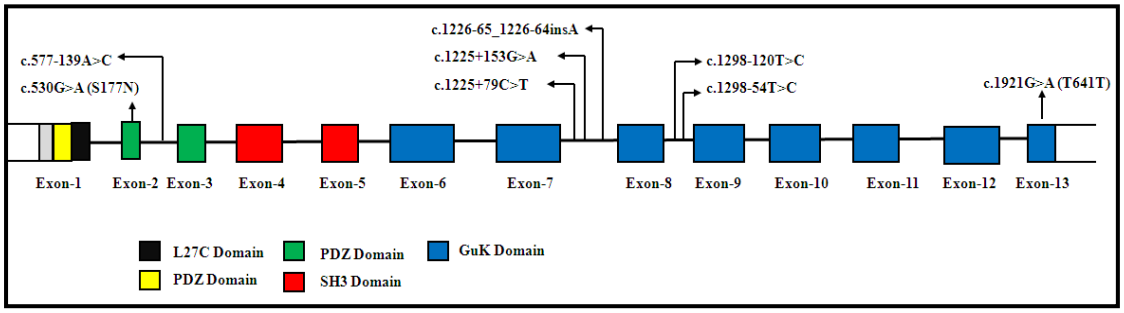

Figure 3.9: Schematic representation of the *PALS1* gene with all the variations identified in this study.

The filled boxes represent the coding region whereas the open boxes represent the untranslated regions of the gene. Protein domains are shown with colored boxes. Reference for domains (Kamberov, Makarova et al. 2000).

Table 3.4: Variants identified in the *PALS1* gene

S.N.	Exon/ Intron	cDNA change	Amino acid change	Database Identifier	No. of probands with variation	MAF	Reference
1	Exon2	c.530G>A	Ser177Asn	rs140810601	1 heterozygous	0.001-0.008	1000G, ESP
2	Intron 2	c.577-139A>C	-	rs7144928	5 homozygous 3 heterozygous	0.008-0.500	1000G
3	Intron 7	c.1225+79C>T	-	rs12588292	3 homozygous 7 heterozygous	0.066-0.608	1000G, HapMap
4	Intron 7	c.1225+153G>A	-	rs12588355	1 homozygous 13 heterozygous	0.017-0.50	1000G
5	Intron 7	c.1226-65_1226-64insA	-	rs5809338	5 homozygous 41 heterozygous	0.024-0.515	1000G
6	Intron 8	c.1298-120T>C	-	rs1475129	1 homozygous	0.24-0.510	1000G
7	Intron 8	c.1298-54T>C	-	rs1475128	2 homozygous	0.024-0.505	1000G,ESP
8	Exon13	c.1921G>A	Thr641Thr	rs143175731	5 heterozygous	0.002-0.005	1000G

Details of variations identified in the *PALS1* gene. Source of allele frequencies- Ensembl genome browser, 1000 genomes browser, ESP- Exome Sequencing Project and HapMap database. *MAF- minor allele frequency, NA- not available

3.5. Nicotinamide mononucleotide adenylyltransferase 1 (*NMNAT1*)

The *NMNAT1* gene encoding the enzyme nicotinamide mononucleotide adenylyltransferase, involved in biosynthesis of nicotinamide adenine dinucleotide (NAD^+) via the salvage pathway, was screened in this study in collaboration with Eric Pierce and co-workers (Harvard Medical School, Boston, Massachusetts, USA), who identified mutations in two Pakistani siblings by exome sequencing (Falk, Zhang et al. 2012)

Screening of 100 probands with LCA for variations in the *NMNAT1* gene revealed 3 novel missense changes in 3 unrelated probands, all homozygous for these changes (Table 3.5; Figure 3.10). These included Val9Met (c.25G>A) in family LCA73; Asp33Gly (c.98A>G) in family LCA79; and Leu72His (c.215T>A) in family LCA128 (Figure 3.11). In addition, proband LCA100 harboured compound heterozygous variations c.565delG (Ala189Leufs*25) and c.709C>T (Arg237Cys) (Figure 3.11). Val178Met (c.532G>A) was identified in 1 proband, who was heterozygous for the change.

All the above changes co-segregated in the family members tested (Figure 3.12). The proband from LCA73 (c.25G>A) presented to the clinic at the age of 1.5 years. Mutational analysis of the proband and both parents was done. It revealed that the parents were heterozygous for the Val9Met (c.25G>A) mutation at (Figure 3.12A).

The proband from LCA79 was born to unaffected consanguineously married parents. This proband was homozygous for c.98 A>G resulting in Asp33Gly. Screening of both the parents revealed that both were heterozygous for this change (Figure 3.12B).

c.215T>A (Leu72His) change was present in proband LCA128. Both the parents were heterozygous for the substitution c.215 T>A (Figure 3.12 C).

In family LCA100, the proband carried compound heterozygous variants-c.565delG (Ala189Leufs*25) and c.709C>T (Arg237Cys) and both the parents were screened for the co-segregation of these variations. Father was heterozygous for c.709C>T

(Arg237Cys) variation and mother was heterozygous for the c.565delG (Ala189Leufs*25) variation (Figure 3.12D).

Amino acids affected by the mutations including Val9, Asp33, Leu72, Val178 and Arg237 are conserved across species in the NMNAT1 protein (shown in Figure: 3.13).

SIFT analysis of Asp33Gly, Leu72His and Arg237Cys predicted that all the 3 variations are damaging with SIFT score of 0.00. The PolyPhen analysis also supported these results with a PolyPhen score of 1.00, interpreted as probably damaging, for all 3 variations. Similarly SIFT and PolyPhen analyses for variant Val9Met gave scores of 0.01 and 0.0983 respectively, also predicted to be probably damaging.

Screening of 150 unrelated normal controls for all the above variations was done by direct sequencing or PCR-RFLP (details are given in Table 2.4; Chapter 2).

Absence of these variations in 150 unrelated normal controls and co-segregation with the disease phenotype in family members supports the conclusion that these mutations are pathogenic.

Two mutations Val9Met and Arg237Cys were not identified in our control population. However Arg237Cys variation is reported in exome sequencing database (http://evs.gs.washington.edu/EVS/) with allele frequency of 0.01% in European American and African American population. Val9Met is not reported in EVS database.

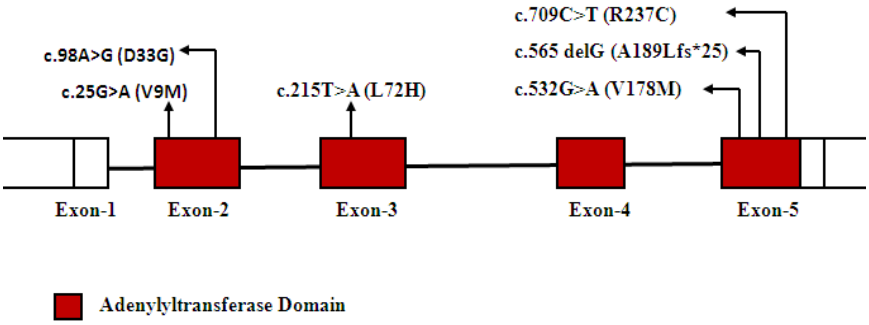

Figure 3.10: Schematic representation of the *NMNAT1* gene with all the variations identified in this study.

The filled boxes represent the coding regions whereas the open boxes represent the untranslated regions of the gene. Protein domains are shown with colored boxes. Reference for domain- (Koenekoop, Wang et al. 2012).

Table 3.5: Variations identified in the *NMNAT1* gene

S.N.	Exon/Intron	cDNA change	Amino acid change	Novel/ Reported	No. of probands with variation
1	Exon 2	c.25G>A	Val9Met	rs387907294*	1Homozygous
2	Exon 2	c.98A>G	Asp33Gly	Novel	1Homozygous
3	Exon 3	c.215T>A	Leu72His	Novel	1Homozygous
4	Exon 5	c.532G>A	Val178Met	Novel	1Heterozygous
5	Exon 5	c.565delG	Ala189Leufs*25	Novel	1Compound Heterozygous
6		c.709C>T	Arg237Cys	rs375110174*	

Details of variations identified in *NMNAT1* gene. * indicates that these variations were not identified in our control population.

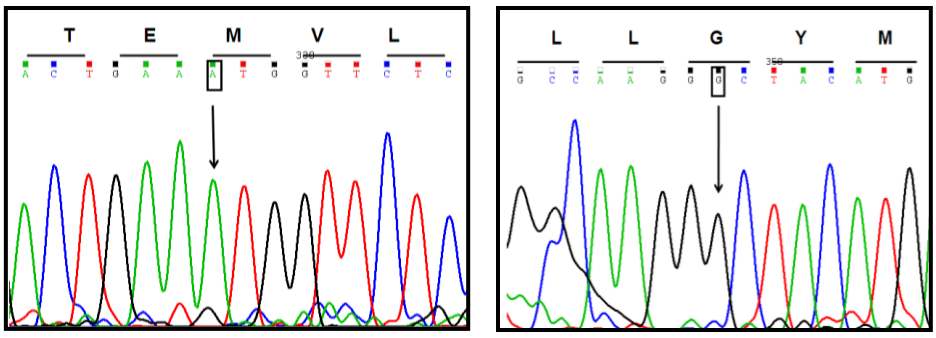

(A) LCA73 (c.25G>A;Val9Met) **(B) LCA79 (c.98A>G; Asp33Gly)**

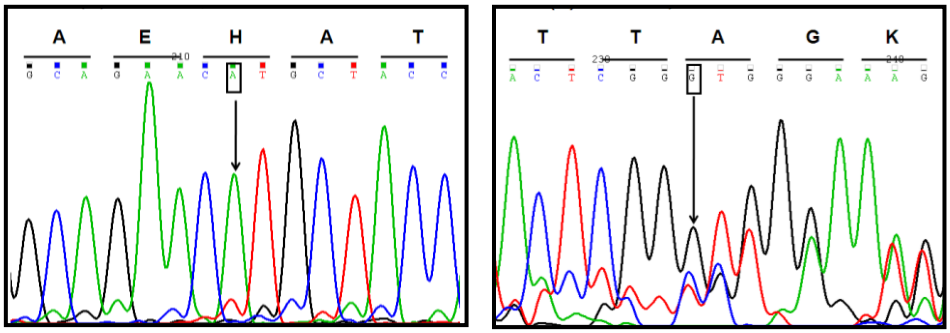

(C) LCA128 (c.215T>A; Leu72His) **(D) LCA100 (c.565delG; Ala189Leufs*25)**

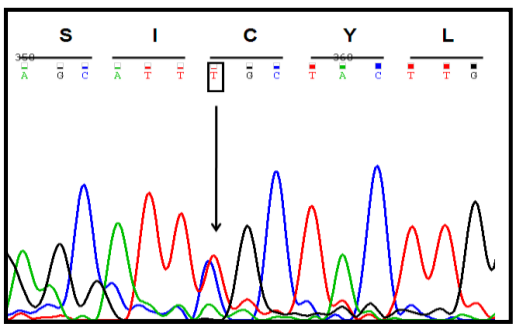

(E) LCA100 (c.709C>T; Arg237Cys)

Figure 3.11: Sequence electropherograms showing pathogenic sequence changes in *NMNAT1* gene in LCA families. Family numbers and sequence changes are shown below each panel and codons in the sequence are indicated by dashes above, along with amino acids encoded.

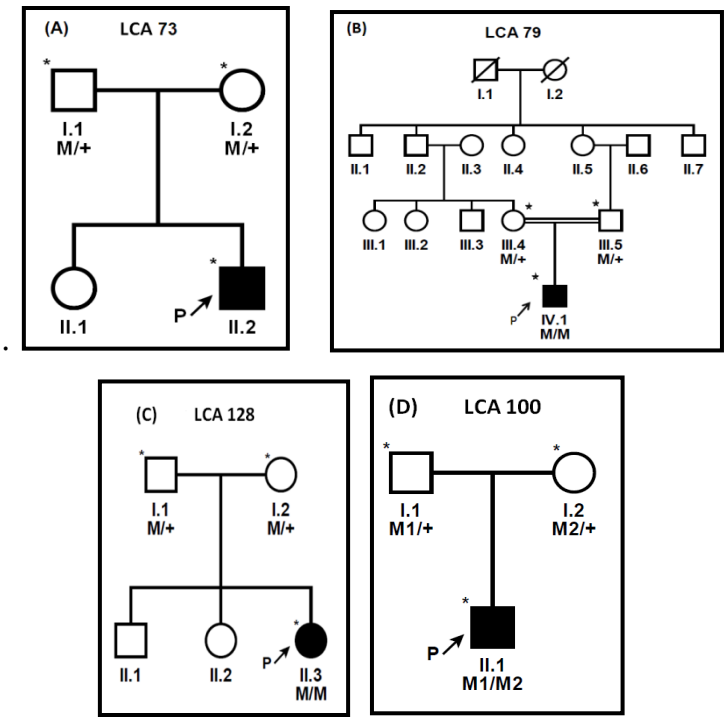

Figure 3.12: Pedigrees of LCA families with pathogenic mutations in *NMNAT1* gene showing affected (solid symbols) and unaffected members (open symbols). The proband in each family is indicated by an arrow. Individuals that were tested are shown by asterisks '*'.Squares and circles represent males and females respectively. M denotes the specific mutant and plus sign (+) denotes the wild type allele present in that family. In case of LCA100, M1 denotes- c.709C>T (Arg237Cys) and M2- c.565delG (Ala189Leufs*25).

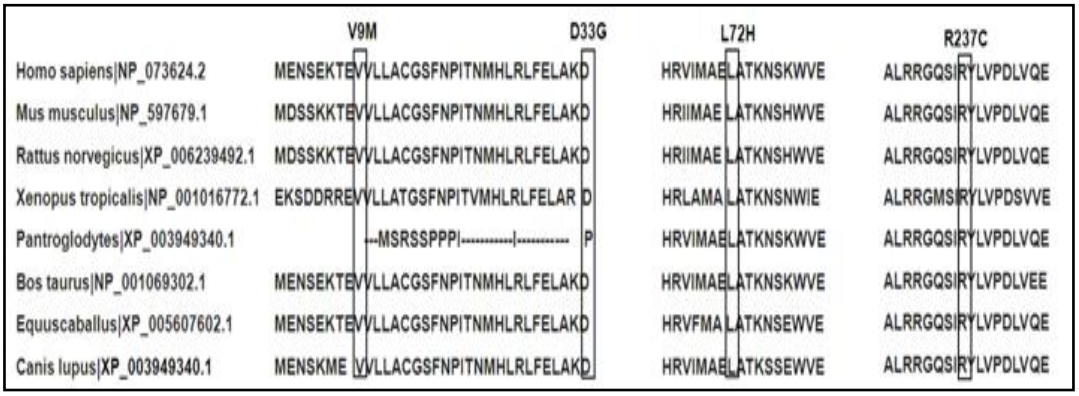

Figure 3.13: Multiple sequence alignment of NMNAT1 protein from different species showing the conservation of amino acids across different species.

The mutated residues are boxed across different species.

Clinical features of patients with *NMNAT1* mutations

Family LCA73: Val9Met mutation was present in the proband from family LCA73, diagnosed at 5 months of age with LCA. He had vision loss since birth with nystagmus. Retinal examination showed the presence of minimal disc pallor, moderate arterial narrowing and diffuse RPE degeneration all over with sparse pigment migration in the periphery of the retina. The macular area showed an atrophic scar of about 1.5 disc diameters in size. The retina around the macular atrophic scar at the posterior pole appeared normal.

Family LCA79: The Asp33Gly mutation was identified in proband from family LCA79 who presented at one year of age. The patient's vision was limited to perception of light. Retinal examination showed moderate disc pallor, moderate arterial narrowing and diffuse RPE degeneration with sparse pigment migration in the periphery of the retina. The macular area showed pigment clumps and RPE degenerative changes of about 2 disc diameters around the fovea but no obvious coloboma at this age. He also reportedly had developmental delay.

Family LCA128: The proband from family LCA128 had mutation Leu72His and presented at 4 years of age. Her visual acuities were 20/380 and 20/150 in the right and left eyes respectively. Retinal examination showed presence of minimal disc pallor, moderate arterial narrowing, diffuse and coarse RPE degeneration all over with sparse pigment migration in periphery. There was more than 3 disc diameter area of macular excavation with pigment hypertrophy at the edges and an atrophic base suggestive of macular coloboma. The retinas of both eyes showed macular colobomata at the posterior pole with the rest of the retina looking essentially normal.

Family LCA100: The proband from family LCA 100 carried compound heterozygous variations -c.565delG (Ala189Leufs*25) and c.709C>T (Arg237 Cys). The proband was diagnosed with LCA at the age of 8 months. The patient was able to perceive light and had hyperopia of + 9.5 dioptors. Retinal examination showed the

presence of minimal disc pallor, moderate arterial narrowing RPE degeneration and macular coloboma (Figure 3.14).

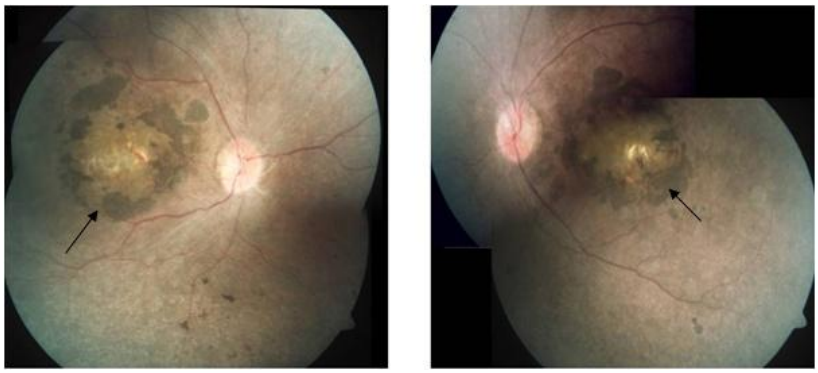

Figure 3.14: Fundus images of a patient LCA100

Fundus images of LCA 100 with mutations in *NMNAT1* gene showing disc pallor, arterial narrowing, diffuse RPE degeneration all over with sparse pigment migration in periphery and macular coloboma as shown by arrow.

Overall involvement of the candidate genes tested in LCA pathogenesis in Indian patients

For the 5 genes (*GUCY2D*, *RD3*, *CRB1*, *PALS1* and *NMNAT1*) screened in 100 unrelated Indian probands with LCA in this study, we identified mutations in a total of 10% (10/100) of cases. *GUCY2D* and *NMNAT1* contributed equally with mutations in 4% of patients in each of the genes whereas *CRB1* gene mutations accounted for 2% of cases. There were no pathogenic changes found in the *RD3* and *PALS1* genes suggesting that they are not significant causes of LCA in our population. A summary of all patients with novel pathogenic mutations and their clinical features is given in Table 3.6.

Table 3.6: Clinical features of LCA probands with homozygous or compound heterozygous variations in the various genes tested

Family ID / Patient ID	Gene/ Mutation	SIFT score	PolyPhen score	Age of presentation	Disease phenotype	Fundus	Visual acuity	Refraction	ERG
LCA72 (III.5)	*GUCY2D* (A353V)	0.15	0.921	6 years	Subnormal vision since birth, nystagmus, astigmatism, amblyopia	RPE degeneration	CF -0.5 Meter	+5.5 D (OU)	Extinguished ERG
LCA105 (II.2)	*GUCY2D* (W640R)	0.36	0.985	3 months	Nystagmus, photophobia	RPE degeneration	Non-oriented LP	+5.78 D (OU)	Extinguished ERG
LCA5 (II.1)	*GUCY2D* (Gln791X)	-	-	3 months	Vision loss since birth, eye poking, nystagmus, compound hyperopic, astigmatism, photophobia	Macular and peripheral pigments/ atrophy and disc pallor	CB	-	Extinguished ERG
LCA15 (V.1)	*GUCY2D* (Gln939X)	-	-	10 months	Visual loss since birth , nystagmus, eye poking	RPE degeneration	LP	+3.5 D (OU)	NA

LCA30 (IV.1)	*CRB1* (Gln1124X)	-	-	6 years	Vision loss since birth, squint, eye poking, alternate esotropia	Diffuse RPE degeneration, arterial narrowing, disc pallor, preserved para arteriolar RPE degeneration, increased foveal thickness	LP	-3.75 D (OD) -4.50 D (OS)	Extinguished ERG
LCA40 (IV.1)	*CRB1* (Tyr1269X)	-	-	10 years	Vision loss since birth, tosis of upper eye lid, sluggishly reacting pupil	Diffuse RPE degeneration, white spots and disc pallor, PPRPE	Non-oriented LP	+2.00 D (OU)	NA
LCA73 (II.2)	*NMNAT1* (Val9Met)	.01	0.983	5 months	Nystagmus, disc pallor	Minimal disc pallor, moderate arterial narrowing, diffuse arterial degeneration all over with sparse pigment migration in periphery	LP	+6.00 D (OD) +7.00 D (OS)	NA
LCA79 (IV.1)	*NMNAT1* (Asp33Gly)	0.00	1.00	1 years	Motor developmental delay, nystagmus	Moderate disc pallor, moderate arterial narrowing, diffuse and coarse RPE degeneration all over with sparse pigment migration in periphery	Non-oriented LP	+5.00 D (OU)	NA

LCA128 (II.3)	*NMNAT1* (Leu72His)	0.00	1.00	4 years	Nystagmus, minimum cone flicker,	Moderate arterial narrowing, diffuse RPE degeneration, Macular coloboma	RE-20/380 LE-20/520	+5.50 D (OU)	Extinguished ERG
LCA100 (II.1)	*NMNAT1* (Ala189Leu fs*25 & Arg237Cys)	0.00	1.00	8 months	Nystagmus, eye poking	RPE degeneration, Macular coloboma, compound hyperopic, optic atrophy, granular appearance of RPE	HM	+9.5 D (OU)	Extinguished ERG

CB: complete blindness; CF: counting fingers; D: diopters; HM: hand movement; LP: light perception; LE: left eye; RE: right eye; LRE: left and right eyes; NA: not available.

Leber congenital amaurosis is one of the most severe forms of childhood blindness with the age of onset within a year of age. Visual acuity of <6/60 in the better eye is defined as blindness (Dandona and Dandona 2003). LCA accounts for 5% of inherited retinal degenerative disorders. Retinal abnormalities, one of the major causes of childhood blindness account for 22% of childhood blindness in India (Gilbert and Foster 2001; Dandona and Dandona 2003). The prevalence of LCA in Western populations is 1/30,000-1/81,000 (Stone 2007; Kaplan 2008). However as it is a rare disorder, prevalence of LCA in India is not estimated.

The main goal of research into the genetics of LCA is to identify the molecular basis of the disease and to develop therapies to treat the disease. Mutations in all LCA-associated genes known till date are found to occur in ~70% of LCA cases especially in Caucasian populations (den Hollander, Roepman *et al*. 2008). It is possible that gene mutation frequencies of individual loci may vary in different ethnic groups. Reliable estimates of mutation frequencies are not available for patients from all regions of the world, as few studies have been done on LCA genetics in non-Caucasian populations.

Therefore establishment of the mutation spectrum for an Indian patient population helps to prioritize the efforts for genetic screening and for the development of new therapies. Currently gene therapy for patients with *RPE65* gene mutations is being tested. Clinical trials for *RPE65* gene therapy have demonstrated safety and efficacy of the gene delivery system. Adeno-associated virus 2 (AAV2) containing the human *RPE65* gene was injected in 3 patients each by 3 groups independently (Bainbridge, Smith *et al*. 2008; Hauswirth, Aleman *et al*. 2008; Maguire, Simonelli *et al*. 2008). Change in vision was compared in LCA patients and controls by using various methods including pupillometry, microperimetry, ability to navigate in an obstacle field and visual acuity. Improved retinal sensitivity and independent navigation in mobility test was observed by all the three studies. Increase in visual acuity was reported by only Maguire *et al*. (Bainbridge, Smith *et al*. 2008; Hauswirth, Aleman *et al*. 2008; Maguire, Simonelli *et al*. 2008).

In the present study, three known LCA genes (*GUCY2D*, *RD3* and *CRB1*) were screened for pathogenic changes in 100 unrelated LCA probands. Two novel genes (*NMNAT1* and *PALS1*) were also screened to establish the role of these genes in LCA.

The two known LCA genes (*GUCY2D* and *CRB1*) were selected for screening based on their relatively high mutation frequencies, as reported in previous studies (Hanein, Perrault *et al*. 2004; Coppieters, Casteels *et al*. 2010). *GUCY2D* is reported to have a frequency of 21% in patients from different ethnicities including Caucasian, Mediterranean and Asians (Hanein, Perrault *et al*. 2004), and *CRB1* mutations are found to occur in 16.5% of cases from Belgium (Coppieters, Casteels *et al*. 2010). However there are very few studies on the mutations in LCA genes in Indian patients. Notably, studies by Sundaresan *et al* and Verma *et al* in Indian patients (Sundaresan, Vijayalakshmi *et al*. 2009; Verma, Perumalsamy *et al*. 2013). Screening of 38 patients for 104 previously reported mutations using SNPlex platform for 8 genes resulted in detectable mutations in one proband of 38 probands tested (Sundaresan, Vijayalakshmi *et al*. 2009). In addition, 784 known disease causing-variations in 15 genes were screened using DNA microarray based LCA chips in 30 probands in another study by Verma *et al*., 2013. Mutations were identified in 11/30 cases (Verma, Perumalsamy *et al*. 2013). These studies indicate the mutational heterogeneity in LCA with very few mutations recurring between families or occurring in mutational hotspots. An important conclusion was that the mutation frequency of the *RPE65* gene (16.6%) was highest followed by the *GUCY2D* gene (10%) (Verma, Perumalsamy *et al*. 2013). The low prevalence of known mutations in these two studies suggests that novel mutations in known and/or new loci could probably be involved in the disease pathogenesis. In contrast, absence of mutations in the *CEP290* gene, reported to be the most frequently mutated gene in European populations with a frequency of ~30 % emphasizes the need for screening Indian patient populations to establish the mutation spectrum in LCA. (Coppieters, Casteels *et al*. 2010)

Many techniques have been used for screening of probands such as direct sequencing of genes, screening of known mutations by the LCA mutation chip, whole genome array/SNP arrays followed by candidate gene analysis and exome sequencing. Every

technique has its advantages/disadvantages. Although direct sequencing is the gold standard, it is cumbersome and time-consuming. Recently, high throughput next generation targeted sequencing has aided in the rapid screening of several genes simultaneously and whole exome sequencing has enabled the identification of novel LCA-associated genes (Sergouniotis, Davidson *et al*. 2011; Wang, Wang *et al*. 2011; Falk, Zhang *et al*. 2012).

Four novel pathogenic mutations (Ala353Val, Trp640Arg, Gln791X and Gln939X) were identified in the *GUCY2D* gene in our cohort. Upon comparison of our data with other reports, none of the mutations present in our cohort were reported previously. The mutation frequencies for *GUCY2D* in LCA range from 2.7-21% between various studies, although the relation to ethnicity is unclear as some studies included patients from multiple ethnic groups. An earlier study from South India reported mutations in the *GUCY2D* gene in 10% of LCA cases although the number of probands studied was only 30 (Verma, Perumalsamy *et al*. 2013).

Other studies of GUCY2D mutations in different ethnic groups conducted in small numbers of patients also do not permit a comparison of mutation frequencies due to small sample sizes screened (Li, Wang *et al.* 2009; Seong, Kim *et al.* 2008; McKibbin, Ali *et al.* 2010).

However a study conducted in a Chinese population including of 87 probands revealed mutations in 16 % cases in *GUCY2D* gene, whereas its frequency was 5.3% in a Italian study of 95 proband (Simonelli, Ziviello *et al.* 2007; Li, Xiao *et al.* 2011).

GUCY2D is a membrane-bound protein consisting of two monomers. Each monomer consists of an extracellular domain, a transmembrane domain, an intracellular protein kinase-like homology domain (KHD), a dimerization (hinge) domain (DD), and a C-terminal catalytic domain (CAT). Among the 4 pathogenic mutations observed in this study, Ala353Val falls in the extracellular domain whereas Trp640Arg is located in the kinase homology domain. Further, two termination mutations Gln791X and Gln939X occur in the dimerization and catalytic domains respectively. The occurrence of premature termination codons may result in the formation of nonfunctional truncated proteins, thus accounting for pathogenicity. In contrast,

Ala353 residue is highly conserved across different species (Figure 3.3) and is predicted as pathogenic by bioinformatics analysis tools like SIFT and Polyphen tools. In addition the other missense variation W640R was also located in the conserved region of the kinase homology domain and was predicted as a pathogenic modification. Both of these changes were also absent in the normal control population (n=150) and are not reported in databases such as Ensembl genome browser database, dbSNP database, 1000 genomes browser, ESP-Exome Sequencing Project .

The W640R mutation identified in this study occurs in the same region as a previously reported mutation of D639Y, shown to lead to defective enzymatic activity of GUCY2D (Peshenko, Olshevskaya *et al*. 2010). Due to its presence in the kinase homology domain, this variation might also interfere with the binding of GCAP with RetGC.

The association of mutations in the *RD3* gene with human LCA was first established in a study in our laboratory in collaboration with Friedman *et al* (Friedman, Chang *et al*. 2006). Screening of the *RD3* gene led to the identification of a pathogenic mutation in one patient out of 103 probands tested from our laboratory (Friedman *et al*. 2006). We wanted to explore further the role of the RD3 gene in LCA and the results presented in this thesis show that it is a very rare cause of LCA, since no mutations were detectable in 100 cases tested.

In this study the *CRB1* gene was also selected for screening due to a relatively high mutation frequency ranging from 2.7-16.5% in various previous reports (Li, Wang *et al*. 2009; Coppieters, Casteels *et al*. 2010). Novel *CRB1* gene mutations were identified in 2/100 (2%) patients with LCA in the present study. This is also the first study to report mutations in *CRB1* gene in Indian patients. Similar to earlier reports on *CRB1* mutations, patients in our study showed perivascular sparing of RPE degeneration in association with *CRB1* mutations. However Coats-like exudative vasculopathy and keratoconus was absent in both patients. An increase in retinal thickness was also observed in one of the probands in the present study (LCA30), with a retinal thickness that was ~1.5 times more than the normal retina. Ptosis and wandering fixation with alternate esotropia were unique clinical features in the present study, not reported previously in patients with *CRB1* mutations. Taken

together, the occurrence of mutations in *CRB1* in association with unique clinical features underscores its relevance for prioritized screening in LCA patients displaying these phenotypes.

In this study screening of the *PALS1* gene in 100 LCA probands failed to show any pathogenic changes and hence no conclusion about its role in LCA pathogenesis is possible from the data. Since the *CRB1* gene is involved in a wide spectrum of retinal dystrophies, further screening of the *PALS1* gene in patients with these *CRB1*-related phenotypes (retinitis pigmentosa with or without preserved PPRPE, retinitis pigmentosa with Coats-like exudative vasculopathy and pigmented paravenous chorioretinal atrophy) would be required to know its role if any, in these conditions.

Screening of the novel gene, *NMNAT1*, showed mutations in 4/100 cases in our population, representing a higher frequency than other patient populations screened so far. Functional assays on missense mutants of *NMNAT1* showed reduction of enzyme activity for mutation of Val9Met (data from laboratory of Dr. Eric A. Pierce, Harvard Medical School, Boston, Massachusetts, USA). The total cellular NAD+ content was also reduced (16%) compared to controls (Falk, Zhang *et al*. 2012). However the retinal delivery of exogenous NAD+ was not effective as shown by Falk *et al*, (2012). NAD+ content of mutant fibroblast cells was also found to be unaffected after treatment with 10 mM nicotinic acid for 24 hours.

The result of this study, with previous literature, suggests ethnic differences in mutation frequencies in different genes. This signifies the need for population-specific screening on large patient populations. Apart from providing information about the mutation spectra, genetic screening in LCA may provide insight into the disease pathogenesis as well as serve as a potential diagnostic/prognostic aid through genotype-phenotype correlations, and be useful in counseling of patients.

Specific conclusions of the study

Disease-causing mutations were identified in 10 families (10/100) in our study. *GUCY2D* and *NMNAT1* both contribute equally in disease pathogenesis with mutation frequencies of about 4% for each. Mutations in the *CRB1* gene account for about 2%

of cases. This study did not provide evidence for the association of mutations of the *RD3* and the *PALS1* genes with LCA.

Specific contributions of the study

This study provides a foundation for mutational data in LCA patients of Indian origin, since no prior mutational data exist for some of the genes tested including *CRB1*, *NMNAT1*, *PALS1* etc. This is the first study that has identified the involvement of *NMNAT1* gene in LCA patients. The presence of macular coloboma was the most characteristic feature of patients with *NMNAT1* gene mutations. Ptosis, wandering fixation with alternate esotropia have not been reported previously in patients with *CRB1* mutations. These clinical features along with other features such as PPRPE can help to develop genotype-phenotype correlations and aid in preferential screening of patients based on these features.

Limitations of the study

This study used the approach of candidate gene screening by conventional methods, and hence is more time-consuming than the newer methods of targeted multiplex sequencing and exome sequencing. Also, the potential for the detection of novel genes is limited since screening of known or suspected candidates was employed. Another limitation may be that screening was limited to exonic and flanking intronic regions. It is possible that mutations in regulatory regions upstream of the gene or within deep intronic sequences could be responsible for disease in some cases.

1. Acland, G. M., G. D. Aguirre, *et al.* (2001). "Gene therapy restores vision in a canine model of childhood blindness." Nat Genet **28**(1): 92-95.

2. Acland, G. M., G. D. Aguirre, *et al.* (2005). "Long-term restoration of rod and cone vision by single dose rAAV-mediated gene transfer to the retina in a canine model of childhood blindness." Mol Ther **12**(6): 1072-1082.

3. Aleman, T. S., A. V. Cideciyan, *et al.* (2011). "Human CRB1-associated retinal degeneration: comparison with the rd8 Crb1-mutant mouse model." Invest Ophthalmol Vis Sci **52**(9): 6898-6910.

4. Ali, Y. O., R. McCormack, *et al.* (2011). "Nicotinamide mononucleotide adenylyltransferase is a stress response protein regulated by the heat shock factor/hypoxia-inducible factor 1alpha pathway." J Biol Chem **286**(21): 19089-19099.

5. Alstrom CH, O. O. (1957). "Heredo-retinopathia congenitalis monohybrida recessiva autosomalis: A genetical-statistical study in clinical collaboration with Olof Olson." Hereditas **43**: 1-178.

6. Anathony J. Bron, R. C. T., Brenda J. Tripathi, Ed. (1997). Wolff's Anatomy of the eye and orbit. Wolff's Anatomy of the eye and orbit. Oxford, Chapman and Hall medical.

7. Araki, T., Y. Sasaki, *et al.* (2004). "Increased nuclear NAD biosynthesis and SIRT1 activation prevent axonal degeneration." Science **305**(5686): 1010-1013.

8. Arshavsky, V. (2002). "Like night and day: rods and cones have different pigment regeneration pathways." Neuron **36**(1): 1-3.

9. Azadi, S., L. L. Molday, *et al.* (2010). "RD3, the protein associated with Leber congenital amaurosis type 12, is required for guanylate cyclase trafficking in photoreceptor cells." Proc Natl Acad Sci U S A **107**(49): 21158-21163.

10. Baehr, W., S. Karan, *et al.* (2007). "The function of guanylate cyclase 1 and guanylate cyclase 2 in rod and cone photoreceptors." J Biol Chem **282**(12): 8837-8847.

11. Bainbridge, J. W., A. J. Smith, *et al.* (2008). "Effect of gene therapy on visual function in Leber's congenital amaurosis." N Engl J Med **358**(21): 2231-2239.

12. Barber, A. C., C. Hippert, *et al.* (2013). "Repair of the degenerate retina by photoreceptor transplantation." Proc Natl Acad Sci U S A **110**(1): 354-359.

13. Batten, M. L., Y. Imanishi, *et al.* (2005). "Pharmacological and rAAV gene therapy rescue of visual functions in a blind mouse model of Leber congenital amaurosis." PLoS Med **2**(11): e333.

14. Baye, L. M., X. Patrinostro, *et al.* (2011). "The N-terminal region of centrosomal protein 290 (CEP290) restores vision in a zebrafish model of human blindness." Hum Mol Genet **20**(8): 1467-1477.

15. Bennett, J., M. Ashtari, *et al.* (2012). "AAV2 gene therapy readministration in three adults with congenital blindness." Sci Transl Med **4**(120): 120ra115.

16. Berger, F., C. Lau, *et al.* (2005). "Subcellular compartmentation and differential catalytic properties of the three human nicotinamide mononucleotide adenylyltransferase isoforms." J Biol Chem **280**(43): 36334-36341.

17. Berger, F., C. Lau, *et al.* (2007a). "Regulation of poly(ADP-ribose) polymerase 1 activity by the phosphorylation state of the nuclear NAD biosynthetic enzyme NMN adenylyl transferase 1." Proc Natl Acad Sci U S A **104**(10): 3765-3770.

18. Berger, S., N. A. Bulgakova, *et al.* (2007). "Unraveling the genetic complexity of Drosophila stardust during photoreceptor morphogenesis and prevention of light-induced degeneration." Genetics **176**(4): 2189-2200.

19. Berger, W., B. Kloeckener-Gruissem, *et al.* (2010). "The molecular basis of human retinal and vitreoretinal diseases." Prog Retin Eye Res **29**(5): 335-375.

20. Booij, J. C., R. J. Florijn, *et al.* (2005). "Identification of mutations in the AIPL1, CRB1, GUCY2D, RPE65, and RPGRIP1 genes in patients with juvenile retinitis pigmentosa." J Med Genet **42**(11): e67.

21. Bowne, S. J., L. S. Sullivan, *et al.* (2006). "Spectrum and frequency of mutations in IMPDH1 associated with autosomal dominant retinitis pigmentosa and leber congenital amaurosis." Invest Ophthalmol Vis Sci **47**(1): 34-42.

22. Boye, S. E., S. L. Boye, *et al.* (2010). "Functional and behavioral restoration of vision by gene therapy in the guanylate cyclase-1 (GC1) knockout mouse." PLoS One **5**(6): e11306.

23. Bringmann, A., T. Pannicke, *et al.* (2006). "Muller cells in the healthy and diseased retina." Prog Retin Eye Res **25**(4): 397-424.

24. Bron AJ, T. R., Tripathi BJ (1997). The Retina, Chapman & Hall, UK.

25. Bulgakova, N. A., O. Kempkens, *et al.* (2008). "Multiple domains of Stardust differentially mediate localisation of the Crumbs-Stardust complex during photoreceptor development in Drosophila." J Cell Sci **121**(Pt 12): 2018-2026.

26. Burns, M. E. and V. Y. Arshavsky (2005). "Beyond counting photons: trials and trends in vertebrate visual transduction." Neuron **48**(3): 387-401.

27. Camuzat, A., H. Dollfus, *et al.* (1995). "A gene for Leber's congenital amaurosis maps to chromosome 17p." Hum Mol Genet **4**(8): 1447-1452.

28. Carlson, A. and D. Bok (1992). "Promotion of the release of 11-cis-retinal from cultured retinal pigment epithelium by interphotoreceptor retinoid-binding protein." Biochemistry **31**(37): 9056-9062.

29. Chang, B., J. R. Heckenlively, *et al.* (1993). "New mouse primary retinal degeneration (rd-3)." Genomics **16**(1): 45-49.

30. Chartier, F. J., E. J. Hardy, *et al.* (2011). "Crumbs controls epithelial integrity by inhibiting Rac1 and PI3K." J Cell Sci **124**(Pt 20): 3393-3398.

31. Chartier, F. J., E. J. Hardy, *et al.* (2012). "Crumbs limits oxidase-dependent signaling to maintain epithelial integrity and prevent photoreceptor cell death." J Cell Biol **198**(6): 991-998.

32. Chen, Y., Q. Zhang, *et al.* (2013). "Comprehensive mutation analysis by whole-exome sequencing in 41 Chinese families with Leber congenital amaurosis." Invest Ophthalmol Vis Sci **54**(6): 4351-4357.

33. Chiang, P. W., J. Wang, *et al.* (2012). "Exome sequencing identifies NMNAT1 mutations as a cause of Leber congenital amaurosis." Nat Genet **44**(9): 972-974.

34. Cho, S. H., J. Y. Kim, *et al.* (2012). "Genetic ablation of Pals1 in retinal progenitor cells models the retinal pathology of Leber congenital amaurosis." Hum Mol Genet **21**(12): 2663-2676.

35. Corton, M., S. D. Tatu, *et al.* (2013). "High frequency of CRB1 mutations as cause of Early-Onset Retinal Dystrophies in the Spanish population." Orphanet J Rare Dis **8**: 20.

36. Corton, M., A. Avila-Fernandez, *et al.* (2014). "Involvement of LCA5 in Leber congenital amaurosis and retinitis pigmentosa in the Spanish population." Ophthalmology **121**(1): 399-407.

37. Chow, R. L. and R. A. Lang (2001). "Early eye development in vertebrates." Annu Rev Cell Dev Biol **17**: 255-296.

38. Chung, D. C. and E. I. Traboulsi (2009). "Leber congenital amaurosis: clinical correlations with genotypes, gene therapy trials update, and future directions." J Aapos **13**(6): 587-592.

39. Cideciyan, A. V., T. S. Aleman, *et al.* (2007). "Centrosomal-ciliary gene CEP290/NPHP6 mutations result in blindness with unexpected sparing of photoreceptors and visual brain: implications for therapy of Leber congenital amaurosis." Hum Mutat **28**(11): 1074-1083.

40. Cideciyan, A. V., T. S. Aleman, *et al.* (2008). "Human gene therapy for RPE65 isomerase deficiency activates the retinoid cycle of vision but with slow rod kinetics." Proc Natl Acad Sci U S A **105**(39): 15112-15117.

41. Cideciyan, A. V., W. W. Hauswirth, *et al.* (2009). "Human RPE65 gene therapy for Leber congenital amaurosis: persistence of early visual improvements and safety at 1 year." Hum Gene Ther **20**(9): 999-1004.

42. Cideciyan, A. V. (2010). "Leber congenital amaurosis due to RPE65 mutations and its treatment with gene therapy." Progress in Retinal and Eye Research **29**: 30.

43. Conforti, L., G. Fang, *et al.* (2007). "NAD(+) and axon degeneration revisited: Nmnat1 cannot substitute for Wld(S) to delay Wallerian degeneration." Cell Death Differ **14**(1): 116-127.

44. Conforti, L., A. Wilbrey, *et al.* (2009). "Wld S protein requires Nmnat activity and a short N-terminal sequence to protect axons in mice." J Cell Biol **184**(4): 491-500.

45. Coppieters, F., I. Casteels, *et al.* (2010). "Genetic screening of LCA in Belgium: predominance of CEP290 and identification of potential modifier alleles in AHI1 of CEP290-related phenotypes." Hum Mutat **31**(10): E1709-1766.

46. Dandona, R. and L. Dandona (2003). "Childhood blindness in India: a population based perspective." Br J Ophthalmol **87**(3): 263-265.

47. den Hollander, A. I., J. B. ten Brink, *et al.* (1999). "Mutations in a human homologue of Drosophila crumbs cause retinitis pigmentosa (RP12)." Nat Genet **23**(2): 217-221.

48. den Hollander, A. I., J. R. Heckenlively, *et al.* (2001). "Leber congenital amaurosis and retinitis pigmentosa with Coats-like exudative vasculopathy are associated with mutations in the crumbs homologue 1 (CRB1) gene." Am J Hum Genet **69**(1): 198-203.

49. den Hollander, A. I., J. Davis, *et al.* (2004). "CRB1 mutation spectrum in inherited retinal dystrophies." Hum Mutat **24**(5): 355-369.

50. den Hollander, A. I., R. K. Koenekoop, *et al.* (2006). "Mutations in the CEP290 (NPHP6) gene are a frequent cause of Leber congenital amaurosis." Am J Hum Genet **79**(3): 556-561.

51. den Hollander, A. I., R. K. Koenekoop, *et al.* (2007). "Mutations in LCA5, encoding the ciliary protein lebercilin, cause Leber congenital amaurosis." Nat Genet **39**(7): 889-895.

52. den Hollander, A. I., R. Roepman, *et al.* (2008). "Leber congenital amaurosis: genes, proteins and disease mechanisms." Prog Retin Eye Res **27**(4): 391-419.

53. Dharmaraj, S. R., E. R. Silva, *et al.* (2000). "Mutational analysis and clinical correlation in Leber congenital amaurosis." Ophthalmic Genet **21**(3): 135-150.

54. Dharmaraj, S., B. P. Leroy, *et al.* (2004). "The phenotype of Leber congenital amaurosis in patients with AIPL1 mutations." Arch Ophthalmol **122**(7): 1029-1037.

55. Dizhoor, A. M., E. V. Olshevskaya, *et al.* (2010). "Mg2+/Ca2+ cation binding cycle of guanylyl cyclase activating proteins (GCAPs): role in regulation of photoreceptor guanylyl cyclase." Mol Cell Biochem **334**(1-2): 117-124.

56. Dryja, T. P., S. M. Adams, *et al.* (2001). "Null RPGRIP1 alleles in patients with Leber congenital amaurosis." Am J Hum Genet **68**(5): 1295-1298.

57. Duke-Elder, S., Ed. (1963). System of ophthalmology. Normal and abnormal development. Londen, The C.V. Mosby company.

58. Ehrenberg, M., E. A. Pierce, *et al.* (2013). "CRB1: one gene, many phenotypes." Semin Ophthalmol **28**(5-6): 397-405.

59. Estrada-Cuzcano, A., R. K. Koenekoop, *et al.* (2011). "IQCB1 mutations in patients with leber congenital amaurosis." Invest Ophthalmol Vis Sci **52**(2): 834-839.

60. Falk, M. J., Q. Zhang, *et al.* (2012). "NMNAT1 mutations cause Leber congenital amaurosis." Nat Genet **44**(9): 1040-1045.

61. Franceschetti, A. and P. Dieterle (1954). Diagnostic and prognostic importance of the electroretinogram in tapetoretinal degeneration with reduction of the visual field and hemeralopia. Confin Neurol **14**(2-3): 184-186.

62. Freund, C. L., Q. L. Wang, *et al.* (1998). "De novo mutations in the CRX homeobox gene associated with Leber congenital amaurosis." Nat Genet **18**(4): 311-312.

63. Friedman, J. S., B. Chang, *et al.* (2006). "Premature truncation of a novel protein, RD3, exhibiting subnuclear localization is associated with retinal degeneration." Am J Hum Genet **79**(6): 1059-1070.

64. Gabriele Thumann, D. R. H. (1998). Retina. Los Angeles, California, Mosby.

65. Gal, A., Y. Li, *et al.* (2000). "Mutations in MERTK, the human orthologue of the RCS rat retinal dystrophy gene, cause retinitis pigmentosa." Nat Genet **26**(3): 270-271.

66. Galvin, J. A., G. A. Fishman, *et al.* (2005). "Evaluation of genotype-phenotype associations in leber congenital amaurosis." Retina **25**(7): 919-929.

67. Gerber, S., I. Perrault, *et al.* (2001). "Complete exon-intron structure of the RPGR-interacting protein (RPGRIP1) gene allows the identification of mutations underlying Leber congenital amaurosis." Eur J Hum Genet **9**(8): 561-571.

68. Gerber, S., S. Hanein, *et al.* (2007). "Mutations in LCA5 are an uncommon cause of Leber congenital amaurosis (LCA) type II." Hum Mutat **28**(12): 1245.

69. Gilbert, C. and A. Foster (2001). "Childhood blindness in the context of VISION 2020--the right to sight." Bull World Health Organ **79**(3): 227-232.

70. Hanein, S., I. Perrault, *et al.* (2004). "Leber congenital amaurosis: comprehensive survey of the genetic heterogeneity, refinement of the clinical definition, and genotype-phenotype correlations as a strategy for molecular diagnosis." Hum Mutat **23**(4): 306-317.

71. Hauswirth, W. W., T. S. Aleman, *et al.* (2008). "Treatment of leber congenital amaurosis due to RPE65 mutations by ocular subretinal injection of adeno-associated virus gene vector: short-term results of a phase I trial." Hum Gene Ther **19**(10): 979-990.

72. Heavner, W. and L. Pevny (2012). "Eye development and retinogenesis." Cold Spring Harb Perspect Biol **4**(12).

73. Henderson, R. H., N. Waseem, *et al.* (2007). "An assessment of the apex microarray technology in genotyping patients with Leber congenital amaurosis

and early-onset severe retinal dystrophy." Invest Ophthalmol Vis Sci **48**(12): 5684-5689.

74. Henderson, R. H., D. S. Mackay, *et al.* (2011). "Phenotypic variability in patients with retinal dystrophies due to mutations in CRB1." Br J Ophthalmol **95**(6): 811-817.

75. Humayun, M. S., J. D. Dorn, *et al.* (2012). "Interim results from the international trial of Second Sight's visual prosthesis." Ophthalmology **119**(4): 779-788.

76. Hurd, T. W., L. Gao, *et al.* (2003). "Direct interaction of two polarity complexes implicated in epithelial tight junction assembly." Nat Cell Biol **5**(2): 137-142.

77. Jacobson, S. G., A. V. Cideciyan, *et al.* (2003). "Crumbs homolog 1 (CRB1) mutations result in a thick human retina with abnormal lamination." Hum Mol Genet **12**(9): 1073-1078.

78. Janaky, M., A. Deak, *et al.* (1994). "Electrophysiologic alterations in patients with optic nerve hypoplasia." Doc Ophthalmol **86**(3): 247-257.

79. Janecke, A. R., D. A. Thompson, *et al.* (2004). "Mutations in RDH12 encoding a photoreceptor cell retinol dehydrogenase cause childhood-onset severe retinal dystrophy." Nat Genet **36**(8): 850-854.

80. Jindrova, H. (1998). "Vertebrate phototransduction: activation, recovery, and adaptation." Physiol Res **47**(3): 155-168.

81. Johnson, K., F. Grawe, *et al.* (2002). "Drosophila crumbs is required to inhibit light-induced photoreceptor degeneration." Curr Biol **12**(19): 1675-1680.

82. Kamberov, E., O. Makarova, *et al.* (2000). "Molecular cloning and characterization of Pals, proteins associated with mLin-7." J Biol Chem **275**(15): 11425-11431.

83. Kamermans, M. and H. Spekreijse (1999). "The feedback pathway from horizontal cells to cones. A mini review with a look ahead." Vision Res **39**(15): 2449-2468.

84. Kantardzhieva, A., I. Gosens, *et al.* (2005). "MPP5 recruits MPP4 to the CRB1 complex in photoreceptors." Invest Ophthalmol Vis Sci **46**(6): 2192-2201.

85. Kaplan, J. (2008). "Leber congenital amaurosis: from darkness to spotlight." Ophthalmic Genet **29**(3): 92-98.

86. Karan, S., J. M. Frederick, *et al.* (2010). "Novel functions of photoreceptor guanylate cyclases revealed by targeted deletion." Mol Cell Biochem **334**(1-2): 141-155.

87. Koenekoop, R. K., I. Lopez, *et al.* (2007). "Genetic testing for retinal dystrophies and dysfunctions: benefits, dilemmas and solutions." Clin Experiment Ophthalmol **35**(5): 473-485.

88. Koenekoop, R. K., H. Wang, *et al.* (2012). "Mutations in NMNAT1 cause Leber congenital amaurosis and identify a new disease pathway for retinal degeneration." Nat Genet **44**(9): 1035-1039.

89. Lagnado, L. (1998). "Retinal processing: amacrine cells keep it short and sweet." Curr Biol **8**(17): R598-600.

90. Lakowski, J., M. Baron, *et al.* (2010). "Cone and rod photoreceptor transplantation in models of the childhood retinopathy Leber congenital amaurosis using flow-sorted Crx-positive donor cells." Hum Mol Genet **19**(23): 4545-4559.

91. Lamb, T. D. and E. N. Pugh, Jr. (2004). "Dark adaptation and the retinoid cycle of vision." Prog Retin Eye Res **23**(3): 307-380.

92. Lamb, T. D. and E. N. Pugh, Jr. (2006). "Phototransduction, dark adaptation, and rhodopsin regeneration the proctor lecture." Invest Ophthalmol Vis Sci **47**(12): 5137-5152.

93. Lavorgna, G., M. Lestingi, *et al.* (2003). "Identification and characterization of C1orf36, a transcript highly expressed in photoreceptor cells, and mutation analysis in retinitis pigmentosa." Biochem Biophys Res Commun **308**(3): 414-421.

94. Lee, B. B., P. R. Martin, *et al.* (2010). "Retinal connectivity and primate vision." Prog Retin Eye Res **29**(6): 622-639.

95. Lemmers, C., E. Medina, *et al.* (2002). "hINADl/PATJ, a homolog of discs lost, interacts with crumbs and localizes to tight junctions in human epithelial cells." J Biol Chem **277**(28): 25408-25415.

96. Leskov, I. B., V. A. Klenchin, *et al.* (2000). "The gain of rod phototransduction: reconciliation of biochemical and electrophysiological measurements." Neuron **27**(3): 525-537.

97. Li, Y., H. Wang, *et al.* (2009). "Mutation survey of known LCA genes and loci in the Saudi Arabian population." Invest Ophthalmol Vis Sci **50**(3): 1336-1343.

98. Li, L., X. Xiao, *et al.* (2011). "Detection of variants in 15 genes in 87 unrelated Chinese patients with Leber congenital amaurosis." PLoS One **6**(5): e19458.

99. Lotery, A. J., P. Namperumalsamy, *et al.* (2000). "Mutation analysis of 3 genes in patients with Leber congenital amaurosis." Arch Ophthalmol **118**(4): 538-543.

100. Lotery, A. J., S. G. Jacobson, *et al.* (2001). "Mutations in the CRB1 gene cause Leber congenital amaurosis." Arch Ophthalmol **119**(3): 415-420.

101. Mack, T. G., M. Reiner, *et al.* (2001). "Wallerian degeneration of injured axons and synapses is delayed by a Ube4b/Nmnat chimeric gene." Nat Neurosci **4**(12): 1199-1206.

102. MacLaren, R. E., R. A. Pearson, *et al.* (2006). "Retinal repair by transplantation of photoreceptor precursors." Nature **444**(7116): 203-207.

103. Maguire, A. M., F. Simonelli, *et al.* (2008). "Safety and efficacy of gene transfer for Leber's congenital amaurosis." N Engl J Med **358**(21): 2240-2248.

104. Makarova, O., M. H. Roh, *et al.* (2003). "Mammalian Crumbs3 is a small transmembrane protein linked to protein associated with Lin-7 (Pals1)." Gene **302**(1-2): 21-29.

105. Mamatha, G., S. Srilekha, *et al.* (2008). "Screening of the RPE65 gene in the Asian Indian patients with leber congenital amaurosis." Ophthalmic Genet **29**(2): 73-78.

106. Marlhens, F., C. Bareil, *et al.* (1997). "Mutations in RPE65 cause Leber's congenital amaurosis." Nat Genet **17**(2): 139-141.

107. Masland, R. H. (2001). "The fundamental plan of the retina." Nat Neurosci **4**(9): 877-886.

108. Mata, N. L., R. A. Radu, *et al.* (2002). "Isomerization and oxidation of vitamin a in cone-dominant retinas: a novel pathway for visual-pigment regeneration in daylight." Neuron **36**(1): 69-80.

109. McKay, G. J., S. Clarke, *et al.* (2005). "Pigmented paravenous chorioretinal atrophy is associated with a mutation within the crumbs homolog 1 (CRB1) gene." Invest Ophthalmol Vis Sci **46**(1): 322-328.

110. Mackay, D. S., L. A. Ocaka, *et al.* (2011). "Screening of SPATA7 in patients with Leber congenital amaurosis and severe childhood-onset retinal dystrophy reveals disease-causing mutations." Invest Ophthalmol Vis Sci **52**(6): 3032-3038.

111. Mackay, D. S., A. D. Borman, *et al.* (2013). "Screening of a large cohort of leber congenital amaurosis and retinitis pigmentosa patients identifies novel LCA5 mutations and new genotype-phenotype correlations." Hum Mutat **34**(11): 1537-1546.

112. McKibbin, M., M. Ali, *et al.* (2010). "Genotype-phenotype correlation for leber congenital amaurosis in Northern Pakistan." Arch Ophthalmol **128**(1): 107-113.

113. Mihelec, M., R. A. Pearson, *et al.* (2011). "Long-term preservation of cones and improvement in visual function following gene therapy in a mouse model of leber congenital amaurosis caused by guanylate cyclase-1 deficiency." Hum Gene Ther **22**(10): 1179-1190.

114. Miller, J. L., A. Picones, *et al.* (1994). "Differences in transduction between rod and cone photoreceptors: an exploration of the role of calcium homeostasis." Curr Opin Neurobiol **4**(4): 488-495.

115. Moiseyev, G., Y. Chen, *et al.* (2005). "RPE65 is the isomerohydrolase in the retinoid visual cycle." Proc Natl Acad Sci U S A **102**(35): 12413-12418.

116. Molday, L. L., H. Djajadi, *et al.* (2013). "RD3 gene delivery restores guanylate cyclase localization and rescues photoreceptors in the Rd3 mouse model of Leber congenital amaurosis 12." Hum Mol Genet **22**(19): 3894-3905.

117. Mustafi, D., A. H. Engel, *et al.* (2009). "Structure of cone photoreceptors." Prog Retin Eye Res **28**(4): 289-302.

118. Nikiforov, A., C. Dolle, *et al.* (2011). "Pathways and subcellular compartmentation of NAD biosynthesis in human cells: from entry of extracellular precursors to mitochondrial NAD generation." J Biol Chem **286**(24): 21767-21778.

119. Pasadhika, S., G. A. Fishman, *et al.* (2010). "Differential macular morphology in patients with RPE65-, CEP290-, GUCY2D-, and AIPL1-related Leber congenital amaurosis." Invest Ophthalmol Vis Sci **51**(5): 2608-2614.

120. Pawlyk, B. S., A. J. Smith, *et al.* (2005). "Gene replacement therapy rescues photoreceptor degeneration in a murine model of Leber congenital amaurosis lacking RPGRIP." Invest Ophthalmol Vis Sci **46**(9): 3039-3045.

121. Pawlyk, B. S., O. V. Bulgakov, *et al.* (2010). "Replacement gene therapy with a human RPGRIP1 sequence slows photoreceptor degeneration in a murine model of Leber congenital amaurosis." Hum Gene Ther **21**(8): 993-1004.

122. Pellikka, M., G. Tanentzapf, *et al.* (2002). "Crumbs, the Drosophila homologue of human CRB1/RP12, is essential for photoreceptor morphogenesis." Nature **416**(6877): 143-149.

123. Perrault, I., J. M. Rozet, *et al.* (1996). "Retinal-specific guanylate cyclase gene mutations in Leber's congenital amaurosis." Nat Genet **14**(4): 461-464.

124. Perrault, I., J. M. Rozet, *et al.* (2000). "Spectrum of retGC1 mutations in Leber's congenital amaurosis." Eur J Hum Genet **8**(8): 578-582.

125. Perrault, I., S. Hanein, *et al.* (2004). "Retinal dehydrogenase 12 (RDH12) mutations in leber congenital amaurosis." Am J Hum Genet **75**(4): 639-646.

126. Perrault, I., N. Delphin, *et al.* (2007). "Spectrum of NPHP6/CEP290 mutations in Leber congenital amaurosis and delineation of the associated phenotype." Hum Mutat **28**(4): 416.

127. Perrault, I., S. Hanein, *et al.* (2010). "Spectrum of SPATA7 mutations in Leber congenital amaurosis and delineation of the associated phenotype." Hum Mutat **31**(3): E1241-1250.

128. Perrault, I., S. Hanein, *et al.* (2012). "Mutations in NMNAT1 cause Leber congenital amaurosis with early-onset severe macular and optic atrophy." Nat Genet **44**(9): 975-977.

129. Perrault, I., A. Estrada-Cuzcano, *et al.* (2013). "Union makes strength: a worldwide collaborative genetic and clinical study to provide a comprehensive survey of RD3 mutations and delineate the associated phenotype." PLoS One **8**(1): e51622.

130. Peshenko, I. V., E. V. Olshevskaya, *et al.* (2010). "Activation of retinal guanylyl cyclase RetGC1 by GCAP1: stoichiometry of binding and effect of new LCA-related mutations." Biochemistry **49**(4): 709-717.

131. Peshenko, I. V., E. V. Olshevskaya, *et al.* (2011). "Retinal degeneration 3 (RD3) protein inhibits catalytic activity of retinal membrane guanylyl cyclase (RetGC) and its stimulation by activating proteins." Biochemistry **50**(44): 9511-9519.

132. Pomares, E., M. Riera, *et al.* (2010). "Comprehensive SNP-chip for retinitis pigmentosa-Leber congenital amaurosis diagnosis: new mutations and detection of mutational founder effects." Eur J Hum Genet **18**(1): 118-124.

133. Preising, M. N., N. Hausotter-Will, *et al.* (2012). "Mutations in RD3 are associated with an extremely rare and severe form of early onset retinal dystrophy." Invest Ophthalmol Vis Sci **53**(7): 3463-3472.

134. Press, C. and J. Milbrandt (2008). "Nmnat delays axonal degeneration caused by mitochondrial and oxidative stress." J Neurosci **28**(19): 4861-4871.

135. Pugh, E. N., Jr. and T. D. Lamb (1993). "Amplification and kinetics of the activation steps in phototransduction." Biochim Biophys Acta **1141**(2-3): 111-149.

136. Raffaelli, N., L. Sorci, *et al.* (2002). "Identification of a novel human nicotinamide mononucleotide adenylyltransferase." Biochem Biophys Res Commun **297**(4): 835-840.

137. Rando, R. R. (2001). "The biochemistry of the visual cycle." Chem Rev **101**(7): 1881-1896.

138. Rivolta, C., N. E. Peck, *et al.* (2001). "Novel frameshift mutations in CRX associated with Leber congenital amaurosis." Hum Mutat **18**(6): 550-551.

139. Roh, M. H., O. Makarova, *et al.* (2002). "The Maguk protein, Pals1, functions as an adapter, linking mammalian homologues of Crumbs and Discs Lost." J Cell Biol **157**(1): 161-172.

140. Ruiz, A., M. H. Kuehn, *et al.* (2001). "Genomic organization and mutation analysis of the gene encoding lecithin retinol acyltransferase in human retinal pigment epithelium." Invest Ophthalmol Vis Sci **42**(1): 31-37.

141. Sasaki, Y., B. P. Vohra, *et al.* (2009a). "Transgenic mice expressing the Nmnat1 protein manifest robust delay in axonal degeneration in vivo." J Neurosci **29**(20): 6526-6534.

142. Sasaki, Y., B. P. Vohra, *et al.* (2009b). "Nicotinamide mononucleotide adenylyl transferase-mediated axonal protection requires enzymatic activity but not increased levels of neuronal nicotinamide adenine dinucleotide." J Neurosci **29**(17): 5525-5535.

143. Sauve, A. A. (2008). "NAD+ and vitamin B3: from metabolism to therapies." J Pharmacol Exp Ther **324**(3): 883-893.

144. Schuster, A., A. R. Janecke, *et al.* (2007). "The phenotype of early-onset retinal degeneration in persons with RDH12 mutations." Invest Ophthalmol Vis Sci **48**(4): 1824-1831.

145. Seebacher, T., E. Beitz, *et al.* (1999). "Expression of membrane-bound and cytosolic guanylyl cyclases in the rat inner ear." Hear Res **127**(1-2): 95-102.

146. Semple-Rowland, S. L., N. R. Lee, *et al.* (1998). "A null mutation in the photoreceptor guanylate cyclase gene causes the retinal degeneration chicken phenotype." Proc Natl Acad Sci U S A **95**(3): 1271-1276.

147. Senechal, A., G. Humbert, *et al.* (2006). "Screening genes of the retinoid metabolism: novel LRAT mutation in leber congenital amaurosis." Am J Ophthalmol **142**(4): 702-704.

148. Seong, M. W., S. Y. Kim, *et al.* (2008). "Molecular characterization of Leber congenital amaurosis in Koreans." Mol Vis **14**: 1429-1436.

149. Sergouniotis, P. I., A. E. Davidson, *et al.* (2011). "Recessive mutations in KCNJ13, encoding an inwardly rectifying potassium channel subunit, cause leber congenital amaurosis." Am J Hum Genet **89**(1): 183-190.

150. Shyjan, A. W., F. J. de Sauvage, *et al.* (1992). "Molecular cloning of a retina-specific membrane guanylyl cyclase." Neuron **9**(4): 727-737.

151. Simo, R., M. Villarroel, *et al.* (2010). "The retinal pigment epithelium: something more than a constituent of the blood-retinal barrier--implications for the pathogenesis of diabetic retinopathy." J Biomed Biotechnol **2010**: 190724.

152. Simon, A., A. Romert, *et al.* (1999). "Intracellular localization and membrane topology of 11-cis retinol dehydrogenase in the retinal pigment epithelium

suggest a compartmentalized synthesis of 11-cis retinaldehyde." J Cell Sci **112 (Pt 4)**: 549-558.

153. Simonelli, F., C. Ziviello, *et al.* (2007). "Clinical and molecular genetics of Leber's congenital amaurosis: a multicenter study of Italian patients." Invest Ophthalmol Vis Sci **48**(9): 4284-4290.

154. Simonelli, F., A. M. Maguire, *et al.* (2010). "Gene therapy for Leber's congenital amaurosis is safe and effective through 1.5 years after vector administration." Mol Ther **18**(3): 643-650.

155. Singh, M. S., P. Charbel Issa, *et al.* (2013). "Reversal of end-stage retinal degeneration and restoration of visual function by photoreceptor transplantation." Proc Natl Acad Sci U S A **110**(3): 1101-1106.

156. Sitorus, R. S., B. Lorenz, *et al.* (2003). "Analysis of three genes in Leber congenital amaurosis in Indonesian patients." Vision Res **43**(28): 3087-3093.

157. Smith, A. J., F. C. Schlichtenbrede, *et al.* (2003). "AAV-Mediated gene transfer slows photoreceptor loss in the RCS rat model of retinitis pigmentosa." Mol Ther **8**(2): 188-195.

158. Smith, A. J., J. W. Bainbridge, *et al.* (2009). "Prospects for retinal gene replacement therapy." Trends Genet **25**(4): 156-165.

159. Sohocki, M. M., L. S. Sullivan, *et al.* (1998). "A range of clinical phenotypes associated with mutations in CRX, a photoreceptor transcription-factor gene." Am J Hum Genet **63**(5): 1307-1315.

160. Sohocki, M. M., S. J. Bowne, *et al.* (2000). "Mutations in a new photoreceptor-pineal gene on 17p cause Leber congenital amaurosis." Nat Genet **24**(1): 79-83.

161. Sohocki, M. M., I. Perrault, *et al.* (2000). "Prevalence of AIPL1 mutations in inherited retinal degenerative disease." Mol Genet Metab **70**(2): 142-150.

162. Stone, E. M. (2007). "Leber congenital amaurosis - a model for efficient genetic testing of heterogeneous disorders: LXIV Edward Jackson Memorial Lecture." Am J Ophthalmol **144**(6): 791-811.

163. Stone, E. M., A. V. Cideciyan, *et al.* (2011). "Variations in NPHP5 in patients with nonsyndromic leber congenital amaurosis and Senior-Loken syndrome." Arch Ophthalmol **129**(1): 81-87.

164. Straight, S. W., K. Shin, *et al.* (2004). "Loss of PALS1 expression leads to tight junction and polarity defects." Mol Biol Cell **15**(4): 1981-1990.

165. Sun, W., C. Gerth, *et al.* (2007). "Novel RDH12 mutations associated with Leber congenital amaurosis and cone-rod dystrophy: biochemical and clinical evaluations." Vision Res **47**(15): 2055-2066.

166. Sun, X., B. Pawlyk, *et al.* (2010). "Gene therapy with a promoter targeting both rods and cones rescues retinal degeneration caused by AIPL1 mutations." Gene Ther **17**(1): 117-131.

167. Sundaresan, P., P. Vijayalakshmi, *et al.* (2009). "Mutations that are a common cause of Leber congenital amaurosis in northern America are rare in southern India." Mol Vis **15**: 1781-1787.

168. Sweeney, M. O., T. L. McGee, *et al.* (2007). "Low prevalence of lecithin retinol acyltransferase mutations in patients with Leber congenital amaurosis and autosomal recessive retinitis pigmentosa." Mol Vis **13**: 588-593.

169. Testa, F., E. M. Surace, *et al.* (2011). "Evaluation of Italian patients with leber congenital amaurosis due to AIPL1 mutations highlights the potential applicability of gene therapy." Invest Ophthalmol Vis Sci **52**(8): 5618-5624.

170. Thompson, D. A., P. Gyurus, *et al.* (2000). "Genetics and phenotypes of RPE65 mutations in inherited retinal degeneration." Invest Ophthalmol Vis Sci **41**(13): 4293-4299.

171. Thompson, D. A., Y. Li, *et al.* (2001). "Mutations in the gene encoding lecithin retinol acyltransferase are associated with early-onset severe retinal dystrophy." Nat Genet **28**(2): 123-124.

172. Thompson, D. A., A. R. Janecke, *et al.* (2005). "Retinal degeneration associated with RDH12 mutations results from decreased 11-cis retinal synthesis due to disruption of the visual cycle." Hum Mol Genet **14**(24): 3865-3875.

173. Tucker, C. L., S. C. Woodcock, *et al.* (1999). "Biochemical analysis of a dimerization domain mutation in RetGC-1 associated with dominant cone-rod dystrophy." Proc Natl Acad Sci U S A **96**(16): 9039-9044.

174. Tucker, C. L., V. Ramamurthy, *et al.* (2004). "Functional analyses of mutant recessive GUCY2D alleles identified in Leber congenital amaurosis patients: protein domain comparisons and dominant negative effects." Mol Vis **10**: 297-303.

175. Ugur Iseri, S. A., Y. K. Durlu, *et al.* (2010). "A novel recessive GUCY2D mutation causing cone-rod dystrophy and not Leber's congenital amaurosis." Eur J Hum Genet **18**(10): 1121-1126.

176. Ulshafer, R. J., C. Allen, *et al.* (1984). "Hereditary retinal degeneration in the Rhode Island Red chicken. I. Histology and ERG." Exp Eye Res **39**(2): 125-135.

177. Vallespin, E., D. Cantalapiedra, *et al.* (2007). "Mutation screening of 299 Spanish families with retinal dystrophies by Leber congenital amaurosis genotyping microarray." Invest Ophthalmol Vis Sci **48**(12): 5653-5661.

178. Vallespin, E., M. A. Lopez-Martinez, *et al.* (2007). "Frequency of CEP290 c.2991_1655A>G mutation in 175 Spanish families affected with Leber congenital amaurosis and early-onset retinitis pigmentosa." Mol Vis **13**: 2160-2162.

179. van de Pavert, S. A., A. Kantardzhieva, *et al.* (2004). "Crumbs homologue 1 is required for maintenance of photoreceptor cell polarization and adhesion during light exposure." J Cell Sci **117**(Pt 18): 4169-4177.

180. van den Hurk, J. A., P. Rashbass, *et al.* (2005). "Characterization of the Crumbs homolog 2 (CRB2) gene and analysis of its role in retinitis pigmentosa and Leber congenital amaurosis." Mol Vis **11**: 263-273.

181. van Rossum, A. G., W. M. Aartsen, *et al.* (2006). "Pals1/Mpp5 is required for correct localization of Crb1 at the subapical region in polarized Muller glia cells." Hum Mol Genet **15**(18): 2659-2672.

182. Verghese, P. B., Y. Sasaki, *et al.* (2011). "Nicotinamide mononucleotide adenylyl transferase 1 protects against acute neurodegeneration in developing CNS by inhibiting excitotoxic-necrotic cell death." Proc Natl Acad Sci U S A **108**(47): 19054-19059.

183. Verma, A., V. Perumalsamy, *et al.* (2013). "Mutational screening of LCA genes emphasizing RPE65 in South Indian cohort of patients." PLoS One **8**(9): e73172.

184. Walia, S., G. A. Fishman, *et al.* (2010). "Visual acuity in patients with Leber's congenital amaurosis and early childhood-onset retinitis pigmentosa." Ophthalmology **117**(6): 1190-1198.

185. Wang, H., A. I. den Hollander, *et al.* (2009). "Mutations in SPATA7 cause Leber congenital amaurosis and juvenile retinitis pigmentosa." Am J Hum Genet **84**(3): 380-387.

186. Wang, X., H. Wang, *et al.* (2011). "Whole-exome sequencing identifies ALMS1, IQCB1, CNGA3, and MYO7A mutations in patients with Leber congenital amaurosis." Hum Mutat **32**(12): 1450-1459.

187. Wang, X., H. Wang, *et al.* (2013). "Comprehensive molecular diagnosis of 179 Leber congenital amaurosis and juvenile retinitis pigmentosa patients by targeted next generation sequencing." J Med Genet **50**(10): 674-688.

188. Weber, M., J. Rabinowitz, *et al.* (2003). "Recombinant adeno-associated virus serotype 4 mediates unique and exclusive long-term transduction of retinal pigmented epithelium in rat, dog, and nonhuman primate after subretinal delivery." Mol Ther **7**(6): 774-781.

189. Werner, E., M. Ziegler, *et al.* (2002). "Crystal structure of human nicotinamide mononucleotide adenylyltransferase in complex with NMN." FEBS Lett **516**(1-3): 239-244.

190. Williams, M. L., J. E. Coleman, *et al.* (2006). "Lentiviral expression of retinal guanylate cyclase-1 (RetGC1) restores vision in an avian model of childhood blindness." PLoS Med **3**(6): e201.

191. Wu, S. M. (1992). "Feedback connections and operation of the outer plexiform layer of the retina." Curr Opin Neurobiol **2**(4): 462-468.

192. Xu, F., Q. Dong, *et al.* (2012). "Novel RPE65 mutations associated with Leber congenital amaurosis in Chinese patients." Mol Vis **18**: 744-750.

193. Yang, R. B., S. W. Robinson, *et al.* (1999). "Disruption of a retinal guanylyl cyclase gene leads to cone-specific dystrophy and paradoxical rod behavior." J Neurosci **19**(14): 5889-5897.

194. Yzer, S., B. P. Leroy, *et al.* (2006). "Microarray-based mutation detection and phenotypic characterization of patients with Leber congenital amaurosis." Invest Ophthalmol Vis Sci **47**(3): 1167-1176.

195. Yu, H., E. Olshevskaya, *et al.* (1999). "Activation of retinal guanylyl cyclase-1 by Ca2+-binding proteins involves its dimerization." J Biol Chem **274**(22): 15547-15555.

196. Zaghloul, N. A., B. Yan, *et al.* (2005). "Step-wise specification of retinal stem cells during normal embryogenesis." Biol Cell **97**(5): 321-337.

197. Zernant, J., M. Kulm, *et al.* (2005). "Genotyping microarray (disease chip) for Leber congenital amaurosis: detection of modifier alleles." Invest Ophthalmol Vis Sci **46**(9): 3052-3059.

198. Zhai, R. G., F. Zhang, *et al.* (2008). "NAD synthase NMNAT acts as a chaperone to protect against neurodegeneration." Nature **452**(7189): 887-891.

199. Zhang, Q., S. Li, *et al.* (2001). "Screening for CRX gene mutations in Chinese patients with Leber congenital amaurosis and mutational phenotype." Ophthalmic Genet **22**(2): 89-96.

200. Zhang, T., J. G. Berrocal, *et al.* (2009). "Enzymes in the NAD+ salvage pathway regulate SIRT1 activity at target gene promoters." J Biol Chem **284**(30): 20408-20417.

201. Zhao, H., J. Y. Zhang, *et al.* (2011). "Nicotinamide mononucleotide adenylyltransferase 1 gene NMNAT1 regulates neuronal dendrite and axon morphogenesis in vitro." Chin Med J (Engl) **124**(20): 3373-3377.

202. Zhou, T., O. Kurnasov, *et al.* (2002). "Structure of human nicotinamide/nicotinic acid mononucleotide adenylyltransferase. Basis for the dual substrate specificity

and activation of the oncolytic agent tiazofurin." J Biol Chem **277**(15): 13148-13154.

203. Zou, X., F. Yao, *et al.* (2013). "De novo Mutations in the Cone-rod Homeobox Gene Associated with Leber Congenital Amaurosis in Chinese Patients." Ophthalmic Genet.

204. Zrenner, E., K. U. Bartz-Schmidt, *et al.* (2011). "Subretinal electronic chips allow blind patients to read letters and combine them to words." Proc Biol Sci **278**(1711): 1489-1497.

APPENDIX

Table 1: The frequencies of mutations in LCA-associated genes as reported in major studies. Each column shows the % of mutation frequency of a particular gene reported in that study.

References	Sample Size	AIPL1	ALMS1	CEP290	CNGA3	CRB1	CRX	GUCY2D	IMPDH1	IQCB1	KCNJ13	LCA5	LRAT	MERTK	MYO7A	NMNAT1	RDH12	RPE65	RD3	RPGRIP1	SPATA7	TULP1
Dharmaraj, Silva *et al*. 2000	100						2	6										3				
Gal, Li *et al*. 2000	328													1								
Sohocki, Bowne *et al*. 2000	188	5.8																				
Lotery, Namperumalsamy *et al*. 2000	176						3	6										7				
Perrault, Rozet *et al*. 2000	118							20														
Thompson, Gyurus *et al*. 2000	114																	11				
Sohocki, Perrault *et al*. 2000	27	11.1					4															
Ruiz, Kuehn *et al*. 2001	38												0									
Zhang, Li *et al*. 2001	27						4															
Rivolta, Peck *et al*. 2001	55						3															
Dryja, Adams *et al*. 2001	57																			5		
den Hollander, Heckenlively *et al*. 2001	98					13																
Gerber, Perrault *et al*. 2001	142																			6		
Thompson, Li *et al*. 2001	267												1.1									
Sitorus, Lorenz *et al*. 2003	21	5						0										10				
Hanein,	179	3				10	1	21										6		4		2

Perrault *et al*. 2004																						
Dharmaraj, Leroy *et al*. 2004	303	9																				
Perrault, Hanein *et al*. 2004	110												0				4					
den Hollander, Davis *et al*. 2004	44					0																
Janecke, Thompson *et al*. 2004	89																3.4					
Zernant, Kulm *et al*. 2005	205	6				5	1	12										2		5		
Booij, Florijn *et al*. 2005	9					11		11										22				
Thompson, Janecke *et al*. 2005	1011																2.2					
Bowne, Sullivan *et al*. 2006	24								8													
Friedman, Chang *et al*. 2006	881																		0.1			
Yzer, Leroy *et al*. 2006	58	5				15	0	10									0	2		0		
Senechal, Humbert *et al*. 2006	216												0.4									
den Hollander, Koenekoop *et al*. 2006	76			21																		
Sweeney, McGee *et al*. 2007	97												0									
Vallespin, Cantalapiedra *et al*. 2007	42	2.4				23	0	0					0	0				0		7.1		
Henderson, Waseem *et al*. 2007	59	6.8				13.5	1.7	15.3										3.4		5.1		
Vallespin, Lopez-Martinez *et al*. 2007	49			8.2																		
Perrault, Delphin *et al*. 2007	192			19.8																		
den Hollander, Koenekoop *et al*. 2007	93											2.2										
Gerber, Hanein *et al*. 2007	179											1.7										
Sun, Gerth *et al*. 2007	36																5.5					
Simonelli, Ziviello *et al*. 2007	95	2.1		4.2		4.2		2.1										8.4				

Mamatha, Srilekha *et al*. 2008	60																1.6				
Seong, Kim *et al*. 2008	20					5											5		20		
Li, Wang *et al*. 2009	37					2.7		2.7									5.4				13.5
Sundaresan, Vijayalakshmi *et al*. 2009	35																2.9				
Perrault, Hanein *et al*. 2010	134																			3	
Coppieters, Casteels *et al*. 2010	91	2.2		29.6		16.5	2.2	7.7									8.8				
Li, Xiao *et al*. 2011	87	1.2		3.4		8		13.8				1.15		1.15			4.6		4.6	2.3	
Wang, Wang *et al*. 2011	37		16.6		16.6					50					16.6						
Mackay, Ocaka *et al*. 2011	141																			3.5	
Testa, Surace *et al*. 2011	260	3.1																			
Sergouniotis, Davidson *et al*. 2011	334										0.50										
Estrada-Cuzcano, Koenekoop *et al*. 2011	225									4.9											
Stone, Cideciyan *et al*. 2011	276									3.3											
Falk, Zhang *et al*. 2012	285															4.9					
Koenekoop, Wang *et al*. 2012	200															4					
Perrault, Hanein *et al*. 2012	261															8.4					
Chiang, Wang *et al*. 2012	51															21.6					
Xu, Dong *et al*. 2012	100																	1			
Preising, Hausotter-Will *et al*. 2012	45																		1.1		
Chen, Zhang *et al*. 2013	41			7.3		2.4	2.4	4.8											4.8		
Verma, Perumalsamy *et al*. 2013	30	3.3						10		3.3								13.3		3.3	
Mackay, Borman *et al*. 2013	797											10									

Wang, Wang *et al*. 2013	**179**	**2.8**		**6.1**		**3.4**		**4.5**	**0.6**	**1.7**		**0.6**	**0.6**				**2.3**	**0.6**		**1.1**	**1.7**	**4.5**
(Corton, Tatu *et al*. 2013	**114**					**14**																
Zou, Yao *et al*. 2013	**109**						**1.8**															
Perrault, Estrada-Cuzcano *et al*. 2013	**574**																		**1.2**			
Corton, Avila-Fernandez *et al*. 2014	**79**											**7.6**										
Yang, Wu *et al*. 2014	**67**					**6**																
Total frequency		**4.9%**	**2.7%**	**13.1%**	**2.7%**	**9%**	**2.1 %**	**10%**	**1.8%**	**3.6%**	**1.5 %**	**2.2%**	**0.5%**	**1%**	**2.7%**	**6.9%**	**2.4 %**	**5.3 %**	**0.60 %**	**4.4 0%**	**2.6 0%**	**1.90 %**

Table 2: Details of primers used for amplification of coding regions of *GUCY2D* gene

S.No	Oligo name	Primer Sequence (5'-3')	Annealing temperature (^{0}C)	$MgCl_2$	Product Size (bp)
1	GUCY2D-2AF	AACTCGGGGTTACGGGGA	57	2 mM	360
	GUCY2D-2AR	AGAGAAGATGGGGTCGCAAG			
2	GUCY2D-2BF	GTGTTCACGGTGGGGGTC	57	2 mM	271
	GUCY2D-2BR	CTTCTTCGGCGAGCAGCT			
3	GUCY2D-2CF	TGGGTCCGGTGAACCCTG	57	2 mM	243
	GUCY2D-2CR	TGAGTGCCGTGGACAGTGA			
4	GUCY2D-2DF	CGCCCCCCAGGACCTGTGG	57	2 mM	233
	GUCY2D-2DR	AGAGGCTTGGCTCGCGGC			
5	GUCY2D-3AF	TAGGCTCCCTTGCAGGGT	60	2 mM	451
	GUCY2D-3BR	TCCCTGCTTTGGCTGTCCT			
6	GUCY2D-4AF	CAGGCAGTGAAAGAATCTGGT	61	2 mM	468
	GUCY2D-4BR	TCCATGGCGATTGTCTCAGT			
7	GUCY2D-5F	AGGGGCCAGCATGTGGCAT	60	2 mM	251
	GUCY2D-5R	GAACCCAGCCTGCTGTTTTT			
8	GUCY2D-6F	GTTATCCCTCCCCCGCATC	60	2 mM	276
	GUCY2D-6R	CAAGTAGGGAGCTGGGGTC			
9	GUCY2D-7F	AACCCAGGACTCTGACACCA	64	2 mM	205
	GUCY2D-7R	TTCTTCCCCCACTGTCTCTCT			
10	GUCY2D-8F	AATGAGGGGGAGGGGTTCTA	60	2 mM	232
	GUCY2D-8R	AGCTGCAAAGAGAAGGCAA			
11	GUCY2D-9F	TAACAGCCCCTTCCCCACATT	59	1.5 mM	301
	GUCY2D-9R	CAGGACGTCACCCCACCA			
12	GUCY2D-10F	GTCCTGGGGGCAGGGATG	59	2mM	292
	GUCY2D-10R	GGGGAGAAGCCCTTGAAATAA			
13	GUCY2D-11F	TTCTGGTGAGGGTGGGAGTCT	59	2 mM	276
	GUCY2D-11R	TGAGGCTGGCTCTTTTCTAAC			
14	GUCY2D-12F	GGTCAGAGGCAGCCTTTGT	59	2 mM	280
	GUCY2D-12R	TCTCAGGTTGCTGACAAGCAT			
15	GUCY2D-13F	ATAAAGAGGGCATGGCAACC	60	2 mM	296
	GUCY2D-13R	TCACCTGGGGGCCACTCTA			
16	GUCY2D-14F	GAGCCCAGCCAGGTAGAGTG	61	2 mM	297
	GUCY2D-14R	TGGTGAAGCTGAATTGAAGG			
17	GUCY2D-15F	GAGGCAATCGCTTCGTGTACT	65	2 mM	295
	GUCY2D-15R	CAGGCCCTAAAGAGGGAGAT			
18	GUCY2D-16F	TACCTAGGTGCAGCCCAGGG	60	2 mM	223
	GUCY2D-16R	TGAGCTCGGGACTCACCTC			
19	GUCY2D-17F	TGAGTGTGACGGGGACAAGA	60	2 mM	239
	GUCY2D-17R	GGATGGGCGGTGCCTCAG			
20	GUCY2D-18F	CAAACCTCAGCTCACCCTTCT	59	2 mM	217
	GUCY2D-18R	CGGGGGGTCAGACACAGA			
21	GUCY2D-19F	ATCGGGACACCTGGCTTG	60	2 mM	265
	GUCY2D-19R	GACGTTCTGCAGGCAGCA			

Table 3: Details of primers used for amplification of coding regions of *RD3* gene

S.No	Oligo name	Primer Sequence (5'-3')	Annealing temperature (^{0}C)	$MgCl_2$	Product Size (bp)
1	RD3-2F	TTCCCAGGTTCCCCACTCTG	63	2 mM	436
	RD3-2R	CCACTGCAGCCACCTTTCCT			
2	RD3-3F	GACGCCCGGGGTGCCAGAC	67	2 mM	439
	RD3-3R	GTTCCAGGGCCCGGCGCT			

Table 4: Details of primers used for amplification of the *CRB1* gene

S.No	Oligo name	Primer Sequence (5'-3')	Annealing temperature (^{0}C)	$MgCl_2$	Product Size (bp)
1	CRB1-1F	TGAAGGAGCTGTAAGTAGGGTG	59	2 mM	433
	CRB1-1R	CCTGAATACCTATTGGAAATCA			
2	CRB1-2AF	TTTGGTTGAGGCAGCACAAA	59	2 mM	454
	CRB1-2AR	GAATCTTCCAGCATATCCAGCA			
3	CRB1-2BF	TTCCTGTGGCAAGAACTCCT	59	2 mM	442
	CRB1-2BR	TGATTCCTGTCAAGAACTTGGC			
4	CRB1-3F	GAACATTTGACAAGTGCTCTGG	59	2 mM	394
	CRB1-3R	CGAGAACGTGAGAGCTCTAAAT			
5	CRB1-4F	ATGGGTCTTGGGTTGATAGACA	59	2 mM	442
	CRB1-4R	TGGGCAGCTTGGTAACCTACTT			
6	CRB1-5F	AATGCCAGTATAGCAGTCAACC	59	2 mM	366
	CRB1-5R	AGCTCTTCCTGCTAATACACCA			
7	CRB1-6AF	GCTATTCATGCACTTCTGCAAG	59	2 mM	402
	CRB1-6AR	TCGCCCTCAAATGAAAGTGT			
8	CRB1-6BF	ATTCAGCTGCCTATGTCCATCT	59	2 mM	415
	CRB1-6BR	TGATTGATCACTTTCAAGTGGA			
9	CRB1-6CF	AATCGACGACTCCTGTAAGGAGA	59	2 mM	447
	CRB1-6CR	TTTGCTGTTTCTGCTCTGCTCT			
10	CRB1-7AF	TCCATCCCTTCTGTCTTTTGAG	59	2 mM	350
	CRB1-7AR	GGCTTGATTTTCAAAGATATCAA			
11	CRB1-7BF	TGACTCCAAACTCTCCCAAA	62	2 mM	468
	CRB1-7BR	TGGTGGGTCAGTAACATCATCT			
12	CRB1-8F	CAGATATGTGGTTTCACCGTCA	59	2 mM	380
	CRB1-8R	TACTCGCATAGGGGAAACAA			
13	CRB1-9AF	GCACAGTATGTAACATGTATCAAATA	59	2 mM	639
	CRB1-9AR	GAAACCATGAACATTTTCAAAG			
14	CRB1-9BF	CCTGCAAGGGTGTCTAAGTACA	59	2 mM	558
	CRB1-9BR	GAGGAGAGAGCTTTCCAATTTG			

15	CRB1-10F	CTCCTCCAGCCTGAGTACTTAA	61	2 mM	368
	CRB1-10R	CAGCATAGATTTTCCTATGGGA			
16	CRB1-11F	GGATGGGTAGATAAGACTGTGC	59	2 mM	356
	CRB1-11R	TGTTCACCCCACTCAACAACT			
17	CRB1-12F	CCTGAGTAGTTCCATTGTCCTGA	61	2 mM	407
	CRB1-12R	TTCCAGTGTAATCCCAGTTGCA			

Table 5: Details of primers used for amplification of the *NMNAT1* gene

S.No	Oligo name	Primer Sequence (5'-3')	Annealing temperature (^{0}C)	$MgCl_2$	Product Size (bp)
1	NMNAT1-2F	GGGTGGCAGAGCAAGACCTTATC	65	2 mM	321
	NMNAT1-2R	ATGCTGGGATTGCAGGTGTG			
2	NMNAT1-3F	GCCGAGATCACTCCAGTGCGG	65	2 mM	515
	NMNAT1-3R	GGAAGACCCATCCTTTGGTGCTGTG			
3	NMNAT1-4F	TGTGCCCAGCTATAAATAATGT	61	2 mM	406
	NMNAT1-4R	AGGCAGGAGAATGGCATGAA			
4	NMNAT1-5F	AAGCCCTCATCCTTGAAAAGCACA	65	2 mM	597
	NMNAT1-5R	AGGCAACAGATCACAACTTCTTTCC			

Table 6: Details of primers used for amplification of coding regions of *PALS1* gene

S.No	Oligo name	Primer Sequence (5'-3')	Annealing temperature(^{0}C)	$MgCl_2$	Product Size (bp)
1	PALS1-1F	TTTCCCCTTAGATTTCCTTCATG	60	2 mM	653
	PALS1-1R	TGGTCTGGAATTCAAACTGTCAT			
2	PALS1-2F	ATGCATGTTGAATTAATACTGAAA	60	2 mM	428
	PALS1-2R	AAATGCATGTAGTAAACTGTCAC			
3	PALS1-3F	GAATTTTATGGTATGTTGGGTGAA	60	2 mM	470
	PALS1-3R	AAACATCAAAATAGGCTAGAGAAT			
4	PALS1-4F	CTTTCATAACCCATTCCAGAGT	63	2 mM	450
	PALS1-4R	AGCACACAACAGCAGAAAAATG			
5	PALS1-5F	AAGCAGAAAGTGTGGGGGAAAT	64	2 mM	656
	PALS1-5R	TTTCCCAAGTGGCTAGTGCATAT			
6	PALS1-6F	AGTGCTGCTGGTCATTTAAGTC	66	2 mM	307
	PALS1-6R	TTGAGTACAGGAAACAGTGACAT			
7	PALS1-7F	ATCGCTTGAGGCTAGAAATTTG	60	2 mM	583
	PALS1-7R	TGGGATTGGCTGAAGTTATACA			

8	PALS1-8F	TTGGAGGCTTACACATCATAGCT	66	2 mM	310
	PALS1-8R	GCAGATTCACACATGGCTCCA			
9	PALS1-9F	AAGACAAGCGTGGCCAACATA	60	2 mM	371
	PALS1-9R	TCAAAACACTGCCTTACTCACA			
10	PALS1-10F	TTTGTCTAATTTTGGGTGAAG	58	2 mM	383
	PALS1-10R	TTCCTCTTTCACTGACAACA			
11	PALS1-11F	TAGGCACTTAGCATTTTCTCAG	65	2 mM	505
	PALS1-11R	AAGAGATTTAGCAACCTGTGTG			
12	PALS1-12F	TGATCACACCACTGCACTCTA	63	2 mM	326
	PALS1-12R	AAGCACCAGGACAAATTAGACC			
13	PALS1-13F	AGAGACAGAAGGAAAGCTATGA	60	2 mM	394
	PALS1-13R	TGCCTTCCATCTTATCCTCAAT			

nature genetics

NMNAT1 mutations cause Leber congenital amaurosis

Marni J Falk[1,2,22], Qi Zhang[3,4,22], Eiko Nakamaru-Ogiso[5], Chitra Kannabiran[6], Zoe Fonseca-Kelly[3,4], Christina Chakarova[7], Isabelle Audo[8–11], Donna S Mackay[7], Christina Zeitz[8–10], Arundhati Dev Borman[7,12], Magdalena Staniszewska[3,4], Rachna Shukla[6], Lakshmi Palavalli[6], Saddek Mohand-Said[8–11], Naushin H Waseem[7], Subhadra Jalali[6,13], Juan C Perin[14], Emily Place[1,3,4], Julian Ostrovsky[1], Rui Xiao[15], Shomi S Bhattacharya[7,16], Mark Consugar[3,4], Andrew R Webster[7,12], José-Alain Sahel[8–11,17,18], Anthony T Moore[7,12,19], Eliot L Berson[4], Qin Liu[3,4], Xiaowu Gai[20,21,23] & Eric A Pierce[3,4,23]

Leber congenital amaurosis (LCA) is an infantile-onset form of inherited retinal degeneration characterized by severe vision loss[1,2]. Two-thirds of LCA cases are caused by mutations in 17 known disease-associated genes[3] (Retinal Information Network (RetNet)). Using exome sequencing we identified a homozygous missense mutation (c.25G>A, p.Val9Met) in *NMNAT1* that is likely to be disease causing in two siblings of a consanguineous Pakistani kindred affected by LCA. This mutation segregated with disease in the kindred, including in three other children with LCA. *NMNAT1* resides in the previously identified LCA9 locus and encodes the nuclear isoform of nicotinamide mononucleotide adenylyltransferase, a rate-limiting enzyme in nicotinamide adenine dinucleotide (NAD^+) biosynthesis[4,5]. Functional studies showed that the p.Val9Met alteration decreased NMNAT1 enzyme activity. Sequencing *NMNAT1* in 284 unrelated families with LCA identified 14 rare mutations in 13 additional affected individuals. These results are the first to link an NMNAT isoform to disease in humans and indicate that *NMNAT1* mutations cause LCA.

Inherited retinal diseases, such as LCA, represent a heterogeneous group of early-onset blindness disorders that are characterized by progressive dysfunction and death of the rod and cone retinal photoreceptor cells[6]. Despite the identification so far of more than 180 different inherited retinal disease–associated genes, the genetic etiology remains uncertain in 40–50% of individuals with inherited retinal disease[7] (RetNet). Additional loci have been identified at which disease-associated genes have not yet been identified, such as the LCA9 locus mapped to chromosome 1p36 (ref. 4). Identifying the genetic basis of inherited retinal diseases is essential to guide the development of potential therapies, as highlighted by the recent success of clinical gene therapy trials for *RPE65*-related LCA[8–12]. Here, we used whole-exome sequencing in a large consanguineous Pakistani family, including five children affected with LCA who did not have mutations in known LCA-causing genes.

Two Pakistani siblings, an 11-year-old girl and her 3-year-old brother (**Fig. 1a**, family 047, subjects IV-1 and IV-3, respectively), initially came to the Ophthalmology-Genetics Clinic at the Children's Hospital of Philadelphia for evaluation of LCA because of severe vision impairment, congenital nystagmus and no detectable (<10 μV) retinal function by full-field electroretinography (ERG) testing in early infancy (see **Supplementary Note** for additional clinical details). Both children also had global developmental delay, nonverbal autism with stereotypies, hypotonia with joint hypermobility and dysmorphic facies. Severe-to-profound bilateral sensorineural hearing loss was present in the 11-year-old proband (IV-1) and in her 8-year-old brother (IV-2), who had a normal eye exam and normal development but exhibited clinical features consistent with mucolipidosis (**Supplementary Note**).

[1]Department of Pediatrics, Division of Human Genetics, The Children's Hospital of Philadelphia and University of Pennsylvania Perelman School of Medicine, Philadelphia, Pennsylvania, USA. [2]Department of Pediatrics, Division of Child Development and Metabolic Disease, The Children's Hospital of Philadelphia and University of Pennsylvania Perelman School of Medicine, Philadelphia, Pennsylvania, USA. [3]Department of Ophthalmology, Ocular Genomics Institute, Massachusetts Eye and Ear Infirmary, Harvard Medical School, Boston, Massachusetts, USA. [4]Berman-Gund Laboratory for the Study of Retinal Degenerations, Department of Ophthalmology, Massachusetts Eye and Ear Infirmary, Harvard Medical School, Boston, Massachusetts, USA. [5]Department of Biochemistry and Biophysics, University of Pennsylvania Perelman School of Medicine, Philadelphia, Pennsylvania, USA. [6]Kallam Anji Reddy Molecular Genetics Laboratory, LV Prasad Eye Institute (LVPEI), Kallam Anji Reddy Campus, LV Prasad Marg, Hyderabad, India. [7]Institute of Ophthalmology, University College of London, London, UK. [8]Institut National de la Santé et de la Recherche Médicale (INSERM) U968, Paris, France. [9]Université Pierre et Marie Curie (UPMC Paris 06), Unité Mixte de Recherche (UMR)_S 968, Institut de la Vision, Paris, France. [10]Centre National de la Recherche Scientifique, UMR 7210, Paris, France. [11]Centre Hospitalier National d'Ophtalmologie des Quinze-Vingts, INSERM–Direction de l'Hospitalisation et de l'Organisation des Soins (DHOS) Centre d'Investigation Clinique 503, Paris, France. [12]Moorfields Eye Hospital, London, UK. [13]Srimati Kanuri Santhamma Centre for Vitreoretinal Diseases, LVPEI, Kallam Anji Reddy Campus, LV Prasad Marg, Hyderabad, India. [14]Center for Biomedical Informatics, Children's Hospital of Philadelphia, Philadelphia, Pennsylvania, USA. [15]Department of Biostatistics and Epidemiology, University of Pennsylvania Perelman School of Medicine, Philadelphia, Pennsylvania, USA. [16]Centro Andaluz de Biología Molecular y Medicina Regenerativa (CABIMER), Isla de Cartuja, Seville, Spain. [17]Fondation Ophtalmologique Adolphe de Rothschild, Paris, France. [18]Académie des Sciences–Institut de France, Paris, France. [19]Great Ormond Street Hospital for Children, London, UK. [20]Department of Molecular Pharmacology and Therapeutics, Loyola University Chicago Health Sciences Division, Maywood, Illinois, USA. [21]Center for Biomedical Informatics, Loyola University Chicago Health Sciences Division, Maywood, Illinois, USA. [22]These authors contributed equally to this work. [23]These authors jointly directed this work. Correspondence should be addressed to E.A.P. (eric_pierce@meei.harvard.edu).

Received 12 February; accepted 29 June; published online 29 July 2012; doi:10.1038/ng.2361

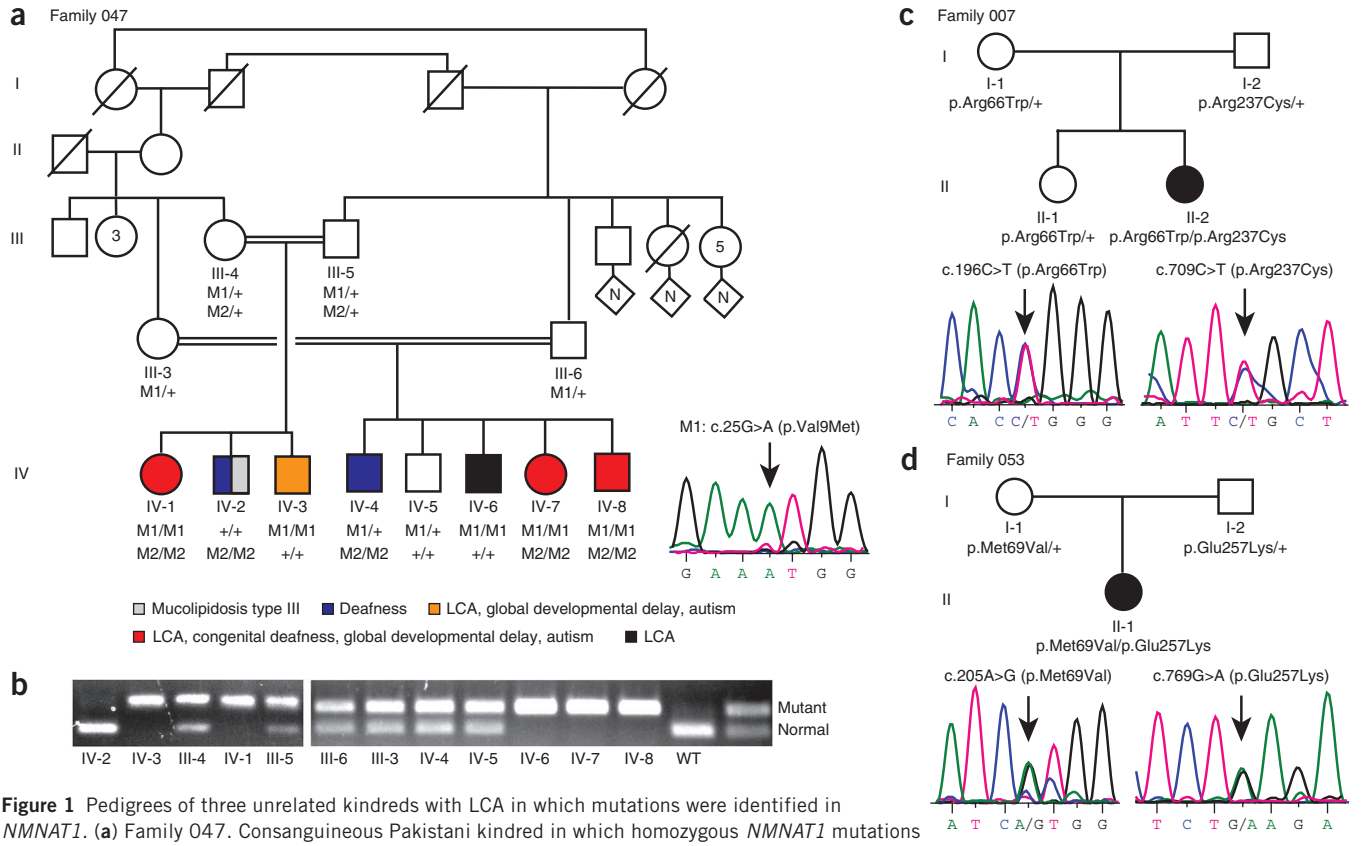

Figure 1 Pedigrees of three unrelated kindreds with LCA in which mutations were identified in *NMNAT1*. (**a**) Family 047. Consanguineous Pakistani kindred in which homozygous *NMNAT1* mutations were identified in five children with LCA by whole-exome sequencing with validation by Sanger sequencing. M1, *NMNAT1* mutation (c.25G>A, p.Val9Met); M2, *GJB2* mutation (c.71G>A, p.Trp24*). A representative sequence trace for M1 is shown. Colored symbols indicate affected individuals. Numbers within symbols indicate multiple offspring of a given gender. Diamonds represent individuals of unknown gender, and N indicates multiple individuals of unknown number. Slashes indicate deceased individuals. (**b**) Genotyping of family 047. Members were genotyped by PCR amplification of exon 2 of *NMNAT1*, and PCR products were digested with AcuI to distinguish wild-type and mutant sequences (sizes of digested wild-type and mutant products shown in the last lane). (**c**) Family 007. A single proband with LCA was shown by Sanger sequencing of *NMNAT1* to harbor compound heterozygous mutations c.196C>T (p.Arg66Trp) and c.709C>T (p.Arg237Cys). (**d**) Family 053. A single proband with LCA was shown by Sanger sequencing of *NMNAT1* to harbor compound heterozygous mutations c.205A>G (p.Met69Val) and c.769G>A (p.Glu257Lys). +, wild type. Sample sequence traces are shown in **c** and **d**.

Their parents were first cousins who were visually and developmentally normal (**Fig. 1a**, subjects III-4 and III-5). Notably, the parents' siblings had married one another (**Fig. 1a**, subjects III-3 and III-6) and together had two children with similar vision and nonverbal autism phenotypes as the proband (subjects IV-7 and IV-8) and one child with isolated LCA (IV-6). Clinical genetic diagnostic testing identified a homozygous mutation in *GJB2* (c.71G>A, p.Trp24*) as the cause of sensorineural hearing loss in subject IV-1, but no mutation was identified in any of the known LCA-causing genes (**Supplementary Note**). Additional sequencing analyses verified that the homozygous mutation encoding p.Trp24* in GJB2 segregated with the hearing loss phenotype in the larger kindred (**Fig. 1a**).

To search for the genetic cause of LCA in this family, we performed whole-exome sequencing of the nuclear family of the 11-year-old proband (**Fig. 1a**, subjects IV-1, IV-2, IV-3, III-4 and III-5). Given known consanguinity, a homozygous mutation of biparental inheritance that was shared by both affected children but not by their sibling with normal visual acuity was postulated to be the most likely mode of LCA inheritance. We identified a total of 113 nonsynonymous variants in 86 genes that met these criteria (**Supplementary Fig. 1**). Four of these variants were rare or novel according to dbSNP 132, 1000 Genomes Project data and National Heart, Lung, and Blood Institute (NHLBI) Exome Sequencing Project (ESP) data[13,14]. The genes harboring these four variants had known retinal expression, which was determined from mouse retina RNA sequencing (RNA-seq) analyses[15]. Only one of these variants was predicted to damage protein function by SIFT, PolyPhen-2 and other programs: c.25G>A (p.Val9Met) in *NMNAT1* (refs. 16–20) (NM_022787). Sanger sequencing of the c.25G>A variant in *NMNAT1* validated its segregation with the LCA phenotype in the original nuclear kindred and in the proband's similarly affected cousins, including the one with isolated LCA (**Fig. 1a**,**b**). Only the mutant M1 allele encoding p.Val9Met NMNAT1 was detected in the five children with LCA in generation IV, whereas the four unaffected parents of these children in generation III carry both the mutant and wild-type alleles, and their three children with normal vision harbor only the wild-type allele (**Fig. 1b**). The p.Val9Met variant was not present in 501 controls or in any public databases[13,14].

No clearly pathogenic mutations were identified that were likely to be the cause of developmental delay, nonverbal autism, hypotonia and dysmorphic facies in family members IV-1, IV-3, IV-7 and IV-8. These presentations likely have a separate genetic etiology from that of LCA and deafness in this family, as individual IV-6 has LCA alone, individual IV-2 has deafness alone and additional *NMNAT1* mutations were identified in individuals with non-syndromic LCA, as described below.

Table 1 Identified *NMNAT1* mutations

	Ancestry or nationality	Alterations		EVS[a]	PolyPhen-2[b]	SIFT[c]
		DNA	Protein			
CHOP/MEEI						
LCA-047	Pakistani	c.25G>A	p.Val9Met (homo)	Novel	PoD	D
LCA-007	Asian American	c.196C>T	p.Arg66Trp	Novel	PrD	D
		c.709C>T	p.Arg237Cys	1/7,019	PrD	D
LCA-053	African American	c.205A>G	p.Met69Val	Novel	PrD	D
		c.769G>A	p.Glu257Lys[d]	13/10,745	B	T
LVPEI						
LCA-73	Indian	c.25G>A	p.Val9Met (homo)	Novel	PoD	D
LCA-79	Indian	c.98A>G	p.Asp33Gly (homo)	Novel	PrD	D
LCA-100	Indian	c.709C>T	p.Arg237Cys	Novel	PrD	D
		c.565delG	p.Ala189Leufs*25	1/7,019		
LCA-128	Indian	c.215T>A	p.Leu72His (homo)	Novel	PrD	D
UCL						
LCA-1	European descent	c.205A>G	p.Met69Val	Novel	PrD	D
		c.769G>A	p.Glu257Lys	13/10,745	B	T
LCA-2	Caribbean, Sri Lankan	c.161C>T	p.Ala54Val	1/10,757	PrD	D
		c.293T>G	p.Val98Gly	Novel	PrD	T
LCA-3	Caribbean	c.37G>A	p.Ala13Thr	1/10,757	PrD	D
		c.293T>G	p.Val98Gly	11/10,747	PrD	T
LCA-4	Caribbean, Irish	c.723delA	p.Pro241Profs*45	Novel	N/A	N/A
		c.769G>A	p.Glu257Lys	13/10,745	B	T
LCA-5	Polish	c.59T>A	p.Ile20Asn	Novel	PrD	D
		c.769G>A	p.Glu257Lys	13/10,745	B	T
LCA-6	British (European descent)	c.552A>G	p.Ile184Met	Novel	PoD	D
		c.769G>A	p.Glu257Lys	13/10,745	B	T
LCA-7	British (European descent)	c.466G>C	p.Gly156Arg	Novel	PrD	D
		c.769G>A	p.Glu257Lys	13/10,745	B	T

CHOP, Children's Hospital of Philadelphia; LVPEI, LV Prasad Eye Hospital; MEEI, Massachusetts Eye and Ear Infirmary; UCL, University College London.

[a]Data from Exome Variant Server, number of times variant detected/number of exomes analyzed. [b]PolyPhen-2 Hum-Var score: PrD, probably damaging; PoD, possibly damaging; B, benign. [c]SIFT: D, damaging; T, tolerated; N/A, not applicable. [d]The p.Glu257Lys variant in NMNAT1 was detected in a total of six families. Although this variant is sufficiently rare to be associated with LCA (estimated prevalence of 1 in 30,000)[33] according to ESP data (13/10,745 = 0.12%), it is not predicted to damage protein function by PolyPhen-2 or SIFT. However, it is known that these prediction programs have significant false positive and negative rates and frequently do not agree with one another[34,35]. We therefore employed Fisher's exact test to estimate the probability that the p.Glu257Lys variant causes disease. This analysis showed that the allele frequency for the p.Glu257Lys variant was significantly higher in the LCA cases (6/568 chromosomes = 1.056%) compared to both our controls (0/1,002 chromosomes = 0%; $P = 0.002$) and ESP samples (13/10,758 chromosomes = 0.121%; $P = 0.0002$), which is consistent with a high likelihood that this variant is pathogenic.

To determine whether *NMNAT1* mutations cause LCA in other families, we sequenced *NMNAT1* in 56 unrelated probands with LCA evaluated at The Children's Hospital of Philadelphia (CHOP) and the Massachusetts Eye and Ear Infirmary (MEEI). We found rare compound heterozygous mutations in *NMNAT1* that segregated with disease in family 007, in which the proband was a 5-year-old girl with isolated LCA and there was no family history of the disease (**Fig. 1c** and **Table 1**). We also identified compound heterozygous variants in *NMNAT1* that segregated with disease in family 053, in which the proband was a 20-year-old man with LCA (**Fig. 1d** and **Table 1**). The four *NMNAT1* variants identified in these subjects were not identified in 501 control samples.

To investigate the frequency of *NMNAT1* mutations in LCA, we screened additional populations of affected individuals from varying ancestry groups. This analysis included 228 additional probands ascertained at Institut de la Vision in Paris, LVPEI in India and University College London (UCL). These analyses identified homozygous or compound heterozygous mutations in *NMNAT1* in 11 additional families with LCA (**Table 1** and **Supplementary Fig. 2**). All of the mutations detected are rare, and all, with the exception of one encoding the p.Glu257Lys variant, were predicted to be damaging by PolyPhen-2 and/or SIFT (**Table 1**). None of the *NMNAT1* variants identified in these subjects were identified by Sanger sequencing in 501 control samples. Review of available clinical information for individuals in whom *NMNAT1* mutations were identified as the cause of LCA (**Supplementary Note**) indicated that the majority have atrophic macular lesions (**Fig. 2**).

NMNAT1 encodes a rate-limiting enzyme that generates NAD^+, both in a biosynthetic pathway from nicotinic acid mononucleotide (NaMN) and in a salvage pathway from nicotinamide mononucleotide (NMN) (**Supplementary Fig. 3**)[21]. Three functionally nonredundant mammalian NMNAT isoforms encoded by different genes have been identified within distinct cellular compartments, with NMNAT1, NMNAT2 and NMNAT3 localizing to the nucleus, Golgi complex and mitochondria, respectively[5,22]. The mitochondrial isoform, NMNAT3, regenerates NAD^+ for cellular energetics, whereas NMNAT1 is involved in the nuclear NAD^+ homeostasis that is necessary for both DNA metabolism and cell signaling[5]. Of interest, Nmnat1 is the principal component of the mouse Wallerian degeneration fusion protein (Wld^S), which also includes a 70-residue N-terminal sequence from the Ube4b multiubiquitination factor, and has been shown to have neuroprotective activity[23]. Homozygous *Nmnat1*-knockout mice are embryonic lethal, whereas heterozygous *Nmnat1*-knockout mice have normal development[24]. Loss of *nmnat* in *Drosophila melanogaster* photoreceptors leads to photoreceptor cell degeneration[25].

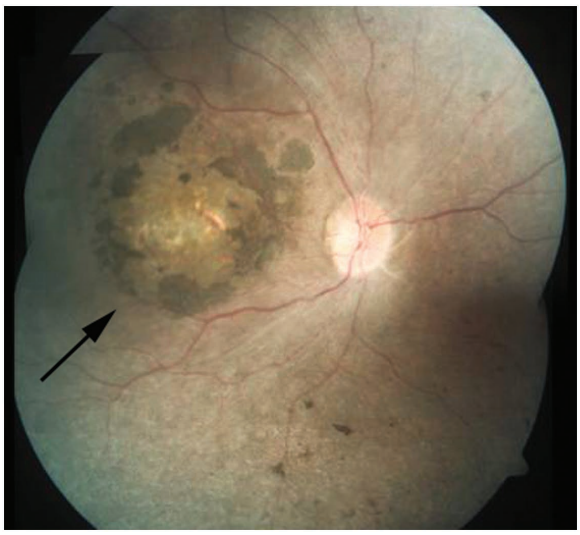

Figure 2 Retinal image from individual with LCA due to mutations in *NMNAT1*. Composite fundus image of the right eye of subject II-1 from LVPEI family LCA-100, showing pallor of the optic disc, attenuation of the retinal blood vessels, pigment disruption, atrophic changes in the macula (arrow) and scattered pigment clumping in the peripheral retina. The optic disc is ~1.75 mm in diameter.

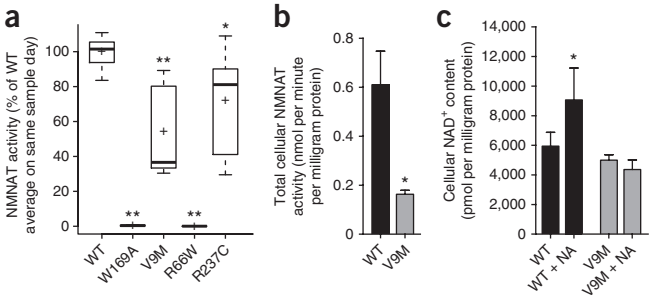

Figure 3 NMNAT1 enzyme activity and cellular NAD+ content. (**a**) The NAD+ biosynthetic activities of wild-type (WT) and mutant purified recombinant NMNAT1 proteins were measured. Box plots show activity measurements from replicate protein preparations that were independently generated and measured. The length of the box represents the 25th to 75th interquartile range, the interior horizontal line represents the median, the interior cross represents the mean, and vertical lines issuing from the box extend to the minimum and maximum values of the analysis variable. The p.Trp169Ala mutant had no NMNAT1 enzyme activity ($n = 6$; $P = 0.0014$), as was previously reported[32]. The p.Val9Met mutant had significantly lower enzyme activity (37% of wild-type NMNAT1 activity) ($n = 7$; $P = 0.0015$). The p.Arg237Cys mutant had 81% of wild-type NMNAT1 activity ($n = 6$; $P = 0.034$). The p.Arg66Trp mutant had no NMNAT1 enzyme activity ($n = 6$; $P = 0.0014$). $^*P < 0.05$; $^{**}P < 0.01$; determined by non-parametric Wilcoxon rank-sum test. (**b**) Total cellular NMNAT enzyme activity was measured in whole-cell extracts of fibroblasts from a healthy control and a proband with LCA (subject IV-1 from family 047) who was homozygous for the p.Val9Met NMNAT1 variant. The mutant cells had 27% of the total cellular NMNAT NAD+ synthetic activity of control cells (two-tailed *t* test $P = 0.016$; $n = 6$ for wild-type, $n = 5$ for mutant cells). (**c**) Cellular NAD+ levels. Total cellular NAD+ content was quantified by HPLC in the same control and mutant fibroblasts as in **b** at baseline and after exposure to 10 mM nicotinic acid (NA) for 24 h. NAD+ content in fibroblasts from the proband with LCA was decreased by 16% relative to that in wild-type cells ($P = 0.067$). Nicotinic acid exposure significantly increased NAD+ content in control cells but had no effect on NAD+ content in the mutant cells. $n = 7$ for both cell lines without treatment, $n = 6$ for control cells exposed to nicotinic acid, and $n = 4$ for mutant cells exposed to nicotinic acid. In **b** and **c**, data are shown as the mean with standard error; $^*P < 0.05$.

We assessed the potential deleterious effects of the novel missense variants p.Val9Met, p.Arg66Trp and p.Arg237Cys on the NMNAT1 protein. These altered residues are located in conserved regions of the protein (**Supplementary Fig. 4**) and are predicted to damage NMNAT1 protein structure and stability by several prediction programs[26,27]. All three of these mutant proteins showed correct nuclear localization and normal expression levels following expression of recombinant NMNAT1 proteins in heterologous cells (**Supplementary Fig. 5a**,**b**). In addition, the p.Val9Met mutant correctly localized to the nucleus of a fibroblast cell line obtained from the proband with LCA in family 047 (**Fig. 1a**, subject IV-1, and **Supplementary Fig. 5c**)[22].

Given the normal nuclear localization and expression of the mutant NMNAT1 proteins, we postulated that the deleterious effect of the p.Val9Met, p.Arg66Trp and p.Arg237Cys variants might be on NMNAT1 enzymatic function. We therefore measured the NAD+ biosynthetic activity of wild-type and mutant purified recombinant NMNAT1 proteins (**Fig. 3a**). Despite variability in enzyme rates between experimental days, the protein activity of the NMNAT1 p.Val9Met variant was reproducibly and significantly lower than that of wild-type protein on the same day (63.4% median reduction, interquartile range 31.4–88.7; Wilcoxon rank-sum test $P = 0.0015$). The enzyme activity of the p.Arg66Trp mutant was also significantly lower (99.5% median reduction, interquartile range 0.01–0.11; Wilcoxon rank-sum test $P = 0.0014$), although we were not able to achieve effective purification of the Flag-tagged version of this mutant (**Supplementary Fig. 6**), despite its clearly normal expression and nuclear localization in CHO and mIMCD3 cells (**Supplementary Fig. 5**). The enzyme activity of the p.Arg237Cys mutant was only marginally lower than that of wild-type protein (18.9% reduction, interquartile range 41.1–90.1; Wilcoxon rank-sum test $P = 0.034$) (**Fig. 3a**), raising the question of how this mutation causes disease. It has been observed that NMNAT1 forms functional homo-oligomers and that amino acids 234–238 participate in these protein interactions[5]. To evaluate whether the pathogenic effect of the p.Arg237Cys alteration could be related to its location in a region of NMNAT1 that is involved in protein multimerization, we measured NMNAT1 activity in recombinant protein purified from cells cotransfected with constructs for both the p.Arg66Trp and p.Arg237Cys variants that were identified in family 007. We observed notably lower enzyme activity (18% of wild-type control rate; data not shown) in the combined protein preparation. Additional studies using extracts from the fibroblast cells of the proband with the p.Val9Met alteration (**Fig. 1a**, subject IV-1) showed 73% lower total cellular NMNAT enzyme activity (two-tailed *t* test $P = 0.016$) relative to wild-type control (**Fig. 3b**). These data suggest that the pathogenic effects of these mutations are related, at least in part, to significantly reduced NMNAT1 enzyme activity. It will be of interest to investigate the function of the mutant NMNAT1 proteins in retinal cells, given the isolated retinal phenotype of LCA.

The total NAD+ concentration of human cells has many contributing determinants[21,28]. We measured NAD+ in the fibroblast cell line from the proband with LCA (**Fig. 1a**, subject IV-1) to determine whether the p.Val9Met alteration in the nuclear-localized NMNAT1 protein significantly affected total cellular NAD+ content. Fibroblasts from the proband with LCA had 16% less NAD+ content than wild-type controls, although this difference was not statistically significant (two-tailed *t* test $P = 0.067$; **Fig. 3c**). These data suggest that the reduction in NMNAT1 enzyme activity caused by the p.Val9Met alteration may be sufficient to affect total cellular NAD+ content.

Cellular NAD+ concentrations can be directly increased by nicotinic acid, which requires NMNAT activity for its conversion to NAD+ (**Supplementary Fig. 3**)[29]. We therefore asked whether cellular NAD+ concentration in the fibroblasts expressing the NMNAT1 p.Val9Met mutant (from subject IV-1) was altered by exposure to 10 mM nicotinic acid for 24 h. Notably, whereas nicotinic acid significantly increased the total cellular NAD+ content by 53% in control cells (two-tailed *t* test $P = 0.021$), it had no effect on NAD+ content in the fibroblasts from the proband with LCA (**Fig. 3c**; two-tailed *t* test $P > 0.05$). The inability of nicotinic acid to increase the NAD+ content in NMNAT1 p.Val9Met mutant fibroblasts provides further evidence that they have a substantial deficiency in cellular NMNAT enzymatic activity.

In summary, we report here the first instance of disease association with an NMNAT isoform[5]. *NMNAT1* mutations cause LCA and are the likely pathogenic basis for disease previously linked to the LCA9 locus, although the family in which disease was originally linked to this locus was not available for analysis in this study[4] (C. Toomes and C. Inglehearn, personal communication). Through exome sequencing in a consanguineous Pakistani kindred with LCA and subsequent Sanger sequencing of *NMNAT1* in 284 additional unrelated probands with LCA, we identified mutations in 14 unrelated

families (14/285 = 4.9% of unrelated cases). This work suggests that mutations in *NMNAT1* are a relatively common cause of LCA[3]. However, because the cohorts of individuals used for these studies are enriched for subjects without mutations in known LCA-causing genes, the proportion of all LCA cases caused by *NMNAT1* mutations is likely to be overestimated by these data.

The identification of *NMNAT1* as an LCA-causing gene raises the intriguing question of how mutations in a widely expressed NAD^+ biosynthetic protein lead to a retina-specific phenotype. The data presented suggest that the retinal degeneration phenotype observed in individuals with *NMNAT1* mutations results from decreased NAD^+ biosynthetic activity. This hypothesis is consistent with findings from studies of the Wld^S protein in mice, which showed that the neuroprotective effect of the Wld^S protein required both the Ube4b component and an enzymatically active NMNAT1 portion of the chimeric protein[30]. However, it seems that, in some systems, such as *Drosophila*, *nmnat* alone has a neuroprotective role that may be independent of its NAD^+ biosynthetic activity[25,31]. Thus, it remains to be determined whether retinal degeneration caused by mutations in *NMNAT1* results primarily from the loss of a potentially novel neuroprotective effect of NMNAT1 or a previously unappreciated role of NAD^+-mediated signaling in retinal health and disease. In either case, *NMNAT1* mutations represent a new pathophysiological cause of LCA, further underscoring the genetic heterogeneity of inherited retinal diseases[3,6]. We postulate that pharmacologic and/or genetic therapies directed at restoring cellular NAD^+ homeostasis in retinal cells may offer a therapeutic strategy for *NMNAT1*-related LCA.

URLs. Exome Variant Server, NHLBI Exome Sequencing Project (ESP), http://evs.gs.washington.edu/EVS/; RetNet Retinal Information Network, https://sph.uth.tmc.edu/retnet/; 1000 Genomes Project, http://www.1000genomes.org/; UCSC Genome Browser, http://genome.ucsc.edu/.

METHODS

Methods and any associated references are available in the online version of the paper.

Accession codes. Exome sequence data for family 047 is available at the NCBI Sequence Read Archive (SRA) under accession SRP013517.

Note: Supplementary information is available in the online version of the paper.

ACKNOWLEDGMENTS

We thank M. Sousa, D. Harnley, M.-E. Lancelot and A. Antonio for their excellent technical assistance, The Children's Hospital of Philadelphia CytoGenomics Laboratory for assistance with the establishment of the fibroblast cell lines and tissue culture and J. Baur for his helpful discussions on NAD^+ metabolism. We are grateful to the individuals with LCA and their relatives for their participation in this study.

This work was supported by grants from the US National Institutes of Health (RO1-EY12910 (E.A.P.), R03-DK082446 (M.J.F.), R01-GM097409 (E.N.-O.), P30HD026979 (M.J.F. and R.X.) and P30EY014104 (Massachusetts Eye and Ear Infirmary core support)); the Foundation Fighting Blindness USA (I.A., A.D.B., E.L.B., S.S.B., Q.L., A.T.M., D.S.M., E.A.P., J.-A.S., S.M.-S. and A.R.W.); the Rosanne Silbermann Foundation (E.A.P.); the Penn Genome Frontiers Institute (E.A.P. and X.G.); the Institutional Fund to the Center for Biomedical Informatics by the Loyola University Stritch School of Medicine (X.G.); the Foerderer Award for Excellence from the Children's Hospital of Philadelphia (M.J.F. and X.G.); the Angelina Foundation Fund from the Division of Child Development and Metabolic Disease at the Children's Hospital of Philadelphia (M.J.F.); the Clinical and Translational Research Center at the Children's Hospital of Philadelphia (UL1-RR-024134) (M.J.F. and E.A.P.); the Department of Biotechnology, the Government of India and the Champalimaud Foundation, Portugal (C.K.); the Hyderabad Eye Research Foundation (C.K.); a senior research fellowship from the Council for Scientific and Industrial Research (R.S.); the Foundation Voir et Entendre, Ville de Paris and Région Ille de France (C.Z.); RP Fighting Blindness (UK)(A.R.W.); Fight For Sight (UK) (A.D.B., S.S.B., A.T.M., D.S.M. and A.R.W.); Moorfields Eye Hospital National Institute of Health Research (NIHR) British Research Council (BRC) for Ophthalmology (A.D.B., S.S.B., A.T.M., D.S.M. and A.R.W.); and the Special Trustees of Moorfields Eye Hospital (A.D.B., S.S.B., A.T.M., D.S.M. and A.R.W.). The content is solely the responsibility of the authors and does not necessarily represent the official views of the funding organizations or the National Institutes of Health. This project is funded, in part, by the Penn Genome Frontiers Institute under a grant with the Pennsylvania Department of Health, which disclaims responsibility for any analyses, interpretations or conclusions.

AUTHOR CONTRIBUTIONS

Experiments were designed by Q.Z., M.J.F., X.G. and E.A.P. LCA case samples and controls were provided by I.A., A.D.B., E.L.B., S.S.B., C.K., M.J.F., S.J., A.T.M., E.P., S.M.-S., J.-A.S., A.R.W. and E.A.P. Pedigrees were compiled by A.D.B., C.C., C.K., S.J. and E.P. Individuals III-4, III-5, IV-1, IV-2 and IV-3 were clinically evaluated by M.J.F. and E.A.P. (individuals III-3, III-6 and IV-4 to IV-7 were not clinically evaluated by the authors). Exome sequencing was performed by M.C. Bioinformatics pipeline development was performed by X.G., M.J.F., E.A.P. and M.C. Exome data analyses were performed by J.C.P., X.G., Z.F.-K. and E.A.P. *NMNAT1* sequencing and segregation analyses were performed by I.A., C.C., M.C., Z.F.-K., D.S.M., L.P., R.S., N.H.W., C.Z. and Q.Z. High-performance liquid chromatography (HPLC)-based NMNAT enzyme activity assay and NAD^+ content assay development was performed by E.N.-O., with data analysis performed by E.N.-O., M.J.F., E.A.P. and R.X. *In vitro* functional studies were carried out by Q.Z., E.N.-O., J.O., Q.L. and M.S. The manuscript was written by M.J.F., Q.Z., X.G. and E.A.P.

COMPETING FINANCIAL INTERESTS

The authors declare no competing financial interests.

Published online at http://www.nature.com/doifinder/10.1038/ng.2361.
Reprints and permissions information is available online at http://www.nature.com/reprints/index.html.

1. Weleber, R.G. Infantile and childhood retinal blindness: a molecular perspective. *Ophthalmic Genet.* **23**, 71–97 (2002).
2. Michaelides, M., Hardcastle, A.J., Hunt, D.M. & Moore, A.T. Progressive cone and cone-rod dystrophies: phenotypes and underlying molecular genetic basis. *Surv. Ophthalmol.* **51**, 232–258 (2006).
3. den Hollander, A.I., Black, A., Bennett, J. & Cremers, F.P. Lighting a candle in the dark: advances in genetics and gene therapy of recessive retinal dystrophies. *J. Clin. Invest.* **120**, 3042–3053 (2010).
4. Keen, T.J. *et al.* Identification of a locus (LCA9) for Leber's congenital amaurosis on chromosome 1p36. *Eur. J. Hum. Genet.* **11**, 420–423 (2003).
5. Lau, C., Niere, M. & Ziegler, M. The NMN/NaMN adenylyltransferase (NMNAT) protein family. *Front. Biosci.* **14**, 410–431 (2009).
6. Pierce, E.A. Pathways to photoreceptor cell death in inherited retinal degenerations. *Bioessays* **23**, 605–618 (2001).
7. Daiger, S.P., Bowne, S.J. & Sullivan, L.S. Perspective on genes and mutations causing retinitis pigmentosa. *Arch. Ophthalmol.* **125**, 151–158 (2007).
8. Maguire, A.M. *et al.* Safety and efficacy of gene transfer for Leber's congenital amaurosis. *N. Engl. J. Med.* **358**, 2240–2248 (2008).
9. Bainbridge, J.W. *et al.* Effect of gene therapy on visual function in Leber's congenital amaurosis. *N. Engl. J. Med.* **358**, 2231–2239 (2008).
10. Cideciyan, A.V. *et al.* Human gene therapy for RPE65 isomerase deficiency activates the retinoid cycle of vision but with slow rod kinetics. *Proc. Natl. Acad. Sci. USA* **105**, 15112–15117 (2008).
11. Maguire, A.M. *et al.* Age-dependent effects of *RPE65* gene therapy for Leber's congenital amaurosis: a phase 1 dose-escalation trial. *Lancet* **374**, 1597–1605 (2009).
12. Jacobson, S.G. *et al.* Gene therapy for Leber congenital amaurosis caused by *RPE65* mutations: safety and efficacy in 15 children and adults followed up to 3 years. *Arch. Ophthalmol.* **130**, 9–24 (2012).
13. Sherry, S.T. *et al.* dbSNP: the NCBI database of genetic variation. *Nucleic Acids Res.* **29**, 308–311 (2001).
14. 1000 Genomes Project Consortium. A map of human genome variation from population-scale sequencing. *Nature* **467**, 1061–1073 (2010).
15. Grant, G.R. *et al.* Comparative analysis of RNA-Seq alignment algorithms and the RNA-Seq unified mapper (RUM). *Bioinformatics* **27**, 2518–2528 (2011).
16. Ramensky, V., Bork, P. & Sunyaev, S. Human non-synonymous SNPs: server and survey. *Nucleic Acids Res.* **30**, 3894–3900 (2002).
17. Ng, P.C. & Henikoff, S. SIFT: predicting amino acid changes that affect protein function. *Nucleic Acids Res.* **31**, 3812–3814 (2003).

18. Sullivan, L.S. *et al.* Prevalence of disease-causing mutations in families with autosomal dominant retinitis pigmentosa: a screen of known genes in 200 families. *Invest. Ophthalmol. Vis. Sci.* **47**, 3052–3064 (2006).
19. Stone, E.M. Leber congenital amaurosis—a model for efficient genetic testing of heterogeneous disorders: LXIV Edward Jackson Memorial Lecture. *Am. J. Ophthalmol.* **144**, 791–811 (2007).
20. Wang, M. & Marin, A. Characterization and prediction of alternative splice sites. *Gene* **366**, 219–227 (2006).
21. Belenky, P., Bogan, K.L. & Brenner, C. NAD^+ metabolism in health and disease. *Trends Biochem. Sci.* **32**, 12–19 (2007).
22. Berger, F., Lau, C., Dahlmann, M. & Ziegler, M. Subcellular compartmentation and differential catalytic properties of the three human nicotinamide mononucleotide adenylyltransferase isoforms. *J. Biol. Chem.* **280**, 36334–36341 (2005).
23. Coleman, M.P. & Freeman, M.R. Wallerian degeneration, wld^S, and nmnat. *Annu. Rev. Neurosci.* **33**, 245–267 (2010).
24. Conforti, L. *et al.* Reducing expression of NAD^+ synthesizing enzyme NMNAT1 does not affect the rate of Wallerian degeneration. *FEBS J.* **278**, 2666–2679 (2011).
25. Zhai, R.G. *et al. Drosophila* NMNAT maintains neural integrity independent of its NAD synthesis activity. *PLoS Biol.* **4**, e416 (2006).
26. Siepel, A. *et al.* Evolutionarily conserved elements in vertebrate, insect, worm, and yeast genomes. *Genome Res.* **15**, 1034–1050 (2005).
27. Worth, C.L., Preissner, R. & Blundell, T.L. SDM—a server for predicting effects of mutations on protein stability and malfunction. *Nucleic Acids Res.* **39**, W215–W222 (2011).
28. Bogan, K.L. & Brenner, C. Nicotinic acid, nicotinamide, and nicotinamide riboside: a molecular evaluation of NAD^+ precursor vitamins in human nutrition. *Annu. Rev. Nutr.* **28**, 115–130 (2008).
29. Nikiforov, A., Dolle, C., Niere, M. & Ziegler, M. Pathways and subcellular compartmentation of NAD biosynthesis in human cells: from entry of extracellular precursors to mitochondrial NAD generation. *J. Biol. Chem.* **286**, 21767–21778 (2011).
30. Conforti, L. *et al.* Wld^S protein requires Nmnat activity and a short N-terminal sequence to protect axons in mice. *J. Cell Biol.* **184**, 491–500 (2009).
31. Avery, M.A., Sheehan, A.E., Kerr, K.S., Wang, J. & Freeman, M.R. Wld^S requires Nmnat1 enzymatic activity and N16-VCP interactions to suppress Wallerian degeneration. *J. Cell Biol.* **184**, 501–513 (2009).
32. Berger, F., Lau, C. & Ziegler, M. Regulation of poly(ADP-ribose) polymerase 1 activity by the phosphorylation state of the nuclear NAD biosynthetic enzyme NMN adenylyl transferase 1. *Proc. Natl. Acad. Sci. USA* **104**, 3765–3770 (2007).
33. den Hollander, A.I., Roepman, R., Koenekoop, R.K. & Cremers, F.P. Leber congenital amaurosis: genes, proteins and disease mechanisms. *Prog. Retin. Eye Res.* **27**, 391–419 (2008).
34. Chun, S. & Fay, J.C. Identification of deleterious mutations within three human genomes. *Genome Res.* **19**, 1553–1561 (2009).
35. Wei, Q., Wang, L., Wang, Q., Kruger, W.D. & Dunbrack, R.L. Jr. Testing computational prediction of missense mutation phenotypes: functional characterization of 204 mutations of human cystathionine β synthase. *Proteins* **78**, 2058–2074 (2010).

ONLINE METHODS

Subject recruitment and clinical evaluations. The clinical study was approved by the institutional review boards of The Massachusetts Eye and Ear Infirmary, the Children's Hospital of Philadelphia, Comité de Protection des Personnes (CDP) Ile de France V, the LV Prasad Eye Hospital and University College London, and conformed to the tenets of the Declaration of Helsinki. Informed consent was obtained from the participants. Complete ophthalmic and clinical genetic evaluations of members of family 047 (subjects IV-1, IV-1 and IV-3), family 007 (subject II-2) and family 053 were performed at the Ophthalmology-Genetics Clinic at the Children's Hospital of Philadelphia.

Exome sequencing. Exome capture was performed using the SureSelect 50 Mb All Exon Targeted Enrichment kit from Agilent Technologies in accordance with the kit manual[36]. The resulting exome-capture libraries underwent 2 × 101-bp paired-end sequencing on an Illumina HiSeq 2000 Next-Generation Sequencing system using v2.5 SBS chemistry, with average flow-cell lane cluster densities of ~800,000/mm^2. One exome sample was analyzed per flow-cell lane to obtain a minimum of 10× read depth for 92–95% of the targeted exome.

Exome data analyses. Burrows-Wheeler Aligner (BWA, version 0.5.9-r16) was used to align the sequence reads to the human reference genome GRCh37 downloaded from the 1000 Genomes Project website (see URLs)[37]. SAMtools (version 0.1.12 or r859) was used to remove potential duplicates (with the rmdup command) and to make initial SNP and insertion and/or deletion (indel) calls (with the pileup command)[38]. A custom program was developed and used to further refine the SNP and indel calls. The custom program used a false discovery rate approach to adjust raw base counts at a candidate position after Benjamini-Hochberg correction was performed using quality values of all bases[39]. A coverage depth cutoff of 10× was then applied. The fraction of a variant base had to be between 0.25 and 0.75 to be called heterozygous and above 0.75 to be called homozygous. Resulting variant calls were annotated using our custom human base-pair codon database. This database maps each base position in the human reference genome on the basis of Ensembl Release 65 gene annotations to its corresponding transcripts, genes, codons, encoded amino acids and translation frames, if any. Additional annotations of each variant call were provided using data sets downloaded from the 1000 Genomes Project website, the NHLBI Exome Sequencing Project Exome Variant Server and the UCSC Genome Browser (see URLs). These annotations include allele frequencies, SIFT and PolyPhen predictions, and phastCons conservation scores[16,17]. Custom scripts were also developed and used to identify candidate variants that fit different filtering criteria, such as genetic models.

***NMNAT1* PCR amplification, Sanger sequencing and genotype confirmation.** Subjects in families 007 and 047 and probands from other families with LCA were selected for Sanger sequence analysis using primers to amplify all four exons and intron-exon boundaries of *NMNAT1* (**Supplementary Table 1**). PCR products were sequenced with the ABI PRISM BigDye Terminator Cycle Sequencing V2.0 Ready Reaction kit on an ABI 3100 or 3730 DNA analyzer (Applied Biosystems). To genotype the members of family 047, the relevant PCR product was digested with AcuI, which cuts the wild-type but not the mutant sequence.

Human fibroblast culture and exposure to nicotinic acid. Skin biopsies were performed on two siblings with LCA and their parents (**Fig. 1a**, subjects IV-1, IV-3, III-4 and III-5) after informed consent was obtained in accordance with the protocol approved by the institutional review board of the Children's Hospital of Philadelphia (08-6177, M.J.F.). Fibroblast cell lines were established in the CytoGenomics Laboratory at the Children's Hospital of Pennsylvania and were subsequently maintained in T75 flasks in a 37 °C CO_2 incubator, per standard protocol, in DMEM (Gibco) supplemented with 20% FBS, 2 mM L-glutamine, 1 mM pyruvate and 50 μg/ml uridine (Calbiochem). Cells were grown to confluence before undergoing functional analyses. Cells in T75 flasks were exposed to 10 mM nicotinic acid (Sigma) for 24 h and were trypsinized, washed twice with Hank's balanced salt solution (Gibco) and flash frozen in liquid nitrogen for HPLC analysis.

Cell culture. CHO-K1 and wild-type mIMCD3 cell lines were purchased from the American Type Culture Collection (ATCC). mIMCD3 cells were maintained in DMEM:F12 medium supplemented with 10% FBS and 0.5 mM sodium pyruvate. CHO cell culture was performed in F12 medium supplemented with 10% FBS. Transfection was performed with Lipofectamine 2000 (Invitrogen), and cells were processed for immunocytochemistry 48–72 h after transfection. Human skin fibroblast cells obtained from two siblings with LCA (**Fig. 1a**, subjects IV-1 and IV-3) and their parents (**Fig. 1a**, subjects III-IV and III-V) were maintained in Medium 106 (Invitrogen) with low-serum growth supplement and were grown to confluence before undergoing immunofluorescence and immunoblot analyses.

Immunofluorescence analyses. Cells were fixed in 4% paraformaldehyde, permeabilized and then blocked with 1% BSA and 0.2% Triton X-100 in PBS, as previously described[40]. Cells were then stained with antibody to V5 (Invitrogen, 46-0705; 1:1,000 dilution) and then with Alexa Fluor 555–conjugated goat secondary antibody to mouse IgG (Invitrogen, A21127; 1:1,000 dilution)[40]. Fluorescent signals were visualized using a Nikon Eclipse fluorescent microscope.

Protein blotting. Total cell lysates from CHO cells transfected with pCAG-V5-*NMNAT1*-IRES-*EGFP* plasmid were separated on a precast NuPAGE 4–12% Bis-Tris Gel (Invitrogen) and were transferred to a PVDF membrane, as previously described[41]. The membrane was probed with antibody to V5 (Invitrogen, 46-0705; 1:5,000 dilution), human NMNAT1 (Novus Biologicals, H00064802-B01P; 1:500 dilution) or β-actin (Santa Cruz Biotechnology, sc-1615; 1:1,000 dilution) and was then incubated with IRDye secondary antibodies (LI-COR, goat anti-mouse 800CW, 926-32210; goat anti-rabbit 680RD, 926-68071; 1:15,000 dilutions). Antibody binding was detected with an Odyssey infrared imager (LI-COR).

Recombinant protein production and purification. Human *NMNAT1* cDNA was amplified by RT-PCR from a cDNA clone (OpenBiosystem) and cloned into a pENTR/D-TOPO entry vector (Invitrogen); the construct was fully verified by sequencing. The coding sequence was moved by recombination to a Gateway-compatible destination expression vector modified to encode a sequence for N-terminal V5 (pCAG-V5-IRES-*EGFP*) or Flag (pCAG-Flag-IRES-*EGFP*) epitope tags in frame. Plasmid DNA was purified using the EndoFree plasmid maxi kit (Qiagen). Recombinant NMNAT1 (with Flag tag) was expressed in CHO cells and was purified using a FLAG M Purification kit (Sigma) for subsequent enzyme activity assay.

NMNAT enzyme activity assay. NMNAT activity was measured by HPLC quantitation of the reaction product, NAD^+. The assay mixture contained 1.5 mM ATP, 1 mM NMN and 10 mM $MgCl_2$ in 25 mM Tris-HCl (pH 7.4) and the appropriate amount of enzyme sample (typically 20 or 40 μl) to achieve a final volume of 0.2 ml. The reaction was started by addition of NMN substrate. After incubation of the reaction mixture for 10, 30 or 120 min at 37 °C, a 40-μl aliquot was removed and added to 20 μl of ice-cold 1.2 M perchloric acid (PCA) containing 20 mM EDTA and 0.15% sodium metabisulfite to stop the reaction. After a 15-min incubation at 4 °C, the mixture was centrifuged for 10 min at 16,000*g* in a Beckman microcentrifuge. A 55-μl aliquot of the supernatant was further neutralized by the addition of 20 μl of ice-cold 1 M K_2CO_3 and was centrifuged again. The supernatant was isolated and stored at −80 °C until HPLC analysis.

Sample preparation for HPLC analyses of NAD^+. Harvested cells were rinsed with Hank's balanced salt solution twice and were centrifuged at 2,150*g* for 5 min. The cell pellet was resuspended in argon-bubbled 20 mM Tris-HCl (pH 7.4) for analysis of the oxidized dinucleotides, including NAD^+. The cell suspension was extracted with four volumes of argon-bubbled, ice-cold 1.2 M PCA containing 20 mM EDTA and 0.15% sodium metabisulfite. After vortexing, the suspension was placed on ice for 15 min and then centrifuged at 16,000*g* for 10 min. The supernatant was neutralized with 1 M potassium carbonate and was centrifuged to remove insoluble material. The pellet from the PCA extraction was used for protein estimation. Samples were stored at −80 °C and were subjected to HPLC analysis.

HPLC conditions for analyses of NAD^+. Separation of the oxidized dinucleotides was carried out on a C18 column (5 µm, 4.6 × 250 mm, Adsorbosphere XL C18 90Å) preceded by a guard column at 40 °C. Flow rate was set at 0.5 ml/min. The mobile phase was initially 100% of mobile phase A (0.1 M sodium phosphate buffer (pH 6.0) containing 3.75% methanol). The methanol concentration was linearly increased with mobile phase B (0.1 M sodium phosphate buffer (pH 6.0) containing 30% methanol), increasing to 50% over 15 min. The column was washed after each separation by increasing mobile phase B to 100% for 5 min. UV absorbance was monitored at 260 and 340 nm with Shimadzu SPD-M20A. Pertinent peak areas were integrated using LabSolution software from Shimadzu and were quantified using standard curves.

Statistical analyses. For comparison of the activity rates of purified recombinant NMNAT1 proteins with that of wild-type protein, rates were normalized by the mean rate of the wild-type protein analyzed on the same day to account for variation in the absolute enzyme activity rates on different analysis dates. The significance of differences between groups was evaluated using a nonparametric Wilcoxon rank-sum test in SAS 4.3 because of skewness observed in the data and small sample size. For measurements of cellular NMNAT activity and NAD^+ concentrations, statistical comparisons between groups were performed using Student's two-tailed *t*-tests.

36. Gnirke, A. *et al.* Solution hybrid selection with ultra-long oligonucleotides for massively parallel targeted sequencing. *Nat. Biotechnol.* **27**, 182–189 (2009).
37. Li, H. & Durbin, R. Fast and accurate short read alignment with Burrows-Wheeler transform. *Bioinformatics* **25**, 1754–1760 (2009).
38. Li, H. *et al.* The Sequence Alignment/Map format and SAMtools. *Bioinformatics* **25**, 2078–2079 (2009).
39. Benjamini, Y. & Hochberg, Y. Controlling the false discovery rate: a practical and powerful approach to multiple testing. *J. Royal Stat. Soc. B (Methodological)* **57**, 289–300 (1995).
40. Liu, Q., Zuo, J. & Pierce, E.A. The retinitis pigmentosa 1 protein is a photoreceptor microtubule-associated protein. *J. Neurosci.* **24**, 6427–6436 (2004).
41. Davis, E.E. *et al. TTC21B* contributes both causal and modifying alleles across the ciliopathy spectrum. *Nat. Genet.* **43**, 189–196 (2011).

doi:10.1038/ng.2361

Supplementary Information

NMNAT1 Mutations Cause Leber Congenital Amaurosis

Marni J. Falk, Qi Zhang, Eiko Nakamaru-Ogiso, Chitra Kannabiran, Zoe Fonseca-Kelly, Christina Chakarova, Isabelle Audo, Donna S. Mackay, Christina Zeitz, Arundhati Dev Borman, Magdalena Staniszewska, Rachna Shukla, Lakshmi Palavalli, Saddek Mohand-Said, Naushin H. Waseem, Subhadra Jalali, Juan C. Perin, Emily Place, Julian Ostrovsky, Rui Xiao, Shomi S. Bhattacharya, Mark Consugar, Andrew R. Webster, José-Alain Sahel, Anthony T. Moore, Eliot L. Berson, Qin Liu, Xiaowu Gai and Eric A. Pierce

Correspondence should be addressed to EAP (eric_pierce@meei.harvard.edu)

Nature Genetics: doi:10.1038/ng.2361

Supplementary Information

Contents

Nature Genetics: doi:10.1038/ng.2361

A. Supplementary Note

1. Clinical information for family members of LCA Pedigrees 047, 007, 053

Family 047:

a) Subject IV-1 is a Pakistani female who had nystagmus onset in the newborn period. Electroretinogram (ERG) performed during early infancy was non-detectable (i.e. < 10 μV), leading to a clinical diagnosis of Leber congenital amaurosis (LCA). She showed oculodigital sign since early childhood. Initial ophthalmological evaluation at The Children's Hospital of Philadelphia at age 11 years was significant for nystagmus and enophthalmos. Her anterior segment O.D. was within normal limits and O.S. was significant for a corneal opacity. She was not able to fix on or follow objects. Dilated fundus exam was significant for bilateral optic nerve atrophy, attenuation of the retinal blood vessels, atrophic changes in the macula, and scattered pigment changes in the retinal peripheries in both eyes.

Her additional medical history was significant for severe to profound sensorineural hearing loss that was diagnosed at 2 months of age. A right ear cochlear implant was placed at age 7 years. Her early development was delayed, with her achieving sitting unassisted at age 1 year and walking at age 3. She remains non-verbal. She has been diagnosed with autism and has stereotypical behaviors.

Clinical Genetics evaluation at the Children's Hospital of Philadelphia evaluation at age 11 years was significant for normal stature and weight with relative microcephaly (OFC 5th percentile, 50th percentile for 5-year-old). Dysmorphic features included low hairline, synophrys, medial eyebrow flare, small forehead, inverted nipples, mild truncal obesity, abdominal protuberance, possible scoliosis, and kyphosis.

Metabolic screening laboratory studies in blood were normal, including comprehensive chemistry panel, quantitative plasma amino acid analysis, blood lactate, blood pyruvate, plasma carnitine, plasma acyl-carnitine profile, very long chain fatty acid analysis, and thyroid hormone screening. Clinical diagnostic sequencing revealed no deleterious mutations in known LCA genes, including *CRB1, LRAT, TUPL1, RPE65, AILP1, CRX, RDH12, GUCY2D, RPGRIP1, CEP290, LCA5, RD3, IMPDH1,* and *SPATA7*. Genome-wide SNP microarray analysis (Illumina HumanQuad610 BeadChip) performed in the CHOP CytoGenomics Laboratory identified several large regions (greater than 10 Mb) of homozygosity, as were consistent with her known consanguinity.

b) Subject IV-2 is a Pakistani boy who underwent initial Ophthalmology and Clinical Genetics evaluations at The Children's Hospital of Philadelphia at age 8 years. His best corrected visual acuity was 20/30 and he had normal dilated fundus examination. He had a history of strabismus, status-post surgical repair in infancy.

He had bilateral sensorineural hearing loss and wears hearing aids. His early developmental milestones were met at age appropriate ages. However, he had recently been given a clinical diagnosis of Mucolipidosis Type III based on having clinical features of acquired short stature by age 2 years, progressive elbow and finger contractures, an unprovoked fracture, coarse facies,

Nature Genetics: doi:10.1038/ng.2361

and hirsutism. Prior metabolite testing had revealed elevated beta-glucuronidase, beta-galactosidase, alpha-fucosidase and beta-hexosaminidase that were suggestive of a pattern consistent with Mucolipidosis types II or III. Enzyme activity screening in skin fibroblasts for MPS-I, MPS-II and MPS-VI were reportedly negative. Sequencing of *GNPTAB* was negative. No additional clinical genetic testing was performed.

c) Subject IV-3 is a Pakistani boy who presented at 1 month of age with no reaction to light and poor visual attention. Ophthalmologic evaluation at age 4 months was significant for myopia, mild pallor of the optic nerves, and vascular attenuation in both retinas. ERG was undetectable for both cone and rod photoreceptor activity in infancy. Brain MRI obtained during early childhood was within normal limits. Initial Ophthalmologic evaluation at The Children's Hospital of Philadelphia at age 3 years, 4 months was significant for light perception only, enophthalmos, normal anterior segments, early atrophy of the optic nerves, attenuation of the retinal blood vessels, as well as atrophy and pigment mottling in the macula and retinal peripheries of both eyes. Follow-up evaluation at The Children's Hospital of Philadelphia at age 4 years was significant for no light perception.

His additional medical history was significant for global developmental delay, with his achieving walking unassisted at age 2 years and he was non-verbal at age 4 years. He had autism spectrum disorder and stereotypical behaviors. He had normal hearing. Clinical Genetics evaluation at age 4 years was significant for relative microcephaly, thick hair, inverted triangular face, enophthalmos, low anterior and lateral hairline with hirsute forehead, synophrys, relative hypertelorism, high arched palate, persistence of the fetal fingertip pads bilaterally, mild 5th finger clinodactyly bilaterally, and soft skin.

d) Additional Kindred Members. Family members IV-4, IV-5, IV-6, IV-7, and IV-8 reside in Pakistan and were not able to be clinically evaluated by members of this study team. However, medical questionnaires completed by the family provided information about each individual. By report, IV-7 and IV-8 have a similar clinical presentation to IV-1, including congenital blindness, hearing loss, developmental delay, and non-verbal autism. Subject IV-6 has isolated congenital blindness but no developmental delay. Subject IV-4 has isolated congenital hearing loss but no developmental delay.

Family 007:

Subject II-2 has a history of reduced vision since early childhood. Ophthalmologic evaluation at The Children's Hospital of Philadelphia at age 3 years was significant for fixing and following and normal anterior segments. Her fundus exam revealed early atrophy of the optic nerves, early attenuation of the retinal blood vessels, and atrophic and pigmentary changes in the retinal peripheries. At this evaluation, her family reported she could recognize colors and preferred bright lights. However, at an annual exam one year later she reported a decline in her visual function and was relying more on tactile sensation, learning Braille, and using a CCTV in the classroom. Visual acuity at age 4 years was significant for light perception only, with an unchanged fundus exam from the prior year. Her medical history was otherwise normal, including normal growth and development. There was no family history of eye disease. Clinical diagnostic sequencing revealed no deleterious mutations in known LCA genes, including *AIPL1*,

Nature Genetics: doi:10.1038/ng.2361

CABP4, CRB1, CRX, GUCY2D, IMPHD1, IQCB1, LCA5, LRAT, OTX2, RD3, RDH12, RPE65, RPGRIP1, SPATA7, and *TULP1*.

Family 053:
Subject II-1 presented with poor vision and nystagmus in the first few months of life. ERG at age 1 was reportedly "flat" and consistent with the diagnosis of LCA. Ophthalmologic exam at The Children's Hospital of Philadelphia at age 20 was significant for no light perception. The fundus exam revealed atrophy of the optic nerves and attenuation of retinal blood vessels, atrophy of the retina and choroid in the central maculas, and atrophic changes in the retinal peripheries. Spectralis OCT analysis showed loss of the retinal architecture centrally and thinning of the retina outside of the maculas. His birth history is significant for being born at 33-weeks' gestational age. He had a history of developmental delay.

2. Clinical information on family members of LVPEI LCA Pedigrees

LVPEI LCA 73:
Subject II-2 was evaluated at 5 months of age, with visual acuity of fixing on and following light. Retinal examination was significant for the presence of only minimal disc pallor, moderate arterial narrowing, and diffuse RPE degeneration throughout the retina with with sparse pigment migration in the retinal peripheries. The macular areas showed atrophic scars of 1.5 disc diameter size. Their condition has remained stable over 3 years of follow-up.

LVPEI LCA 79:
Subject IV:1 was evaluated at 1-year-old, with visual acuity of light perception. Retinal examination revealed the presence of moderate disc pallor, moderate arterial narrowing, as well as diffuse and somewhat coarse RPE degeneration throughout the retina with sparse pigment migration in retinal peripheries. In the macular area, there were pigment clumps and RPE degeneration of 2 disc diameters in area around the fovea. The condition has remained stable over 2 years of follow-up. This subject also had a history of motor developmental delay observed at one year of age, for which appropriate physical therapy was started and improvement over the next year was observed.

LVPEI LCA 100:
Subject II-2 was evaluated at the age of 3 months, with visual acuity of following and fixing light. Refraction showed hyperopia of + 9.5 D sph with -1.00D cylinder at 180 degrees. Retinal examination showed the presence of only minimal disc pallor, moderate arterial narrowing, as well as diffuse and somewhat coarse RPE degeneration throughout the retina with sparse pigment migration in retinal peripheries. There was a >4 disc diameter area of macular excavation with pigment hypertrophy at the edges and atrophic base. Their condition has remained static at 7 years of follow-up.

LVPEI LCA 128:
Subject II-3 was evaluated at 28 years of age. His visual acuity was 20/380 for the right eye and 20/150 for the left eye. Retinal examination showed the presence of only minimal disc pallor, moderate arterial narrowing, as well as diffuse and somewhat coarse RPE degeneration all over

Nature Genetics: doi:10.1038/ng.2361

with sparse pigment migration in retinal peripheries. There was a >3 disc diameter area of macular excavation with pigment hypertrophy at the edges and atrophic base in both eyes.

3. Clinical information for family members of UCL LCA Pedigrees

UCL LCA 1:
Subject II-1 presented to the pediatric ophthalmology clinic at the age of four years. She had poor vision from birth with roving nystagmus and an oculodigital reflex. She was systemically normal. There was no family history of any ocular disease and no evidence of consanguinity. The family are of Caucasian descent. At presentation, her vision in either eye was no perception of light. She had a hypermetropic refractive error at +11.0 diopter sphere in either eye. Ocular examination showed a normal anterior segment. The fundus examination showed bilateral optic disc pallor and severe macular atrophy. There was widespread retinal pigment epithelium atrophy with minimal bone spicule pigmentation in the retinal periphery. ERG revealed an undetectable retinal responses.

UCL LCA 2:
Subject II-2 had poor vision and nystagmus from birth. She was systemically normal and there was no family history of any ocular disease. The proband had Caribbean and Sri Lankan ancestry. There was no parental consanguinity. When reviewed at age 13 months, the vision in either eye was perception of light. She had a hypermetropic refractive error of +3.0 diopter sphere in each eye. The anterior segments were normal. Fundoscopy showed severe macular atrophy and pigmentation. The retinal vessels were attenuated and there was bilateral pigment epithelial atrophy and retinal pigment deposition. Her ERG showed undetectable retinal responses.

UCL LCA 3:
Subject II-1 presented with poor vision and nystagmus from birth. She was systemically normal and there was no family history of any ocular disease. The family were from Caribbean descent and there was no parental consanguinity. At the age of 10 years, the corrected vision was 1.5 logMAR in each eye. She had a refractive error of +3.0 diopter sphere in the right eye and +5.0 diopter sphere in the left eye. The anterior segments were normal. Fundus examination revealed severe macular atrophy and pigmentation bilaterally with severe peripheral retinal pigment epithelium atrophy and pigment migration. The retinal blood vessels were attenuated. The ERG was undetectable.

UCL LCA 4:
Subject II-1 presented with poor vision and nystagmus from birth. He was systemically normal and there was no family history of any ocular disease. He was of mixed race origin with Irish and Caribbean ancestry. At aged 13 months, his vision was perception of light only in either eye and he had a hypermetropic refractive error of +6.5 diopter sphere in either eye. His anterior segments were normal, he had sluggish pupiliary responses and fundoscopy showed bilateral severe macular atrophy with peripheral pigment migration. Electroretinography using surface electrodes and non-Ganzfeld stimulation identified a generalised retinal dysfunction affecting the rod and cone photoreceptors, in keeping with a severe photoreceptor dystrophy.

Nature Genetics: doi:10.1038/ng.2361

UCL LCA 5:
Subject II-2 presented with poor vision from birth with roving nystagmus and an oculodigital reflex. She was systemically and developmentally normal. There was no family history of any ocular disease, but an older sibling was developmentally delayed and had features consistent with an autistic spectrum disorder. This was a non-consanguineous family of Polish descent. At age 18 months, her vision was perception of light in either eye and she had a hypermetropic refractive error of +6.0 diopter sphere in either eye. An adnexal exam showed bilateral enophthalmos and a mild left ptosis. The enophthalmos is likely to have occurred subsequent to her oculodigital reflex. She had normal anterior segments and fundoscopy showed severe bilateral macular atrophy with retinal pigment epithelium atrophy and granularity throughout the fundus. The ERG showed undetectable responses.

UCL LCA 6:
Subject II-1 had poor vision from infancy and was systemically normal. He was diagnosed as having a retinal dystrophy. He was of British Caucasian descent and there was no parental consanguinity. When reviewed at the age of 41 years, his vision was hand movements bilaterally. He had mild nystagmus and bilateral posterior chamber intraocular lens implants *in situ*, relfecting prior cataract extraction surgery. Fundoscopy showed extensive bilateral macular atrophy with extensive retinal pigmentation in the periphery.

UCL LCA 7:
Subject II-1 presented with poor vision and nystagmus from birth. He was systemically normal and there was no family history of any ocular disease. He was of British Caucasian descent and there was no known consanguinity. At the age of 36 months, his vision was recorded as no perception of light. He had normal anterior segments. Fundoscopy showed severe macular atrophy with bilateral optic disc pallor and retinal vessel attenuation. There was widespread retinal pigment epithelium atrophy in the periphery. An ERG performed in infancy showed non-recordable retinal responses.

Nature Genetics: doi:10.1038/ng.2361

B. Supplementary Figures

4. Supplementary Figure 1

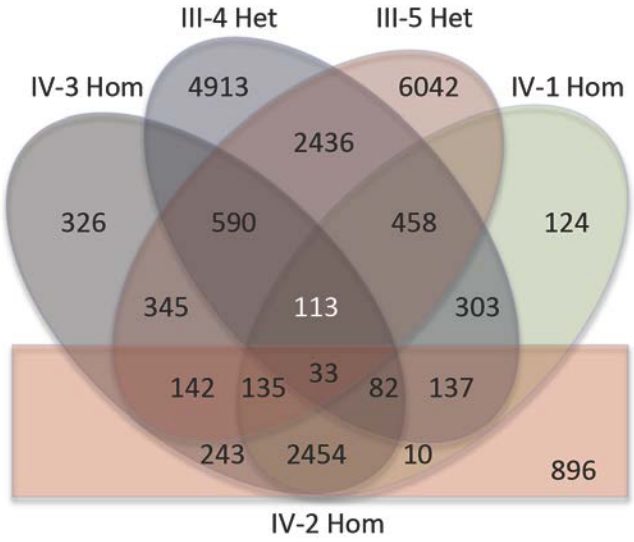

Supplementary Figure 1. **Exome Data Filtering**
Exome sequence data was filtered to identify genes containing non-synonymous homozygous variants present in subjects IV-1 and IV-3 that demonstrated biparental inheritance. Variants that were also found to be homozygous in the visually unaffected sibling (IV-2) were excluded to obtain 113 variants in 86 genes as potentially pathogenic for their LCA phenotype.

Nature Genetics: doi:10.1038/ng.2361

5. Supplementary Figure 2

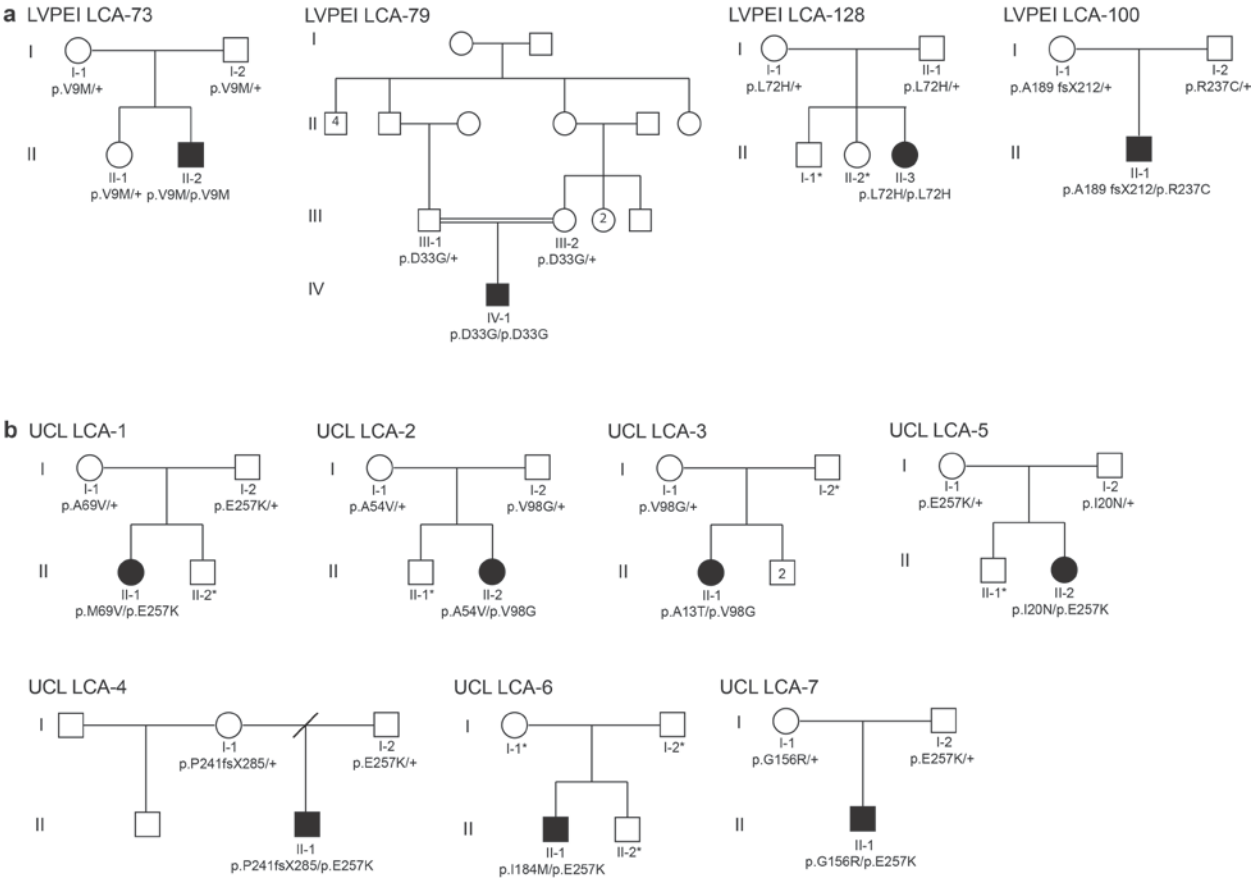

Supplementary Figure 2. **Pedigrees of additional LCA kindreds in which *NMNAT1* mutations were identified.**

(a) Pedigrees of LCA families from LVPEI with mutations identified in *NMNAT1* by Sanger sequencing. (b) Pedigrees of LCA families from UCL with mutations identified in *NMNAT1* by Sanger sequencing. The identified mutations are indicated. The '+' represents a wild-type allele. Squares and circles indicate male or female, respectively, and numbers within symbols indicate multiple offspring of a given gender. Slashes depict deceased individuals. Individual affected by LCA are indicated by black symbols. * indicates individuals for which DNA samples are not available. As shown, mutations were detected in an additional individual who was homozygous for the previously identified p.V9M mutation (but apparently unrelated to family 047), as well as in two additional families from LVPEI in which the probands were homozygous for either the c.98A>G (p.D33G) or c.215T>A (p.L72H) mutations, respectively. One LCA family from LVPEI and all 7 LCA families from UCL had compound heterozygous mutations, including one family with the same p.M69V and p.E257K mutations as were identified in CHOP/MEEI family 053.

Nature Genetics: doi:10.1038/ng.2361

6. Supplementary Figure 3

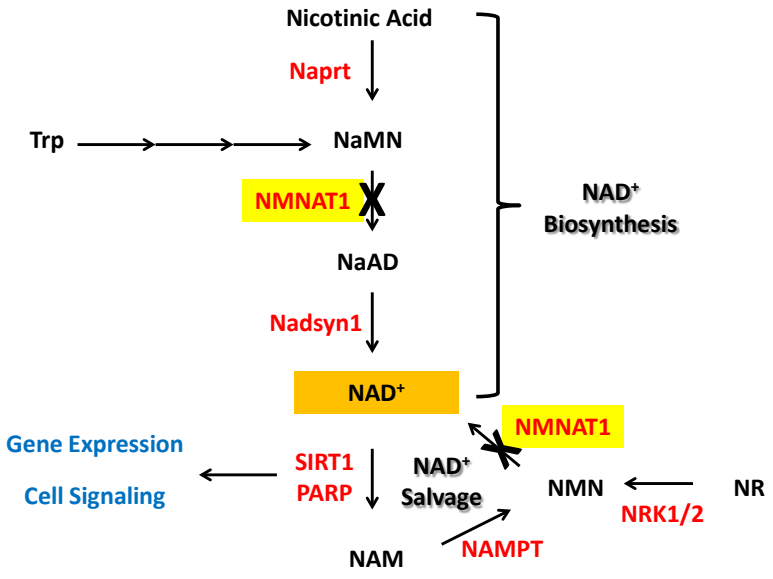

Supplementary Figure 3. **Schematic overview of the role of the NMNAT1 enzyme in NAD^+ biosynthetic and salvage pathways.** The site of the NMNAT1 enzyme deficiency (yellow highlight) caused by a homozygous p.V9M mutation in Penn 047 is indicated by an "X", which impacts NAD^+ biosynthetic and salvage pathways. NMNAT1, nicotinamide mononucleotide adenylyltransferase isoform 1; NAD^+, nicotinamide adenine dinucleotide; NAM, nicotinamide; NMN, nicotinamide mononucleotide; NR, nicotinamide riboside; NaMN, nicotinic acid mononucleotide; NaAD, nicotinic acid adenine dinucleotide; TRP, tryptophan; Naprt, nicotinic acid phosphoribosyltransferase; Nadsyn1, NAD^+ synthetase; NRK, nicotinamide riboside kinases; NAMPT, nicotinamide phosphoribosyltransferase; SIRT1, sirtuin 1; PARP, poly-ADP-ribosyl polymerase

Nature Genetics: doi:10.1038/ng.2361

7. Supplementary Figure 4

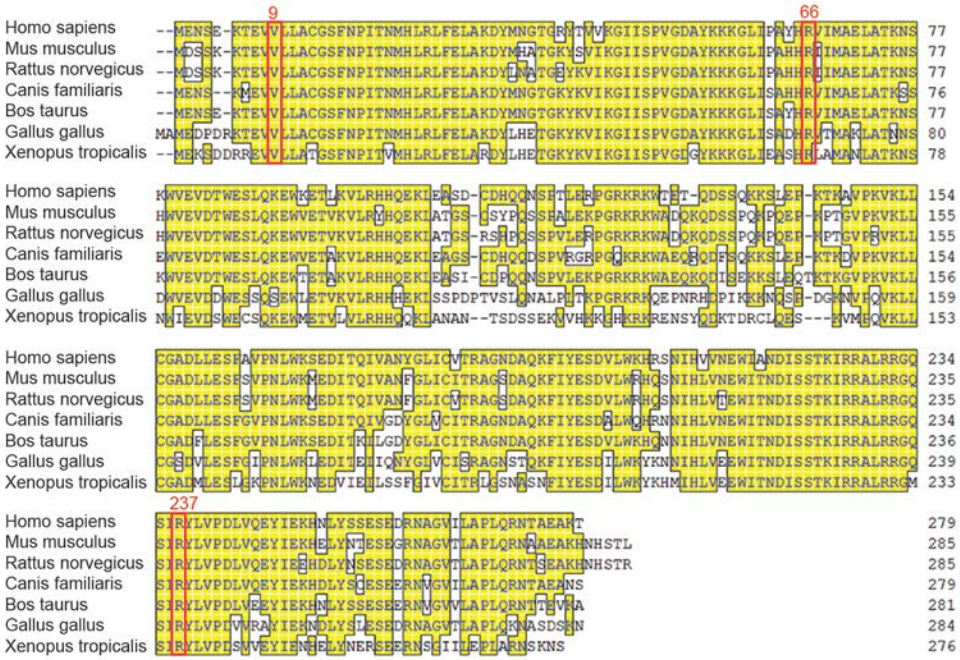

***Supplementary Figure 4. NMNAT1* sequence conservation.** Polypeptide sequences of NMNAT1 from NCBI (human, NP_073624; mouse, NP_597679; rat, NP_001032645; dog, XP_536739; cow, NP_001069302; chicken, XP_417605; Xenopus tropicalis, NP_001016772) were aligned via Clustal W. Conserved residues are highlighted and boxed. The locations of V9, R66 and R237 are indicated. The crystal structure of the NMNAT1 protein is a barrel-like hexamer, where V9, R66 and R237 are predicted to localize to the outside surface (PDB ID: 1KQN) [1].

Nature Genetics: doi:10.1038/ng.2361

8. Supplementary Figure 5

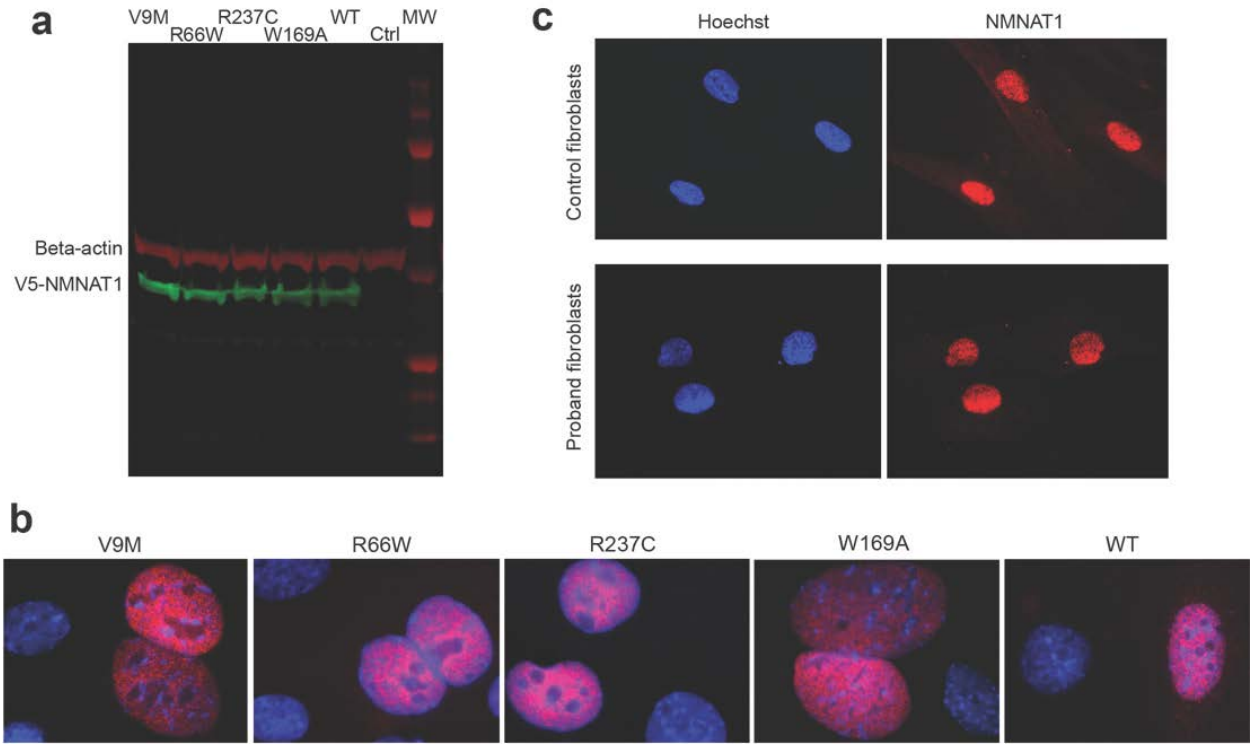

Supplementary Figure 5. Expression and localization of mutant NMNAT1 protein. **(a) Recombinant mutant NMNAT1 proteins showed correct expression size and levels in CHO cells.** CHO cells were transfected with plasmids encoding V5-tagged wild-type (WT) NMNAT1, mutant NMNAT1 (p.V9M, p.R66W, or p.R237C mutations identified in LCA families), or a negative control NMNAT1 mutation (p.W169A) having known loss of catalytic activity [2]. Non-transfected cells were also included as a control (Ctrl). Protein extracts harvested from the transfected and control cells were subjected to immunoblotting with anti-V5 antibodies. All five forms of the NMNAT1 protein showed normal size and expression levels. Antibodies to β-actin were used as a gel loading control. **(b) Recombinant mutant NMNAT1 proteins showed correct nuclear localization in the nuclei of transfected mIMCD3 cells.** Mouse IMCD3 cells were transfected with plasmids encoding V5-tagged wild-type (WT), mutant (p.V9M, p.R66W, p.R237C mutations identified in LCA families), or p.W169A (loss of catalytic activity) NMNAT1 proteins. Transfected cells were stained with anti-V5 antibodies (red), and Hoechst dye to demonstrate nuclei (blue). **(c) Endogenous NMNAT1 protein showed correct nuclear localization in the LCA proband's fibroblasts.** Fibroblasts from a normal control and the LCA proband from Family 047 (subject IV-1) were fixed and stained with antibodies to human NMNAT1 (red). The p.V9M mutant NMNAT1 protein localized correctly to the nuclei (Hoechst dye, blue) of the LCA proband's fibroblasts.

Nature Genetics: doi:10.1038/ng.2361

9. Supplementary Figure 6

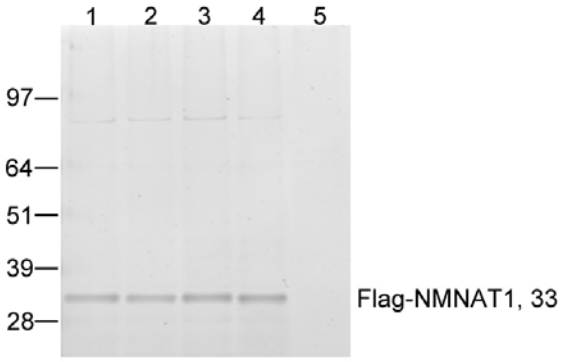

Supplementary Figure 6. Purified, recombinant mutant NMNAT1 proteins
Flag-tagged recombinant NMNAT1 proteins were produced and affinity purified as described in Methods. 0.4 µg of of WT (lane 1), p.Trp169Ala (lane 2), p.Val9Met (lane 3), p.Arg237Cys (lane 4), and p.Arg66Trp (lane 5) proteins were subjected to SDS-PAGE, and the gel stained with Coomassie blue. The wild-type and first three NMNAT1 protein variants are readily detectable, and highly enriched following affinity purification. The p.Arg66Trp protein was not detected. Futher experiments will be needed to determine if the Flag-tagged p.Arg66Trp protein is unstable to purification, or if the mutation prevents affinity purification via another mechanism.

Nature Genetics: doi:10.1038/ng.2361

C. Supplementary Table

10. Supplementary Table 1 - *NMNAT1* primers

Gene	Exon	Annealing Temperature (°C)	Primer Sequence
NMNAT1	2	61	F- GGGTGGCAGAGCAAGACCTTATC
			R- ATGCTGGGATTGCAGGTGTG
NMNAT1	3	60	F- TGAGCCGAGATCACTCCAGTG
			R- CATCCTTTGGTGCTGTGCTCTAC
NMNAT1	4	58	F- TATAGACACCATCAAGAGAAATTGGAGGC
			R- TCAACTCTAGTCCGTGGGTCCTGC
NMNAT1	5	60	F- TTTCCACTTGGAGGAGGTAGAGG
			R- ACTCCCAGATTGTTTCAGATCCC

11. References for Supplementary Information

1. Zhou, T. *et al.* Structure of human nicotinamide/nicotinic acid mononucleotide adenylyltransferase. Basis for the dual substrate specificity and activation of the oncolytic agent tiazofurin. *J Biol Chem* **277**, 13148-54 (2002).
2. Berger, F., Lau, C. & Ziegler, M. Regulation of poly(ADP-ribose) polymerase 1 activity by the phosphorylation state of the nuclear NAD biosynthetic enzyme NMN adenylyl transferase 1. *Proc.Nat.Acad.Sci.* **104**, 3765-70 (2007).

Nature Genetics: doi:10.1038/ng.2361

EXPERT REVIEWS

Genetics of Leber congenital amaurosis: an update

Expert Rev. Ophthalmol. 7(2), 141–151 (2012)

Rachna Shukla[1], Chitra Kannabiran*[1] and Subhadra Jalali[2]

[1]*Kallam Anji Reddy Molecular Genetics Laboratory, Hyderabad Eye Research Foundation, LV Prasad Eye Institute, LV Prasad Marg, Banjara Hills, Hyderabad 500034, India*
[2]*Smt Kannuri-Santhamma Retina-Vitreous Services, LV Prasad Eye Institute, LV Prasad Marg, Banjara Hills, Hyderabad 500034, India*
**Author for correspondence: chitra@lvpei.org*

Leber congenital amaurosis (LCA) is a hereditary condition involving severe visual loss or blindness that develops within the first year of life. LCA occurs as syndromic and nonsyndromic forms, and is mostly of autosomal-recessive inheritance. To date, mutations in 19 genes are known to be associated with nonsyndromic LCA phenotypes. Mutations in all known genes account for disease in 70% or less of LCA patients, suggesting that unidentified genes are responsible in the remaining cases. High-throughput screening methods such as mutation chips and exome sequencing have accelerated the pace of genetic discovery in LCA. Genetic testing is useful in counseling families and in confirming diagnosis in ambiguous cases. Gene-based therapy with the *RPE65* gene has completed the first phase of clinical trials and shows promising results. Various other gene-specific and other modes of therapy are in experimental stages and are expected to progress to human trials in the near future.

Keywords: gene therapy • genetics • genotype–phenotype correlation • LCA • Leber congenital amaurosis • mutations

Leber congenital amaurosis (LCA), first described by Theodore Leber in 1869 as tapeto-retinal degeneration with amaurosis, is a severe, congenital form of hereditary retinal disease involving loss of vision and blindness. The underlying photoreceptor defects giving rise to LCA are recognized to be of three types: abnormal development, degeneration and death, and dysfunction [1]. LCA is congenital in onset and characterized by blindness or severe visual impairment before the age of 1 year, nystagmus, amaurotic pupils and attenuated electroretinographic (ERG) responses. The appearance of the retina is very variable and does not show any features characteristic of LCA as a whole. LCA shows clinical overlap with other childhood retinal disorders, a group of conditions that include stationary, progressive, syndromic and nonsyndromic diseases, and careful evaluation of both ocular and systemic features is required to diagnose and differentiate it from these disorders (for reviews see [1,2]). In particular, nonsyndromic early-onset retinitis pigmentosa (RP) and other disorders belonging to the category of early-onset severe retinal dystrophies show similarities with LCA and may be difficult to differentiate. Distinguishing features of LCA include the characteristics noted above; in particular, autosomal-recessive inheritance, congenital onset of visual loss with ERG documented within the first year of life, early nystagmus and loss of pupillary responses. In contrast to LCA, early-onset RP is not congenital and manifests in early childhood, and it shows all types of mendelian inheritance patterns. LCA accounts for 5% of inherited retinal degenerative disorders [3]. The prevalence of LCA is one in 30,000 to one in 81,000 as reported mainly in Western populations [2,4]. It is mostly inherited as an autosomal-recessive form and is genetically heterogeneous. Autosomal-dominant inheritance has also been reported in LCA [5,6].

Advances in the molecular genetics of LCA have progressed rapidly since the mapping and identification of the first locus (*LCA1*) [7,8], and in a span of one and a half decades, 19 genes have been found to be associated with LCA (Table 1). Genetic screening is recognized as an important tool in the diagnosis of LCA, particularly in view of conflicting or overlapping clinical presentation. Knowledge of the disease gene in LCA patients is also important in counseling parents and in determining their suitability for gene-specific therapies. The success of the *RPE65* gene-therapy trials in LCA patients has catalyzed efforts to develop other gene-based therapies for LCA [9–11]. This review is aimed at giving a brief update on recent developments in the genetics of LCA, genotype–phenotype correlations and progress in gene therapy.

 10.1586/EOP.12.14 ISSN 1746-9899

LCA genes & mutations

Genes identified so far for LCA, the prevalence of mutations in each, and functions of the genes are summarized in Table 1. Knowledge of mutation frequencies of LCA genes can help in guiding efforts at developing gene therapy that targets genes that are more commonly mutated in a given population. Frequencies of mutations in LCA genes range from <1–2% at the lower end of the frequency spectrum for *RD3* [12], *LRAT* [13] and *LCA5*/Lebercilin [14–16], to 'intermediate' frequencies of 4–5% for *RDH12* and *AIPL1* [17–19], and relatively high frequencies of mutations (~10–20%) for *CRB1* and *GUCY2D* [18,20–23]. The most frequently mutated gene known to date is *CEP290*, with a mutation frequency in some Caucasian populations of approximately 20–30% of cases [23–25]. Interestingly, one founder mutation in *CEP290* involving an intronic change (c2991+1655A>G) is the most common mutation reported in LCA, and occurs in 15–40% of cases [23,25,26]. Thus the *IMPDH1* gene has been identified as causing LCA in one study (two out of 24 patients) [5] and for a better estimate of its mutation frequency in LCA we will have to await the results of further studies.

The mutation frequencies and other attributes of most LCA genes have been reviewed previously [2], and so are not repeated here. Novel LCA genes have been added to the list using single nucleotide polymorphisms (SNP) microarrays and exome-sequencing approaches. The *SPATA7* gene, known to be expressed in spermatocytes, was identified as the *LCA3* gene, with mutations in families mapping to the LCA3 locus [27]. It is also expressed in the human and mouse retina in all layers and at different developmental stages [27], with high expression levels in the brain, retina and testis [28]. Screening of LCA patients for *SPATA7* revealed mutations in approximately 2% of cases [28,29]. By means of homozygosity mapping and exome sequencing, *KCNJ13*, a potassium channel gene was found to have mutations in LCA, identified in two families out of >300 screened [30]. The *IQCB1*/*NPHP5* gene, which is implicated in Senior–Loken syndrome, was also found to have mutations in LCA patients without nephronophthisis [31]. Some of the mutations in *IQCB1* are common to LCA and Senior–Loken syndrome [32]. Mutations in *IQCB1* were also identified in three additional LCA families from Saudi Arabia [33]. Other genes recently identified as to having pathogenic mutations in LCA, based on a study in Saudi Arabian patients, are: *ALMS1*, *CNGA3* and *MYO7A* (Usher 1B), all of which were not previously associated with LCA, although they are known to be responsible for other retinal disease phenotypes [33]. However, potential limitations exist with reference to the associations of *ALMS1* and *CNGA3* with LCA. In the case of a patient with a mutation in *ALMS1*, one cannot exclude the possibility that the phenotype may in fact be Alstrom syndrome rather than just LCA, since the other features of the syndrome can appear later in the course of the disease. As *CNGA3* is a cone-specific gene, there is no evident explanation for its involvement in a phenotype that includes rod cell degeneration (as in LCA). This may be due to criteria for diagnosis of LCA being more expansive in this study; on the other hand, it is possible that *CNGA3* has an, as yet, unknown function that may explain the association of this gene with LCA. Further confirmation of these observations may have to await future studies.

Mutations in all LCA-associated genes account for approximately 70% of all cases, especially in North American and European patients [2,24]. There are population-dependent variations in the overall frequency of mutations, as well as in frequencies of specific genes. Screening in a Saudi Arabian patient population revealed that approximately 24% of cases had mutations when 13 of the LCA genes were tested [34]. In a study in Chinese patients with LCA, 50% of patients had mutations when 15 genes were tested, but the percentage of patients with at least two mutant alleles was less than 50% [16]. A smaller study in Korean patients covering nine genes found mutations in three out of 20 cases (15%) [35]. In Italian and Chinese patients, the frequency of mutations in *CEP290* was approximately 4% [16,36], which is far less than in patients of other populations studied [23]. A survey of the most common mutations in eight different genes responsible for 30% of LCA in various populations showed mutation in one out of 38 cases among Indian patients [37].

Functions of genes involved in LCA

Vision is mediated by the photoreceptor cells present in the retina. Most of the genes associated with LCA are expressed exclusively or predominantly in the eye, except a few genes that are expressed in other tissues. These genes are involved in a variety of functions, such as photoreceptor morphogenesis, phototransduction, outer segment (OS) phagocytosis and ciliary transport (summarized in Table 1) and have been reviewed [2]. The following sections briefly outline functional aspects, highlighting more recent studies and discussing newly identified LCA genes.

The genes that are ubiquitously expressed are *IMPDH1*, *CEP290*, *MERTK*, *LCA5*, *ALMS1* and *IQCB1*. *IMPDH1* is involved in nucleotide biosynthesis where it catalyzes the conversion of inosine monophosphate to xanthosine monophosphate, which is a rate-limiting step. IMPDH1 also binds to single-strand nucleic acid; this interaction is mediated by a subdomain distinct from the catalytic domain [38]. MERTK stimulates the phagocytosis of photoreceptor OSs by retinal pigment epithelium (RPE), as evident by ingestion of OS by cultured RPE cells [39].

The *CEP290*-encoded protein is a centrosomal protein and is involved in cilia-associated transport [40]. Apart from *CEP290*, proteins encoded by four other LCA genes *TULP1*, *RPGRIP1*, *RD3* and *LCA5* are also involved in protein transport. TULP1 is involved in the vesicular protein transport of photoreceptor proteins, particularly of the OSs. It is also essential for photoreceptor cell survival and is required for proper development of the photoreceptor synapse [41,42]. TULP1 also acts as a ligand that binds to and helps in phagocytosis by RPE cells [43]. RPGRIP1 plays a role in vesicular trafficking and disc morphogenesis [44]. RD3 co-localizes and interacts with retinal guanyl cyclase (retGC1; GUCY2D). It plays an important role in the stable expression and trafficking of retGC1 from endoplasmic reticulum to endosomal vesicles [45]. Lebercilin plays an important role in anterograde and retrograde transport of proteins across the connecting cilium [46].

Table 1. Leber congenital amaurosis genes known to date, and their functions, expression and mutation frequencies.

Gene symbol	Locus	Function	Expression	Phenotype associated with LCA	Mutation frequency (%)	Ref.
GUCY2D *RETGC1*	17p13.1	Phototransduction (cGMP synthesis)	PRCs	Poor vision (CF-LP), mild-to-severe hyperopia, normal fundus appearance, photophobia, retained lamellar structures	2.7–21	[2,23,34]
RPE65 *RP20*	1p31.3–1p31.2	Visual cycle (retinyl esters to 11-cis-retinol)	RPE	Night blindness, photo attraction, nystagmus, mild-to-moderate hyperopia, relatively good vision early in life and later deterioration, bull's eye maculopathy, geographic atrophic lesions at later age and disorganized lamellar structures	1.7–9	[20,23]
SPATA7	14q31.3		Retina	Poor vision, retinal atrophy, attenuated vessels	1.7–2.9	[28,29]
AIPL1	17p13.2	Maintenance of rod photoreceptor, chaperone and protein farnesylation	In rods of central and peripheral retina, pineal gland	Poor vision, night blindness, late onset, pigmentary retinal changes, maculopathy in the form of a bull's eye lesion or atrophic lesion, keratoconus or cataracts, decreased macular thickness	1.1–7.8	[16,21]
LCA5	6q14.1	Protein transport	Ubiquitous expression in early embryonic stages, connecting cilium, centriole and microtubules of PRCs in adults	Low vision (CF-20/100), severe hyperopia, macular coloboma, peripheral pigment mottling	1.7–6	[14,15]
RPGRIP1	14q11.2	Protein transport	Outer segment of rod photoreceptor cells, kidney, brain, heart, liver and spleen	Occasional night blindness, initially normal retinal appearance, progressive pigmentary retinopathy and loss of vision (20/200-LP), drusen-like deposits, retained central laminar organization, intact ONL	4–28	[2,16,74]
CRX *CORD2* *CRD* *OTX3*	19q13.33	Transcription factor	PRCs, retinal inner nuclear layer and pineal gland	Severe vision loss (20/300-LP), infantile nystagmus, cataract, pigmentary retinopathy	0.6–3.4	[16,18]
CRB1	1q31.3	Cell–cell interaction	PRCs, retinal inner nuclear layer and iris	PPRPE, Coats-like response, keratoconous, optic nerve pallor, thickened and disorganized retina	9–16	[2,16,23]
LCA9	1p36					[73]
CEP290 *NPHP6* *BBS14*	12q21.32	Cilia-associated protein transport	Ubiquitous	Hyperopia, extremely poor vision, cataracts and keratoconus, nummular pigmentary retinopathy, pigmentary maculopathy, preservation of ONL at the fovea with distorted inner retina, thinning of ONL with age	4–30	[16,23,25]
IMPDH1 *RP10* *MPD*	7q32.1	Regulation of cell growth	Ubiquitous	Rare, diffuse RPE mottling, no pigmentary deposits, moderate hyperopia, low vision (20/40-LP)	8.3	[5]
RD3 *C1ORF36*	1q32.3	Transport of retinal guanylate cyclase	Subnuclear localization	Poor vision, atrophic and pigmentary maculopathy, peripheral mottling and RPE atrophy, moderate-to-severe optic nerve pallor	0.1	[12]

Frequencies shown are the range of frequencies (lowest–highest) reported.
†Genes are tentatively associated with LCA with only one case each reported so far.
CF: Counting finger; LCA: Leber congenital amaurosis; LP: Light perception; NA: Not available; ONL: Outer nuclear layer; OS: Outer segment; PPRPE: Preservation of para-arteriolar retinal pigment epithelium; PRC: Photoreceptor cell; RPE: Retinal pigment epithelium.

Table 1. Leber congenital amaurosis genes known to date, and their functions, expression and mutation frequencies (cont.).

Gene symbol	Locus	Function	Expression	Phenotype associated with LCA	Mutation frequency (%)	Ref.
RDH12 *SDR7C2*	14q24.1	Vitamin A cycle (converts all-trans/11-cis-retinal to all-trans/11-cis-retinol)	RPE	RPE atrophy, pronounced attenuation of retinal arterioles and intraretinal bone spicule pigmentation, fishnet or reticular pattern, maculopathy, visual function in early life, followed by a progressive decline	1–2	[2,16,23]
LRAT	4q32.1	Visual cycle (converts all-trans-retinol to retinyl esters)	RPE	Night blindness, retinal atrophy, peripheral RPE atrophy, maculopathy, moderate optic nerve pallor	<1.0	[2]
TULP1 *RP14* *LCA15* *TUBL1*	6p21.31	Protein transport and synaptic development	PRCs	Reading vision in early stages, severe pigmentary retinopathy, early bull's eye maculopathy, moderate-to-severe myopia, color vision anomalies	<1–13	[2,34,73]
KCNJ13	2q37.1	Regulation of K^+ transport	RPE, neural retina, CNS and epithelial cells of kidney, lung, testis and small intestine	NA	0.9	[30]
MERTK *MER* *RP38*	2q13	OS phagocytosis	Macrophages, dendritic cells and RPE	NA	0.9–2.3	[16]
IQCB1 *NPHP5* *SLSN5*	3q13.33	Protein transport across cilia	Photoreceptor cilia and primary cilia of renal epithelial cells	NA	8	[33]
ALMS1†	2p13.1	Probably intracellular trafficking	Ubiquitous	NA	2	[33]
CNGA3†	2q11.2	Phototransduction	Cone PRCs	NA	2	[33]
MYO7A†						[33]

Frequencies shown are the range of frequencies (lowest–highest) reported.
†Genes are tentatively associated with LCA with only one case each reported so far.
CF: Counting finger; LCA: Leber congenital amaurosis; LP: Light perception; NA: Not available; ONL: Outer nuclear layer; OS: Outer segment; PPRPE: Preservation of para-arteriolar retinal pigment epithelium; PRC: Photoreceptor cell; RPE: Retinal pigment epithelium.

CRB1 protein occurs as part of a protein complex that is apparently required for maintenance of the integrity of photoreceptor cell layers, particularly the adherence junctions that maintain cell–cell contact between photoreceptors and Müller glial cells. In mammals, Crumbs 1 is shown to localize to the subapical region adjacent to the adherence junctions at the outer limiting membrane (OLM) of the photoreceptor layer [47]; a subsequent study showed Crb1 expression by immune-electron microscopy in the subapical region of mainly the Müller cells, with little expression in the photoreceptors [48]. *Crb1*$^{-/-}$ mice developed changes in the retina at 3 months with subsequent retinal degeneration. Retinal changes included ruptured OLM with protrusion of photoreceptor cell bodies into the inter-photoreceptor matrix, outer plexiform and inner nuclear layers and formation of half rosettes [47]. This suggested that formation of adherence junctions was not dependent on Crb1 expression since the mice had normal retinas at birth. Similar disruption of the OLM along with disturbances of Müller cell layer was observed in Crb1$^{-/-}$ retinal explant cultures [48].

Two LCA genes (*AIPL1* and *GUCY2D*) are involved in the phototransduction cascade. GUCY2D is required for restoration of cGMP. Decreased Ca^{2+} concentration stimulates synthesis of cGMP by retGC1, thus leading to reopening of the cGMP-gated channels, influx of ions (Ca^{2+}), depolarization of the cell and return to the dark state. GUCY2D is also involved in the peripheral membrane protein transport from the endoplasmic reticulum to the OS [49]. AIPL1 is involved in chaperoning/assembly of subunits of the *PDE6* gene and may be important for farnesylation of PDE6 [50,51]. Three LCA genes (*RDH12*, *RPE65* and *LRAT*) are involved in the visual cycle.

The newly identified LCA genes play diverse roles. Two are channel proteins (*KCNJ13* and *CNGA3*). KCNJ13 is a member of a family of inwardly rectifying potassium channels (Kir channels) possibly involved in regulation of K^+ transport [52], whereas the *CNGA3* gene encodes the α3 subunit of the cone photoreceptor cyclic nucleotide-gated channel, and plays an important role in the phototransduction cascade [53]. IQCB1 or NPHP5 forms a complex with other proteins such as RPGR, and localizes at the base of the connecting cilium of photoreceptors. It probably controls ciliary transport [54]. MYO7A is involved in various processes, including the apical localization of RPE melanosomes, light-dependent translocation of RPE65, removal of phagosomes from the apical RPE for their delivery to lysosomes and normal functioning of the visual retinoid cycle [55]. ALMS1 protein localizes to the centrosome and probably plays a role in intracellular trafficking [56].

Genotype–phenotype correlations

Clinical manifestations in LCA show a wide range of heterogeneity. Variable features that may be present in LCA patients include hypermetropia, cataract, eye-poking behavior, photophobia and keratoconus. The evaluation of patients having LCA associated with mutations in different genes has suggested gene-specific patterns in phenotypes, although there is a considerable degree of variation between individuals and overlap between different genes [18,57,58].

Visual acuities (VAs) of patients with *RPE65* mutations may vary from mild, moderate or severe loss of VA in the first three decades, with worsening after the third decade [59]. Progressive decline in VAs with increasing age is also a feature of *RDH12* mutations, although patients are found to have useful levels of VA during childhood [60]. Mutations in *GUCY2D* and *AIPL1* are associated with very poor VA in the majority of patients even at very early stages of life [17,59,61,62]. Similarly, profound early loss of vision is a feature of *RPGRIP1* mutations [59,62,63]. Patients with *CRB1* mutations have variable VA ranging from <20 out of 200 to no light perception. Hyperopia of ≥1.0 diopter (D) is a feature of this group of patients [59,64]. In cases of CEP290-LCA, patients have stable but severe vision loss. VA of counting fingers or less was found to occur in most cases with an early decline of vision [25,59].

Mutations in different genes are associated with characteristic fundus features. Methods ranging from conventional ophthalmoscopy to more sophisticated imaging techniques aimed at retinal microstructure have been used to derive associations. Patients with *GUCY2D* mutations generally have a normal-appearing fundus [36,58,63,65]. Even at the microstructural level, retinas of GUCY2D-LCA patients show preservation of retinal layers and organization comparable with normal individuals. Macular imaging with spectral domain optical coherence tomography (OCT) showed six retinal layers with a visible photoreceptor inner/OS juncture [66]. In cases of *CRB1* mutation, the fundus shows white dots, develops nummular pigmentation especially in later ages, macular atrophy, and a thickened and delaminated retina is evident on OCT [64,67,68]. Preserved para-arteriolar RPE, and Coats-like exudative vasculopathy are infrequent features of patients with *CRB1* mutations, although regarded as characteristic of CRB1-LCA. Preserved para-arteriolar RPE is reported in 9.4% of cases [36,68–70] and Coats-like reaction in 17% of cases [20,63,64,68]. Patients with *CEP290* mutations are found to have sparing of the macular area on gross retinal examination, with marbleized fundus in the first decade of life and retinal atrophy in later stages [23]. Preservation of photoreceptors in the foveal and macular regions has also been detected on OCT of CEP290-LCA patients, with peripheral thinning [66,71], albeit with loss of the retinal laminar structure that is more pronounced eccentric to the fovea. Pigmentary retinopathy of varying degrees is characteristic of *RPE65*-, *RDH12*- and *AIPL1*-related LCA [17,60,63,72]. Maculopathy is found to be a predominant feature of AIPL1-LCA [17,73,74]; retinal imaging of AIPL1-LCA cases showed loss of photoreceptors from the central retina [20,61–63].

Modifier alleles

Though LCA is considered to be a mendelian disease, the presence of non-mendelian patterns has also been proposed, especially to explain differences in phenotype resulting from mutations in the same locus. Presence of a third variant allele in 7% of patients suggested that these are second site modifiers, and in a subset of families these alleles were correlated to variations in phenotype [21]. A recent study on 60 families from North America found that 12% of cases have a third mutant allele [24]; the presence of this third allele, usually at a LCA locus, was more than would

be expected by chance, but no phenotypic correlations could be drawn from the presence of the third allele. A study of a large series of patients with various ciliopathy phenotypes for potential modifying effects found that a common allele of *RPGRIP1L* (RPGRIP1-like) is significantly associated with retinal degeneration phenotypes, including LCA, Joubert syndrome and SLS, as compared with nonretinal ciliopathies such as nephronophthisis and normal controls [75]. This allele was shown to be functionally defective and interpreted as a phenotypic modulator to the retinal degeneration found in LCA and other ciliopathies, although the primary mutations are different.

Models for gene therapy

Animal models of LCA that carry similar mutations to humans have helped in understanding the pathology and testing the effectiveness of gene-replacement therapy for these disorders. Mouse models of LCA with targeted knockouts of the relevant genes, as well as naturally occurring mutants, have been described [2,76]. Here, we will discuss models of gene replacement in LCA, since these models provide a basis for therapy. Clinical trials involving gene therapy with *RPE65* for LCA patients have provided proof of principle for translation into clinical treatment of knowledge obtained from many different streams of basic and clinical research [201–204].

The most extensively studied animal model of gene replacement to date is the Briard dog, a breed that is affected with congenital blindness due to mutation of *RPE65*. The subretinal administration of recombinant adeno-associated virus (AAV) serotype 2 (AAV2/2) carrying a chicken h-actin-promoter/ cytomegalovirus (CMV) enhancer-driven wild-type canine *RPE65* cDNA to three dogs led to visual recovery [77]. Further studies also established efficacy of the treatment as loss of nystagmus, increased ERG responses and depletion of lipid droplets in the RPE were observed in treated eyes [78]. Stable restoration of rod and cone photoreceptor function was observed even after 3 years of gene therapy in this canine model [77,79]. AAV were chosen because of their ability to efficiently transduce both rod and cone photoreceptors and the RPE (AAV2/4), nontoxic nature, nonimmunogenic and long-lasting effect, usually a single dose being needed [80]. Safety and dosage was established in canine and a nonhuman primate model, cynomolgus monkey, which laid the background for gene therapy clinical trials for LCA [81,82].

Clinical trials of AAV-*RPE65* gene replacement, employing an AAV-based vector to deliver the *RPE65* gene through subretinal injection to LCA patients, were initiated in 2007 at three sites, independently [9,10,83]. Bainbridge and coworkers enrolled three LCA patients with *RPE65* mutations (aged 17–23 years); the AAV 2/2-hR*PE65* with a human *RPE65* promoter was used for subretinal injection, which covered a third of the retina [9]. Maguire and coworkers used AAV particles containing AAV2-h*RPE65*v2 with a chicken β-actin promoter in three LCA patients (aged 19–26 years) [10]. Hauswirth and coworkers used AAV2-*hRPE65* in three patients aged 21–24 years [83]. No significant intraocular or systemic inflammation was observed by any of the groups. Improvement in vision was observed as evident from improved early treatment diabetic retinopathy study acuities (ranging from 3 to 4.5 lines), improvement in the pupillary light reflex and reduced nystagmus in one study [10]. Improvement in visual function and retinal sensitivity for both light- and dark-adapted settings (microperimetry), and improvement in mobility through the obstacle course was observed in one patient by Bainbridge and coworkers [9]. These studies are an important landmark in gene therapy for ocular diseases, since they have demonstrated the feasibility of gene therapy for LCA in terms of safety and efficacy of the AAV2 vectors used as a gene-delivery system and the potential for improvement in visual function [84,85]. Encouragingly, the improvement in visual outcome and safety observed in the first few weeks of the trials are shown to be retained after 1–1.5 years [84,86].

Gene-replacement studies on knockout models of a few other LCA genes have also shown restoration of the structural and functional defects, including *MERTK*, *LRAT*, *AIPL1*, *RPGRIP1* and *GUCY2D*. A naturally occurring chicken model that has a knockout of *GUCY2D* is the GUCY1*B chicken, which is blind, and has retinal degeneration with loss of rod and cone function [87]. Partial restoration of vision, as assessed by behavioral and ERG testing, was demonstrated in this model after transfer of the lentiviral-bovine RetGC-1 cDNA gene construct in prehatch embryos [88]. A mouse model of *Gucy2D* or GC1 deficiency (guanylate cyclase 1 knockout) shows defects in cone function and degeneration of cones while rods are preserved. Studies have shown stable restoration of visual functions and cone preservation in a guanylate cyclase 1 knockout model using rAAV2/5 and AAV2/8 vectors for subretinal gene transfer [89,90]. Maintenance of retinal structure in LCA1 patients suggests that *GUCY2D* may be a suitable candidate for gene therapy trial in humans [66].

Using similar approaches as mentioned above, gene therapy for *AIPL1* in mouse models showed promising results. In mice, AIPL1 is present in the outer plexiform layer and inner segments of photoreceptors. *Aipl1*$^{-/-}$ mice are found to have normal development of the retina although retinal degeneration is very rapid and complete degeneration is observed by 4 weeks. Similar to LCA patients, *Aipl1*-null mice showed no ERG response [91], whereas in hypomorphic mice, production of AIPL1 is reduced (~20% of wild-type) and photoreceptor degeneration is slow compared with null mice and results in RP-like features [92]. Stable and long-term restoration of vision was obtained by using AAV-*Aipl1* gene transfer using a rhodopsin kinase (RK) promoter that is specific to both rods and cones in both null and hypomorphic mice [93]. Gene transfer using AAV8-RK-*hAIPL1* resulted in increased *AIPL1* gene expression followed by PDE synthesis in both rod and cone photoreceptors in null mice, which was evident from ERG responses. Improved photoreceptor cell survival, stabilization of retinal functions and preservation of OS morphology was observed following subretinal delivery of this gene, with the effect persisting at 5 months postinjection [93]. These results provided experimental support for the feasibility of human gene therapy with the *AIPL1* gene.

The gene-delivery system mentioned above, AAV-mediated gene delivery using the RK promoter, was also attempted for the human *RPGRIP1* gene. RPGRIP1 is localized in

photoreceptor-connecting cilium. It forms a complex with RPGR and other proteins and a mutation in this gene affects the functioning of the whole complex [94]. RPGRIP1 is also required for OS morphogenesis [95]. In *Rpgrip1*$^{-/-}$ mice, photoreceptor degeneration starts at around postnatal day 15 and most of the cells degenerate by 3 months of age. The first attempt to treat photoreceptor degeneration was made by subretinal delivery of AAV-*RPGRIP* under the control of murine opsin promoter fragment in *Rpgrip1*$^{-/-}$ mutant mice. Retinal function was restored as evident by restored localization of RPGR to connecting cilia, a thicker photoreceptor nuclear layer, well-organized OSs and higher ERG amplitudes as compared with controls [96]. In continuation of this, the human RK promoter–RPGRIP gene construct was used to test the efficacy of gene therapy for *RPGRIP1* using AAV8 in the mouse model [97]. Improved retinal function was observed at the fifth month as measured by ERG. Introduced human RPGRIP1 localized correctly in the mouse retina and was able to anchor RPGR. Morphology of treated eyes was comparable to the wild-type. Photoreceptor survival was increased. Expression level of transgenic human RPGRIP1 was lower than endogenous RPGRIP1 in mice, which could be the reason for incomplete rescue of the phenotype in treated mice. Despite this fact, this model provides a possible background for a future human trial [97]. Preservation of central retina in these patients will aid the success of gene therapy if the gene is injected into the central retina [98].

Another candidate being explored for gene therapy is *CEP290*, which is the most frequently mutated gene in LCA. Patients with *CEP290* gene mutations show preservation of the ONL at the fovea [66,71]. Preservation of ONL seems to be associated with the c2991+1655A>G mutation, as all the patients studied in these two reports had this particular mutation except one [66,71]. Specific roles of different subdomains of CEP290 protein were determined in *cep290* knockdown zebrafish model (mimicking hypomorphic c.2991+1655A>G mutation in humans). These *cep290* morphant embryos had normal retinal structure yet reduced VA. Owing to its large size, the CEP290 protein was divided into two-part-N-terminal regions, the first 1059 amino acids containing c.2991+1655A residue and the C-terminal 1765–2479 amino acids. The N-terminal CEP290 construct was able to rescue the visual defects in the *cep290*$^{-/-}$ zebrafish model [99].

MERTK gene expression is found mainly in the RPE and macrophages, both of them being involved in phagocytosis. Mutations in this gene cause accumulation of OS material in the subretinal space which ultimately leads to retinal degeneration as evident in the Royal College of Surgeons (RCS) rat model with a 409-bp deletion in the *Mertk* gene [100]. Adenoviral-mediated delivery of rat *Mertk* under the control of the CMV promoter in RPE of RCS rat was attempted. The transgene was able to prevent photoreceptor degeneration as well as correct the RPE phagocytosis defect. Numbers of photoreceptors were higher near the site of injection after 1 month [101]. However, short-term expression from adenovirus makes this system unsuitable for gene therapy trials. This problem can be overcome by the use of recombinant (r)AAV vectors or lentiviruses [102,103]. AAV-CMV-*Mertk*- or AAV-RPE-*Mertk*-mediated gene delivery prolonged the survival of photoreceptor cells. Functional photoreceptors were present even after 9 weeks postinjection in treated eyes. The number of photoreceptors was also approximately 2.5-times higher than in the control eye after 9 months [103].

rAAV-mediated gene therapy in *Lrat*-deficient mice was successful at restoring visual function in *Lrat*$^{-/-}$ mice as measured by recovery of visual chromophore and pigment, and ERG responses [104]. In treated mice, ERG amplitude was restored to approximately 50% of that of wild-type mice. Pupillary light responses were also increased after treatment. Oral administration of retinoids in *Lrat*$^{-/-}$ mice also had the same beneficial effects [104].

Expert commentary

Recent developments in the genetics of LCA and in gene therapy in particular have been tremendous. Although one has to await the results of further stages of clinical trials with *RPE65*, the initial results are very promising and have suggested the possibility of at least a partial recovery of visual responses. At the same time, various gene-delivery systems have been developed and these have paved the way for clinical trials for other LCA genes. Gene therapy would require functional photoreceptors to be applicable. In cases of early photoreceptor degeneration, which usually happens with several LCA subtypes, photoreceptor replacement by cell-based therapies may be a better option. Research in this field had proved the feasibility of rod as well as cone cell transplantation in retinas in animal models. Apart from these, attempts to develop electronic prosthesis are also being made, which will convert visual information to electrical impulses that will be able to stimulate the visual pathways to restore vision. Success of these nongenetic methods will help patients who are not eligible for gene therapy. Taken together, these developments hold promise for treatments for LCA patients in the near future.

Five-year view

In at least approximately 30% of LCA, the underlying genetic etiology is still unknown. The vast genetic heterogeneity of LCA makes it cumbersome to use conventional Sanger sequencing as a routine clinical tool. The LCA mutation chip has proved effective for rapid screening of all existing mutations [20,21,105]. Conventional methods of gene mapping in families or candidate gene screening for discovery of new genes have given way to next-generation sequencing (NGS), which facilitates a screen of the whole exome for finding pathogenic changes, and thereby enables a simultaneous screen of known and novel genes. Over the next few years, it is expected that gene discovery will proceed at a very advanced pace through the application of NGS. Other high-throughput methods that have recently been in use include resequencing and genotyping arrays that can cover all known loci at once. Screening devices based on these are the retina-array which has 93 genes involved in retinal diseases [106] and an SNP chip representing SNPs covering 40 genes for retinal diseases [107].

These methods enable more rapid screening for the large number of known genes, and thereby facilitate diagnostic screening. Another approach employed in retinitis pigmentosa is targeted capture of several genes for, and high-throughput NGS of, the captured sequences [108]. These methods are rather expensive at present for routine use in most parts if the world, but will possibly make genetic testing in LCA faster, and hopefully, less expensive in the near future. Simultaneously, the next few years should see efforts towards gene therapy, which is in the preclinical stages at present, to allow this progress to more clinical trials.

Financial & competing interests disclosure

The authors are supported by the Hyderabad Eye Research Foundation, Champalimaud Foundation (Portugal) and by a grant from the Department of Biotechnology, Government of India. The authors have no other relevant affiliations or financial involvement with any organization or entity with a financial interest in or financial conflict with the subject matter or materials discussed in the manuscript apart from those disclosed.

No writing assistance was utilized in the production of this manuscript.

Key issues

- Leber congenital amaurosis (LCA) is a genetically heterogeneous disorder with 19 genes known to date. Genes are not yet known in a subset of patients. Genetic heterogeneity is an obstacle to genetic testing for diagnostic and predictive purposes.
- There are variations in mutation frequencies for specific genes across different ethnic groups.
- Rapid advances in genomic technologies over the last few years have led to the increasing application of high-throughput platforms based on microarray and next-generation sequencing for genetic screening. These new technologies facilitate screening of multiple genes as well as discovery of new genes.
- Genotype–phenotype correlations described for different LCA genes can aid in grouping of patients for prioritized genetic testing. However, significant phenotypic overlaps exist between different sets of genotypes.
- Gene therapy with the *RPE65* gene in clinical trials of patients with LCA has shown promise and has spurred efforts at developing gene-delivery systems for other major LCA genes.

References

Papers of special note have been highlighted as:
• of interest
•• of considerable interest

1 Ahmed E, Loewenstein J. Leber congenital amaurosis: disease, genetics and therapy. *Semin. Ophthalmol.* 23(1), 39–43 (2008).

2 Den Hollander AI, Roepman R, Koenekoop RK, Cremers FP. Leber congenital amaurosis: genes, proteins and disease mechanisms. *Prog. Retin. Eye Res.* 27(4), 391–419 (2008).

• **Comprehensive review on genetics of Leber congenital amaurosis (LCA), covering various aspects in detail.**

3 Koenekoop RK. An overview of Leber congenital amaurosis: a model to understand human retinal development. *Surv. Ophthalmol.* 49(4), 379–398 (2004).

4 Stone EM. Leber congenital amaurosis – a model for efficient genetic testing of heterogeneous disorders: LXIV Edward Jackson Memorial Lecture. *Am. J. Ophthalmol.* 144(6), 791–811 (2007).

• **Overview of methods of screening of LCA genes and a strategy for molecular testing.**

5 Bowne SJ, Sullivan LS, Mortimer SE *et al.* Spectrum and frequency of mutations in IMPDH1 associated with autosomal dominant retinitis pigmentosa and Leber congenital amaurosis. *Invest. Ophthalmol. Vis. Sci.* 47(1), 34–42 (2006).

6 Sohocki MM, Sullivan LS, Mintz-Hittner HA *et al.* A range of clinical phenotypes associated with mutations in *CRX*, a photoreceptor transcription-factor gene. *Am. J. Hum. Genet.* 63(5), 1307–1315 (1998).

7 Camuzat A, Dollfus H, Rozet JM *et al.* A gene for Leber's congenital amaurosis maps to chromosome 17p. *Hum. Mol. Genet.* 4(8), 1447–1452 (1995).

8 Perrault I, Rozet JM, Calvas P *et al.* Retinal-specific guanylate cyclase gene mutations in Leber's congenital amaurosis. *Nat. Genet.* 14(4), 461–464 (1996).

9 Bainbridge JW, Smith AJ, Barker SS *et al.* Effect of gene therapy on visual function in Leber's congenital amaurosis. *N. Engl. J. Med.* 358(21), 2231–2239 (2008).

• **Reports results of the first clinical trials for *RPE65* gene-replacement therapy.**

10 Maguire AM, Simonelli F, Pierce EA *et al.* Safety and efficacy of gene transfer for Leber's congenital amaurosis. *N. Engl. J. Med.* 358(21), 2240–2248 (2008).

• **Report of the first gene therapy trial for *RPE65* gene delivery in LCA.**

11 Cideciyan AV, Aleman TS, Boye SL *et al.* Human gene therapy for RPE65 isomerase deficiency activates the retinoid cycle of vision but with slow rod kinetics. *Proc. Natl Acad. Sci. USA* 105(39), 15112–15117 (2008).

12 Friedman JS, Chang B, Kannabiran C *et al.* Premature truncation of a novel protein, RD3, exhibiting subnuclear localization is associated with retinal degeneration. *Am. J. Hum. Genet.* 79(6), 1059–1070 (2006).

13 Sweeney MO, Mcgee TL, Berson EL, Dryja TP. Low prevalence of lecithin retinol acyltransferase mutations in patients with Leber congenital amaurosis and autosomal recessive retinitis pigmentosa. *Mol. Vis.* 13, 588–593 (2007).

14 Gerber S, Hanein S, Perrault I *et al.* Mutations in LCA5 are an uncommon cause of Leber congenital amaurosis (LCA) type II. *Hum. Mutat.* 28(12), 1245 (2007).

15 Den Hollander AI, Koenekoop RK, Mohamed MD *et al.* Mutations in *LCA5*, encoding the ciliary protein Lebercilin, cause Leber congenital amaurosis. *Nat. Genet.* 39(7), 889–895 (2007).

16 Li L, Xiao X, Li S *et al.* Detection of variants in 15 genes in 87 unrelated Chinese patients with Leber congenital amaurosis. *PLoS One* 6(5), e19458 (2011).

17 Dharmaraj S, Leroy BP, Sohocki MM *et al.* The phenotype of Leber congenital amaurosis in patients with AIPL1 mutations. *Arch. Ophthalmol.* 122(7), 1029–1037 (2004).

18 Hanein S, Perrault I, Gerber S *et al.* Leber congenital amaurosis: comprehensive survey of the genetic heterogeneity, refinement of the clinical definition, and genotype–phenotype correlations as a strategy for molecular diagnosis. *Hum. Mutat.* 23(4), 306–317 (2004).

19 Perrault I, Hanein S, Gerber S *et al.* Retinal dehydrogenase 12 (RDH12) mutations in Leber congenital amaurosis. *Am. J. Hum. Genet.* 75(4), 639–646 (2004).

20 Yzer S, Leroy BP, De Baere E *et al.* Microarray-based mutation detection and phenotypic characterization of patients with Leber congenital amaurosis. *Invest. Ophthalmol. Vis. Sci.* 47(3), 1167–1176 (2006).

21 Zernant J, Kulm M, Dharmaraj S *et al.* Genotyping microarray (disease chip) for Leber congenital amaurosis: detection of modifier alleles. *Invest. Ophthalmol. Vis. Sci.* 46(9), 3052–3059 (2005).

22 Vallespin E, Cantalapiedra D, Riveiro-Alvarez R *et al.* Mutation screening of 299 Spanish families with retinal dystrophies by Leber congenital amaurosis genotyping microarray. *Invest. Ophthalmol. Vis. Sci.* 48(12), 5653–5661 (2007).

23 Coppieters F, Casteels I, Meire F *et al.* Genetic screening of LCA in Belgium: predominance of CEP290 and identification of potential modifier alleles in AHI1 of CEP290-related phenotypes. *Hum. Mutat.* 31(10), E1709–E1766 (2010).

24 Wiszniewski W, Lewis RA, Stockton DW *et al.* Potential involvement of more than one locus in trait manifestation for individuals with Leber congenital amaurosis. *Hum. Genet.* 129(3), 319–327 (2011).

25 Perrault I, Delphin N, Hanein S *et al.* Spectrum of NPHP6/CEP290 mutations in Leber congenital amaurosis and delineation of the associated phenotype. *Hum. Mutat.* 28(4), 416 (2007).

26 Den Hollander AI, Koenekoop RK, Yzer S *et al.* Mutations in the *CEP290* (*NPHP6*) gene are a frequent cause of Leber congenital amaurosis. *Am. J. Hum. Genet.* 79(3), 556–561 (2006).

27 Wang H, Den Hollander AI, Moayedi Y *et al.* Mutations in *SPATA7* cause Leber congenital amaurosis and juvenile retinitis pigmentosa. *Am. J. Hum. Genet.* 84(3), 380–387 (2009).

28 Perrault I, Hanein S, Gerard X *et al.* Spectrum of *SPATA7* mutations in Leber congenital amaurosis and delineation of the associated phenotype. *Hum. Mutat.* 31(3), E1241–E1250 (2010).

29 Mackay DS, Ocaka LA, Borman AD *et al.* Screening of SPATA7 in patients with Leber congenital amaurosis and severe childhood-onset retinal dystrophy reveals disease-causing mutations. *Invest. Ophthalmol. Vis. Sci.* 52(6), 3032–3038 (2011).

30 Sergouniotis PI, Davidson AE, Mackay DS *et al.* Recessive mutations in *KCNJ13*, encoding an inwardly rectifying potassium channel subunit, cause Leber congenital amaurosis. *Am. J. Hum. Genet.* 89(1), 183–190 (2011).

31 Stone EM, Cideciyan AV, Aleman TS *et al.* Variations in NPHP5 in patients with nonsyndromic Leber congenital amaurosis and Senior–Loken syndrome. *Arch. Ophthalmol.* 129(1), 81–87 (2011).

32 Estrada-Cuzcano A, Koenekoop RK, Coppieters F *et al. IQCB1* mutations in patients with Leber congenital amaurosis. *Invest. Ophthalmol. Vis. Sci.* 52(2), 834–839 (2011).

33 Wang X, Wang H, Cao M *et al.* Whole-exome sequencing identifies *ALMS1*, *IQCB1*, *CNGA3*, and *MYO7A* mutations in patients with Leber congenital amaurosis. *Hum. Mutat.* 32(12), 1450–1459 (2011).

34 Li Y, Wang H, Peng J *et al.* Mutation survey of known LCA genes and loci in the Saudi Arabian population. *Invest. Ophthalmol. Vis. Sci.* 50(3), 1336–1343 (2009).

35 Seong MW, Kim SY, Yu YS, Hwang JM, Kim JY, Park SS. Molecular characterization of Leber congenital amaurosis in Koreans. *Mol. Vis.* 14, 1429–1436 (2008).

36 Simonelli F, Ziviello C, Testa F *et al.* Clinical and molecular genetics of Leber's congenital amaurosis: a multicenter study of Italian patients. *Invest. Ophthalmol. Vis. Sci.* 48(9), 4284–4290 (2007).

37 Sundaresan P, Vijayalakshmi P, Thompson S, Ko AC, Fingert JH, Stone EM. Mutations that are a common cause of Leber congenital amaurosis in Northern America are rare in southern India. *Mol. Vis.* 15, 1781–1787 (2009).

38 Mclean JE, Hamaguchi N, Belenky P, Mortimer SE, Stanton M, Hedstrom L. Inosine 5'-monophosphate dehydrogenase binds nucleic acids *in vitro* and *in vivo*. *Biochem. J.* 379(Pt 2), 243–251 (2004).

39 Feng W, Yasumura D, Matthes MT, Lavail MM, Vollrath D. Mertk triggers uptake of photoreceptor outer segments during phagocytosis by cultured retinal pigment epithelial cells. *J. Biol. Chem.* 277(19), 17016–17022 (2002).

40 Chang B, Khanna H, Hawes N *et al.* In-frame deletion in a novel centrosomal/ciliary protein CEP290/NPHP6 perturbs its interaction with RPGR and results in early-onset retinal degeneration in the rd16 mouse. *Hum. Mol. Genet.* 15(11), 1847–1857 (2006).

41 Grossman GH, Pauer GJ, Narendra U, Hagstrom SA. Tubby-like protein 1 (Tulp1) is required for normal photoreceptor synaptic development. *Adv. Exp. Med. Biol.* 664, 89–96 (2010).

42 Grossman GH, Watson RF, Pauer GJ, Bollinger K, Hagstrom SA. Immunocytochemical evidence of Tulp1-dependent outer segment protein transport pathways in photoreceptor cells. *Exp. Eye Res.* 93, 658–668 (2011).

43 Caberoy NB, Zhou Y, Li W. Tubby and tubby-like protein 1 are new MerTK ligands for phagocytosis. *EMBO J.* 29(23), 3898–3910 (2010).

44 Roepman R, Bernoud-Hubac N, Schick DE *et al.* The retinitis pigmentosa GTPase regulator (RPGR) interacts with novel transport-like proteins in the outer segments of rod photoreceptors. *Hum. Mol. Genet.* 9(14), 2095–2105 (2000).

45 Azadi S, Molday LL, Molday RS. RD3, the protein associated with Leber congenital amaurosis type 12, is required for guanylate cyclase trafficking in photoreceptor cells. *Proc. Natl Acad. Sci. USA* 107(49), 21158–21163 (2010).

46 Boldt K, Mans DA, Won J *et al.* Disruption of intraflagellar protein transport in photoreceptor cilia causes Leber congenital amaurosis in humans and mice. *J. Clin. Invest.* 121(6), 2169–2180 (2011).

47 Van De Pavert SA, Kantardzhieva A, Malysheva A *et al.* Crumbs homologue 1 is required for maintenance of photoreceptor cell polarization and adhesion during light exposure. *J. Cell Sci.* 117(Pt 18), 4169–4177 (2004).

48 Van Rossum AG, Aartsen WM, Meuleman J *et al.* Pals1/Mpp5 is required for correct localization of Crb1 at the subapical region in polarized Müller glia cells. *Hum. Mol. Genet.* 15(18), 2659–2672 (2006).

49 Karan S, Frederick JM, Baehr W. Novel functions of photoreceptor guanylate cyclases revealed by targeted deletion. *Mol. Cell. Biochem.* 334(1–2), 141–155 (2010).

50 Kirschman LT, Kolandaivelu S, Frederick JM *et al.* The Leber congenital amaurosis protein, AIPL1, is needed for the viability and functioning of cone photoreceptor cells. *Hum. Mol. Genet.* 19(6), 1076–1087 (2010).

51 Kolandaivelu S, Huang J, Hurley JB, Ramamurthy V. AIPL1, a protein associated with childhood blindness, interacts with alpha-subunit of rod phosphodiesterase (PDE6) and is essential for its proper assembly. *J. Biol. Chem.* 284(45), 30853–30861 (2009).

52 Derst C, Doring F, Preisig-Müller R *et al.* Partial gene structure and assignment to chromosome 2q37 of the human inwardly rectifying K^+ channel (*Kir7.1*) gene (*KCNJ13*). *Genomics* 54(3), 560–563 (1998).

53 Ding XQ, Fitzgerald JB, Quiambao AB, Harry CS, Malykhina AP. Molecular pathogenesis of achromatopsia associated with mutations in the cone cyclic nucleotide-gated channel CNGA3 subunit. *Adv. Exp. Med. Biol.* 664, 245–253 (2010).

54 Otto EA, Loeys B, Khanna H *et al.* Nephrocystin-5, a ciliary IQ domain protein, is mutated in Senior–Loken syndrome and interacts with RPGR and calmodulin. *Nat. Genet.* 37(3), 282–288 (2005).

55 Williams DS, Lopes VS. The many different cellular functions of MYO7A in the retina. *Biochem. Soc. Trans.* 39(5), 1207–1210 (2011).

56 Collin GB, Cyr E, Bronson R *et al.* Alms1-disrupted mice recapitulate human Alstrom syndrome. *Hum. Mol. Genet.* 14(16), 2323–2333 (2005).

57 Kaplan J. Leber congenital amaurosis: from darkness to spotlight. *Ophthalmic Genet.* 29(3), 92–98 (2008).

58 Dharmaraj SR, Silva ER, Pina AL *et al.* Mutational analysis and clinical correlation in Leber congenital amaurosis. *Ophthalmic Genet.* 21(3), 135–150 (2000).

59 Walia S, Fishman GA, Jacobson SG *et al.* Visual acuity in patients with Leber's congenital amaurosis and early childhood-onset retinitis pigmentosa. *Ophthalmology* 117(6), 1190–1198 (2010).

60 Schuster A, Janecke AR, Wilke R *et al.* The phenotype of early-onset retinal degeneration in persons with RDH12 mutations. *Invest. Ophthalmol. Vis. Sci.* 48(4), 1824–1831 (2007).

61 Jacobson SG, Cideciyan AV, Aleman TS *et al.* Human retinal disease from AIPL1 gene mutations: foveal cone loss with minimal macular photoreceptors and rod function remaining. *Invest. Ophthalmol. Vis. Sci.* 52(1), 70–79 (2011).

62 Chung DC, Traboulsi EI. Leber congenital amaurosis: clinical correlations with genotypes, gene therapy trials update, and future directions. *J. AAPOS* 13(6), 587–592 (2009).

63 Galvin JA, Fishman GA, Stone EM, Koenekoop RK. Evaluation of genotype-phenotype associations in Leber congenital amaurosis. *Retina* 25(7), 919–929 (2005).

64 Henderson RH, Mackay DS, Li Z *et al.* Phenotypic variability in patients with retinal dystrophies due to mutations in *CRB1*. *Br. J. Ophthalmol.* 95(6), 811–817 (2011).

65 Koenekoop RK, Lopez I, Den Hollander AI, Allikmets R, Cremers FP. Genetic testing for retinal dystrophies and dysfunctions: benefits, dilemmas and solutions. *Clin. Experiment. Ophthalmol.* 35(5), 473–485 (2007).

66 Pasadhika S, Fishman GA, Stone EM *et al.* Differential macular morphology in patients with RPE65-, CEP290-, GUCY2D-, and AIPL1-related Leber congenital amaurosis. *Invest. Ophthalmol. Vis. Sci.* 51(5), 2608–2614 (2010).

• **Describes macular imaging as a tool to study fine structural details of macular phenotypes in LCA.**

67 McKay GJ, Clarke S, Davis JA, Simpson DA, Silvestri G. Pigmented paravenous chorioretinal atrophy is associated with a mutation within the crumbs homolog 1 (*CRB1*) gene. *Invest. Ophthalmol. Vis. Sci.* 46(1), 322–328 (2005).

68 Jacobson SG, Cideciyan AV, Aleman TS *et al.* Crumbs homolog 1 (*CRB1*) mutations result in a thick human retina with abnormal lamination. *Hum. Mol. Genet.* 12(9), 1073–1078 (2003).

69 Lotery AJ, Jacobson SG, Fishman GA *et al.* Mutations in the *CRB1* gene cause Leber congenital amaurosis. *Arch. Ophthalmol.* 119(3), 415–420 (2001).

70 Den Hollander AI, Heckenlively JR, Van Den Born LI *et al.* Leber congenital amaurosis and retinitis pigmentosa with Coats-like exudative vasculopathy are associated with mutations in the crumbs homologue 1 (*CRB1*) gene. *Am. J. Hum. Genet.* 69(1), 198–203 (2001).

71 Cideciyan AV, Aleman TS, Jacobson SG *et al.* Centrosomal-ciliary gene *CEP290*/*NPHP6* mutations result in blindness with unexpected sparing of photoreceptors and visual brain: implications for therapy of Leber congenital amaurosis. *Hum. Mutat.* 28(11), 1074–1083 (2007).

72 Valverde D, Pereiro I, Vallespin E, Ayuso C, Borrego S, Baiget M. Complexity of phenotype–genotype correlations in Spanish patients with *RDH12* mutations. *Invest. Ophthalmol. Vis. Sci.* 50(3), 1065–1068 (2009).

73 Mckibbin M, Ali M, Mohamed MD *et al.* Genotype–phenotype correlation for Leber congenital amaurosis in northern Pakistan. *Arch. Ophthalmol.* 128(1), 107–113 (2010).

74 Testa F, Surace EM, Rossi S *et al.* Evaluation of Italian patients with Leber congenital amaurosis due to *AIPL1* mutations highlights the potential applicability of gene therapy. *Invest. Ophthalmol. Vis. Sci.* 52(8), 5618–5624 (2011).

75 Khanna H, Davis EE, Murga-Zamalloa CA *et al.* A common allele in *RPGRIP1L* is a modifier of retinal degeneration in ciliopathies. *Nat. Genet.* 41(6), 739–745 (2009).

•• **Study of *RPGRIP1L* variants across several ciliopathies that reports on a common allele involved in retinal phenotypes of these disorders.**

76 Den Hollander AI, Black A, Bennett J, Cremers FP. Lighting a candle in the dark: advances in genetics and gene therapy of recessive retinal dystrophies. *J. Clin. Invest.* 120(9), 3042–3053 (2010).

77 Acland GM, Aguirre GD, Ray J *et al.* Gene therapy restores vision in a canine model of childhood blindness. *Nat. Genet.* 28(1), 92–95 (2001).

• **First report of *RPE65* gene therapy in a canine model.**

78 Narfstrom K, Katz ML, Bragadottir R *et al.* Functional and structural recovery of the retina after gene therapy in the *RPE65* null mutation dog. *Invest. Ophthalmol. Vis. Sci.* 44(4), 1663–1672 (2003).

79 Acland GM, Aguirre GD, Bennett J *et al.* Long-term restoration of rod and cone vision by single dose rAAV-mediated gene transfer to the retina in a canine model of childhood blindness. *Mol. Ther.* 12(6), 1072–1082 (2005).

80 Weber M, Rabinowitz J, Provost N *et al.* Recombinant adeno-associated virus serotype 4 mediates unique and exclusive long-term transduction of retinal pigmented epithelium in rat, dog, and nonhuman primate after subretinal delivery. *Mol. Ther.* 7(6), 774–781 (2003).

81 Jacobson SG, Acland GM, Aguirre GD *et al.* Safety of recombinant adeno-associated virus type 2-RPE65 vector delivered by ocular subretinal injection. *Mol. Ther.* 13(6), 1074–1084 (2006).

82 Jacobson SG, Boye SL, Aleman TS *et al.* Safety in nonhuman primates of ocular AAV2-RPE65, a candidate treatment for blindness in Leber congenital amaurosis. *Hum. Gene Ther.* 17(8), 845–858 (2006).

83 Hauswirth WW, Aleman TS, Kaushal S *et al.* Treatment of Leber congenital amaurosis due to *RPE65* mutations by ocular subretinal injection of adeno-

associated virus gene vector: short-term results of a Phase I trial. *Hum. Gene Ther.* 19(10), 979–990 (2008).

- **Report of the first gene therapy trial for *RPE65* gene delivery in LCA.**

84 Cideciyan AV. Leber congenital amaurosis due to *RPE65* mutations and its treatment with gene therapy. *Prog. Retin. Eye Res.* 29(5), 398–427 (2010).

85 Cideciyan AV, Hauswirth WW, Aleman TS *et al.* Human *RPE65* gene therapy for Leber congenital amaurosis: persistence of early visual improvements and safety at 1 year. *Hum. Gene Ther.* 20(9), 999–1004 (2009).

86 Simonelli F, Maguire AM, Testa F *et al.* Gene therapy for Leber's congenital amaurosis is safe and effective through 1.5 years after vector administration. *Mol. Ther.* 18(3), 643–650 (2010).

87 Semple-Rowland SL, Lee NR, Van Hooser JP, Palczewski K, Baehr W. A null mutation in the photoreceptor guanylate cyclase gene causes the retinal degeneration chicken phenotype. *Proc. Natl Acad. Sci. USA* 95(3), 1271–1276 (1998).

88 Williams ML, Coleman JE, Haire SE *et al.* Lentiviral expression of retinal guanylate cyclase-1 (RetGC1) restores vision in an avian model of childhood blindness. *PLoS Med.* 3(6), e201 (2006).

89 Boye SE, Boye SL, Pang J *et al.* Functional and behavioral restoration of vision by gene therapy in the guanylate cyclase-1 (*GC1*) knockout mouse. *PLoS One* 5(6), e11306 (2010).

90 Mihelec M, Pearson RA, Robbie SJ *et al.* Long-term preservation of cones and improvement in visual function following gene therapy in a mouse model of Leber congenital amaurosis caused by guanylate cyclase-1 deficiency. *Hum. Gene Ther.* 22(10), 1179–1190 (2011).

91 Ramamurthy V, Niemi GA, Reh TA, Hurley JB. Leber congenital amaurosis linked to AIPL1: a mouse model reveals destabilization of cGMP phosphodiesterase. *Proc. Natl Acad. Sci. USA* 101(38), 13897–13902 (2004).

92 Liu X, Bulgakov OV, Wen XH *et al.* AIPL1, the protein that is defective in Leber congenital amaurosis, is essential for the biosynthesis of retinal rod cGMP phosphodiesterase. *Proc. Natl Acad. Sci. USA* 101(38), 13903–13908 (2004).

93 Sun X, Pawlyk B, Xu X *et al.* Gene therapy with a promoter targeting both rods and cones rescues retinal degeneration caused by *AIPL1* mutations. *Gene Ther.* 17(1), 117–131 (2010).

94 Gerner M, Haribaskar R, Putz M, Czerwitzki J, Walz G, Schafer T. The retinitis pigmentosa GTPase regulator interacting protein 1 (RPGRIP1) links RPGR to the nephronophthisis protein network. *Kidney Int.* 77(10), 891–896 (2010).

95 Won J, Gifford E, Smith RS *et al.* RPGRIP1 is essential for normal rod photoreceptor outer segment elaboration and morphogenesis. *Hum. Mol. Genet.* 18(22), 4329–4339 (2009).

96 Pawlyk BS, Smith AJ, Buch PK *et al.* Gene replacement therapy rescues photoreceptor degeneration in a murine model of Leber congenital amaurosis lacking RPGRIP. *Invest. Ophthalmol. Vis. Sci.* 46(9), 3039–3045 (2005).

97 Pawlyk BS, Bulgakov OV, Liu X *et al.* Replacement gene therapy with a human RPGRIP1 sequence slows photoreceptor degeneration in a murine model of Leber congenital amaurosis. *Hum. Gene Ther.* 21(8), 993–1004 (2010).

98 Jacobson SG, Cideciyan AV, Aleman TS *et al.* Leber congenital amaurosis caused by an *RPGRIP1* mutation shows treatment potential. *Ophthalmology* 114(5), 895–898 (2007).

99 Baye LM, Patrinostro X, Swaminathan S *et al.* The N-terminal region of centrosomal protein 290 (CEP290) restores vision in a zebrafish model of human blindness. *Hum. Mol. Genet.* 20(8), 1467–1477 (2011).

100 D'Cruz PM, Yasumura D, Weir J *et al.* Mutation of the receptor tyrosine kinase gene *Mertk* in the retinal dystrophic RCS rat. *Hum. Mol. Genet.* 9(4), 645–651 (2000).

101 Vollrath D, Feng W, Duncan JL *et al.* Correction of the retinal dystrophy phenotype of the RCS rat by viral gene transfer of *Mertk*. *Proc. Natl Acad. Sci. USA* 98(22), 12584–12589 (2001).

102 Tschernutter M, Schlichtenbrede FC, Howe S *et al.* Long-term preservation of retinal function in the RCS rat model of retinitis pigmentosa following lentivirus-mediated gene therapy. *Gene Ther.* 12(8), 694–701 (2005).

103 Smith AJ, Schlichtenbrede FC, Tschernutter M, Bainbridge JW, Thrasher AJ, Ali RR. AAV-mediated gene transfer slows photoreceptor loss in the RCS rat model of retinitis pigmentosa. *Mol. Ther.* 8(2), 188–195 (2003).

104 Batten ML, Imanishi Y, Tu DC *et al.* Pharmacological and rAAV gene therapy rescue of visual functions in a blind mouse model of Leber congenital amaurosis. *PLoS Med.* 2(11), e333 (2005).

105 Henderson RH, Waseem N, Searle R *et al.* An assessment of the apex microarray technology in genotyping patients with Leber congenital amaurosis and early-onset severe retinal dystrophy. *Invest. Ophthalmol. Vis. Sci.* 48(12), 5684–5689 (2007).

106 Song J, Smaoui N, Ayyagari R *et al.* High-throughput retina-array for screening 93 genes involved in inherited retinal dystrophy. *Invest. Ophthalmol. Vis. Sci.* 52(12), 9053–9060 (2011).

107 Pomares E, Riera M, Permanyer J *et al.* Comprehensive SNP-chip for retinitis pigmentosa–Leber congenital amaurosis diagnosis: new mutations and detection of mutational founder effects. *Eur. J. Hum. Genet.* 18(1), 118–124 (2010).

108 Simpson DA, Clark GR, Alexander S, Silvestri G, Willoughby CE. Molecular diagnosis for heterogeneous genetic diseases with targeted high-throughput DNA sequencing applied to retinitis pigmentosa. *J. Med. Genet.* 48(3), 145–151 (2011).

Websites

201 Clinical Trials.gov. Phase I Trial of Gene Vector to Patients With Retinal Disease Due to RPE65 Mutations (LCA). http://clinicaltrials.gov/ct2/show/NCT00481546

202 Clinical Trials.gov. Safety Study of RPE65 Gene Therapy to Treat Leber Congenital Amaurosis. http://clinicaltrials.gov/ct2/show/NCT00643747

203 Clinical Trials.gov. Safety Study in Subjects With Leber Congenital Amaurosis (LCARPE). http://clinicaltrials.gov/ct2/show/NCT00516477

204 Clinical Trials.gov. Genetic Study of Patients Suffering From Congenital Amaurosis of Leber or From an Early Severe Retinal Dystrophy. http://clinicaltrials.gov/ct2/show/NCT00422721